Chapter 2

Modulation and Demodulation

The most fundamental building block of a digital communication system is the modulator-demodulator (MODEM) pair. In this chapter, we study the theory that underlies the design of the MODEM in a digital communication.

We start with the simple baseband binary communication system over the AWGN channel to introduce the concept of a matched £lter. In many cases, we have to modulate the transmitted signal to higher frequency bands, usually known as the *radio frequency* (RF) bands, to suit the propagation characteristics of the communication channels. The simplest RF channel is the *non-dispersive* channel which changes the amplitude and phase of the transmitted signal. There are two ways to perform demodulation over the non-dispersive channel. The £rst way is to estimate the phase distortion and use the matched £lter as in a baseband communication system. This method is usually referred to as *coherent* demodulation. The second approach, known as *noncoherent* demodulation, is to avoid using the phase information in the demodulation process at all. We discuss and compare the two approaches.

Binary modulation is the simplest modulation format. An immediate extension is to send one out of M signals instead of one out of two signals. This is called M*-ary communications*. Beside introducing M-ary communications, we present a very useful technique, namely the *union bound*, to evaluate the performance of complex communication systems such as a M-ary system.

The discussion of the modulation and demodulation methods above provide us a solid introduction to the topic. Our next goal is to study the optimal demodulators, both coherent and noncoherent, in the sense of achieving the minimum symbol error probability over the non-dispersive channel. It

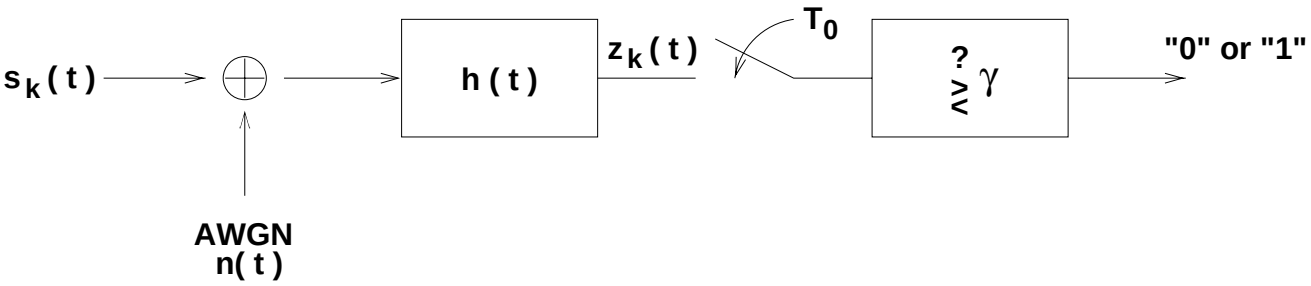

Figure 2.1: Baseband binary communication system

turns out that the optimal demodulators can be characterized by maximizing some likelihood functions of the received signal. Hence, the optimal demodulators are also called *maximum likelihood (ML)* demodulators.

For the developments in this chapter, we restrict ourselves to the simple AWGN and non-dispersive channels. The effect of other channel distortions and techniques to overcome them will be discussed in later chapters.

2.1 Baseband Binary Communications

Consider the baseband binary communication system over the AWGN channel as shown in Figure 2.1. The goal is to send one bit only (one-shot analysis).

Assumptions:

1. The modulator outputs the signal $s_0(t)$ if the input bit value is "0" and it outputs the signal $s_1(t)$ if the input bit value is "1". In other words, we use $s_0(t)$ to represent "0" and $s_1(t)$ to represent "1".

2. The additive noise $n(t)$ introduced by the channel is an AWGN process with a two-sided noise spectral density of $N_0/2$.

3. The demodulator passes the received signal $s_k(t) + n(t)$ ($k = 0$ or 1) to an LTI filter whose impulse response is $h(t)$ and samples the filter output at time T_0 to provide the *decision statistic* $z_k(T_0)$.

4. The receiver checks the decision statistic against the threshold γ to decide whether the transmitted bit is "0" or "1". We assume that $s_0 * h(T_0) > s_1 * h(T_0)$. Therefore, we decide "0" if $z_k(T_0) \geq \gamma$, and "1" otherwise.

Goals:

1. To determine the probability of error for chosen threshold γ, £lter $h(t)$, sampling time T_0, and signal pair $s_0(t)$ and $s_1(t)$.

2. To determine the "best"

   (a) threshold γ,

   (b) linear £lter $h(t)$ and sampling time T_0,

   (c) signal pair $s_0(t)$ and $s_1(t)$.

2.1.1 Bit error probability

Suppose that "0" is sent. Let $\hat{s}_0(t)$ and $\hat{n}(t)$ represent the output of the £lter $h(t)$ due to the signal and the noise, respectively, i.e.,

$$\hat{s}_0(t) = s_0 * h(t), \tag{2.1}$$

$$\hat{n}(t) = n * h(t). \tag{2.2}$$

The overall output $z_0(t)$ is the sum $\hat{s}_0(t) + \hat{n}(t)$. The decision is made according to the sample of $z_0(t)$ at time T_0. Therefore, the decision statistic is $z_0(T_0)$ given by

$$z_0(T_0) = \hat{s}_0(T_0) + \hat{n}(T_0). \tag{2.3}$$

The signal contribution $\hat{s}_0(T_0)$ is deterministic. We consider the noise contribution $\hat{n}(T_0)$. Since $n(t)$ is a WSS zero-mean Gaussian random process, $\hat{n}(t)$ is also a WSS zero-mean Gaussian random process. Therefore, $\hat{n}(T_0)$ is a zero-mean Gaussian random variable. The variance of $\hat{n}(T_0)$ is $\mathrm{E}[\hat{n}^2(T_0)] = R_{\hat{n}}(0)$. Therefore, $z_0(T_0)$ is a Gaussian random variable with mean $\hat{s}_0(T_0)$ and variance $R_{\hat{n}}(0)$. Given

that "0" is sent, the probability of error is given by

$$\begin{aligned} P_{b,0} &= \Pr(z_0(T_0) < \gamma) \\ &= \Phi\left(\frac{\gamma - \hat{s}_0(T_0)}{\sqrt{R_{\hat{n}}(0)}}\right) \\ &= Q\left(\frac{\hat{s}_0(T_0) - \gamma}{\sqrt{R_{\hat{n}}(0)}}\right). \end{aligned} \tag{2.4}$$

Similarly, if "1" is sent, then the decision statistic $z_1(T_0)$ is a Gaussian random variable with mean $\hat{s}_1(T_0)$ and variance $R_{\hat{n}}(0)$. Given that "1" is sent, the probability of error is given by

$$\begin{aligned} P_{b,1} &= \Pr(z_1(T_0) \geq \gamma) \\ &= Q\left(\frac{\gamma - \hat{s}_1(T_0)}{\sqrt{R_{\hat{n}}(0)}}\right). \end{aligned} \tag{2.5}$$

Suppose that we send "0" with probability p_0 and "1" with probability $p_1 = 1 - p_0$. Then the average bit error probability is given by

$$P_b = p_0 P_{b,0} + p_1 P_{b,1}. \tag{2.6}$$

2.1.2 Threshold optimization

The goal of the optimization is to determine the decision threshold γ which minimizes the average bit error probability P_b. Depending on the knowledge available to the receiver, one of the following approaches is taken.

Minimax approach

Suppose that the receiver has no knowledge of p_0 and p_1. To guarantee a certain performance no matter whether "0" or "1" is sent, we minimize the maximum of $P_{b,0}$ and $P_{b,1}$. The best way to solve this optimization problem is to look at the plots of $P_{b,0}$ and $P_{b,1}$ versus γ as those shown in Figure 2.2. Consider the following diagram. First, we note from (2.4) and (2.5) that as γ increases, $P_{b,0}$ increases while $P_{b,1}$ decreases. It is obvious from Figure 2.2 that the maximum of $P_{b,0}$ and $P_{b,1}$ reaches its minimum at where $P_{b,0} = P_{b,1}$. Therefore under this minimax criterion, the best choice of γ is the one

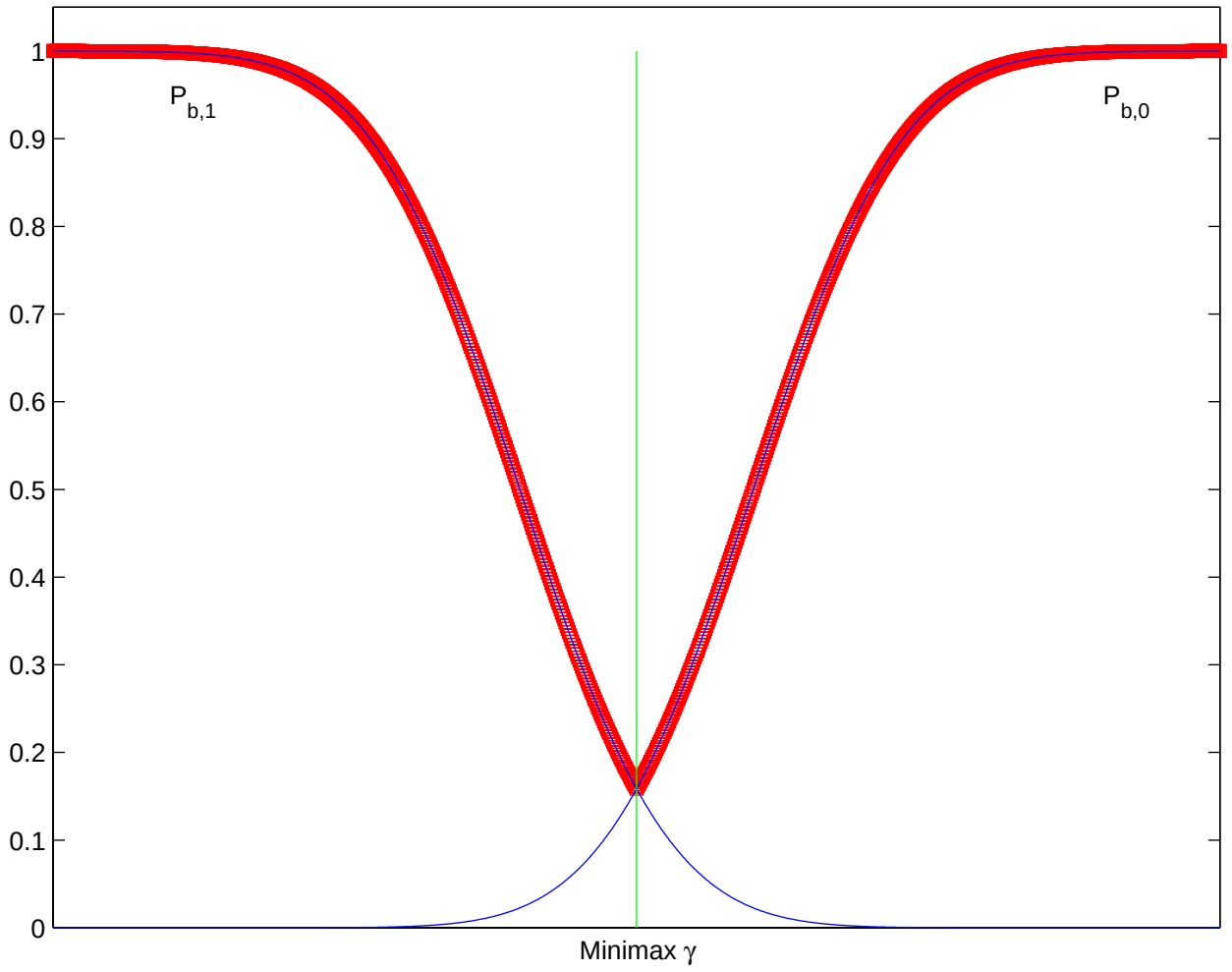

Figure 2.2: Typical plots of $P_{b,0}$ and $P_{b,1}$ versus γ

that makes

$$\begin{aligned} P_{b,0} &= P_{b,1} \\ Q\left(\frac{\hat{s}_0(T_0)-\gamma}{\sqrt{R_{\hat{n}}(0)}}\right) &= Q\left(\frac{\gamma-\hat{s}_1(T_0)}{\sqrt{R_{\hat{n}}(0)}}\right). \end{aligned} \tag{2.7}$$

Therefore, the best choice of γ is

$$\gamma = \frac{\hat{s}_0(T_0)+\hat{s}_1(T_0)}{2}. \tag{2.8}$$

With this choice of γ, the average bit error probability becomes

$$P_b = P_{b,0} = P_{b,1} = Q\left(\frac{\hat{s}_0(T_0)-\hat{s}_1(T_0)}{2\sqrt{R_{\hat{n}}(0)}}\right). \tag{2.9}$$

Minimum average bit error probability approach

Suppose that the receiver has clear knowledge of p_0 and p_1. Then the obvious approach is to choose γ that minimizes P_b. We recall that

$$P_b = p_0 Q\left(\frac{\hat{s}_0(T_0)-\gamma}{\sqrt{R_{\hat{n}}(0)}}\right) + p_1 Q\left(\frac{\gamma-\hat{s}_1(T_0)}{\sqrt{R_{\hat{n}}(0)}}\right). \tag{2.10}$$

Differentiating it wrt γ, we have

$$\frac{dP_b}{d\gamma} = \frac{p_0}{\sqrt{2\pi R_{\hat{n}}(0)}}\exp\left[\frac{-(\hat{s}_0(T_0)-\gamma)^2}{2R_{\hat{n}}(0)}\right] - \frac{p_1}{\sqrt{2\pi R_{\hat{n}}(0)}}\exp\left[\frac{-(\gamma-\hat{s}_1(T_0))^2}{2R_{\hat{n}}(0)}\right]. \tag{2.11}$$

Setting the result to zero and solving for γ, we have

$$\gamma = \frac{\hat{s}_0(T_0)+\hat{s}_1(T_0)}{2} + \frac{R_{\hat{n}}(0)}{\hat{s}_0(T_0)-\hat{s}_1(T_0)}\ln\frac{p_1}{p_0}. \tag{2.12}$$

We notice that when $p_0 = p_1$, γ reduces to the minimax threshold. When p_0 is larger, γ is reduced so that the average bit error probability P_b is reduced. Likewise, when p_1 is larger, γ is increased so that the average bit error probability P_b is reduced.

2.1.3 Filter and sampling time optimization

We consider the best £lter when the *a priori* probabilities p_0 and p_1 are the same and the minimax threshold is used. With the minimax γ, P_b is given by (2.9). Since $Q(\cdot)$ is monotone decreasing, we can minimize P_b by maximizing

$$\frac{\hat{s}_0(T_0)-\hat{s}_1(T_0)}{2\sqrt{R_{\hat{n}}(0)}}. \tag{2.13}$$

First, let us determine the noise variance $R_{\hat{n}}(0)$:

$$\begin{aligned} R_{\hat{n}}(0) &= \int_{-\infty}^{\infty} \Phi_{\hat{n}}(f)df \\ &= \frac{N_0}{2}\int_{-\infty}^{\infty} |H(f)|^2 df \\ &= \frac{N_0}{2}\int_{-\infty}^{\infty} |h(t)|^2 dt \\ &= \frac{N_0}{2}\|h\|^2 \end{aligned} \tag{2.14}$$

where the norm $\|\cdot\|$ of any function x is de£ned by

$$\|x\| = \sqrt{\int_{-\infty}^{\infty} x^2(t)dt}. \tag{2.15}$$

Moreover,

$$\hat{s}_0(T_0) - \hat{s}_1(T_0) = \int_{-\infty}^{\infty} [s_0(T_0 - t) - s_1(T_0 - t)]h(t)dt. \tag{2.16}$$

Therefore, in order to minimize P_e, we can choose $h(t)$ such that the expression

$$\frac{1}{\|h\|}\int_{-\infty}^{\infty} [s_0(T_0 - t) - s_1(T_0 - t)]h(t)dt \tag{2.17}$$

is maximized.

We can use the Cauchy-Schwartz inequality to solve the maximization problem in (2.17). The Cauchy-Schwartz inequality says that for any two functions f and g such that $\|f\|, \|g\| < \infty$,

$$\left|\int_{-\infty}^{\infty} f(t)g(t)dt\right| \leq ||f|| \cdot ||g|| \tag{2.18}$$

with equality if and only if $f(t) = \lambda g(t)$ where λ is a constant. Applying (2.18) with $f(t) = s_0(T_0 - t) - s_1(T_0 - t)$ and $g(t) = h(t)$, we have[1]

$$\int_{-\infty}^{\infty} [s_0(T_0 - t) - s_1(T_0 - t)]h(t)dt \leq \|s_0(T_0 - t) - s_1(T_0 - t)\| \cdot \|h\| \tag{2.19}$$

with equality if and only if $h(t) = \lambda[s_0(T_0 - t) - s_1(T_0 - t)]$ where λ is a constant. Therefore, the expression in (2.17) is maximized if we choose

$$h(t) = s_0(T_0 - t) - s_1(T_0 - t). \tag{2.20}$$

[1] $\hat{s}_0(T_0) - \hat{s}_1(T_0) = \int_{-\infty}^{\infty}[s_0(T_0 - t) - s_1(T_0 - t)]h(t)dt > 0$.

This best linear £lter is called the *matched £lter*. The minimum P_b achieved by the matched £lter is

$$\begin{aligned} P_b &= Q\left(\sqrt{\frac{\|s_0(T_0-t)-s_1(T_0-t)\|^2}{2N_0}}\right) \\ &= Q\left(\sqrt{\frac{\|s_0-s_1\|^2}{2N_0}}\right). \end{aligned} \tag{2.21}$$

We note that the choice of the constant λ is immaterial in terms of minimizing P_b. Therefore, we may just choose $\lambda = 1$ as above. From (2.20), we see that the matched £lter depends on the choice of the signal pair and the sampling time T_0. On the other hand, the last expression of (2.21) indicates that the choice of the sampling time T_0 does not affect the minimum P_b provided that $h(t)$ is chosen accordingly. In general, we choose T_0 so that $h(t)$ is a causal £lter and the delay before making the decision is minimized.

With the matched £lter, some expressions before can be simpli£ed. The expression for the minimax threshold reduces to

$$\begin{aligned} \gamma &= \frac{1}{2}[\hat{s}_0(T_0)+\hat{s}_1(T_0)] \\ &= \frac{1}{2}\left[\int_{-\infty}^{\infty} s_0^2(T_0-t)dt - \int_{-\infty}^{\infty} s_1^2(T_0-t)dt\right] \\ &= \frac{1}{2}(E_0-E_1) \end{aligned} \tag{2.22}$$

where E_0 and E_1 are the energies of $s_0(t)$ and $s_1(t)$, respectively. Let us de£ne $\bar{E}$ as the average energy and r as the correlation coef£cient of the signals $s_0(t)$ and $s_1(t)$, i.e.,

$$\bar{E} = \frac{1}{2}(E_0+E_1) \tag{2.23}$$

$$r = \frac{1}{\bar{E}}\int_{-\infty}^{\infty} s_0(t)s_1(t)dt. \tag{2.24}$$

Then

$$P_b = Q\left(\sqrt{\frac{\bar{E}(1-r)}{N_0}}\right). \tag{2.25}$$

2.1.4 Signal pair optimization

We see from the previous discussion that the minimum average bit error probability achieved by the matched £lter depends on the choice of the signal pair. Our goal here is to determine which pair

of signals give the smallest P_b. From (2.25), it is clear that P_b is minimized when the correlation coef£cient r is minimized.

First, by the Cauchy-Schwartz inequality,

$$\left| \int_{-\infty}^{\infty} s_0(t) s_1(t) dt \right| \leq \sqrt{E_0 E_1}. \tag{2.26}$$

Moreover, since the geometric mean (of positive numbers) is less than the arithmetic mean,

$$\sqrt{E_0 E_1} \leq \bar{E}. \tag{2.27}$$

Together, the two inequalites imply that $|r| \leq 1$. Therefore, the minimum possible value of r is -1. To achieve $r = -1$, we must achieve equality for (2.26) and equality for (2.27). For (2.26), equality is achieved when

$$s_1(t) = \lambda s_0(t) \tag{2.28}$$

where λ is a constant. For (2.27), equality is achieved when

$$E_0 = E_1 = \bar{E}. \tag{2.29}$$

Therefore, $|\lambda| = 1$. By direct calculation, $r = -1$ is achieved when $\lambda = -1$, i.e.,

$$s_1(t) = -s_0(t). \tag{2.30}$$

Such a pair of signals, where one is the negation of the other, are called *antipodal signals*. With antipodal signals, P_b is minimized at

$$P_b = Q\left(\sqrt{\frac{2E_b}{N_0}}\right) \tag{2.31}$$

where $E_b = E_0 = E_1$ is the *energy per bit*. For antipodal signals, The matched £lter reduces to

$$h(t) = s_0(T_0 - t) \tag{2.32}$$

and the minimax threshold is 0.

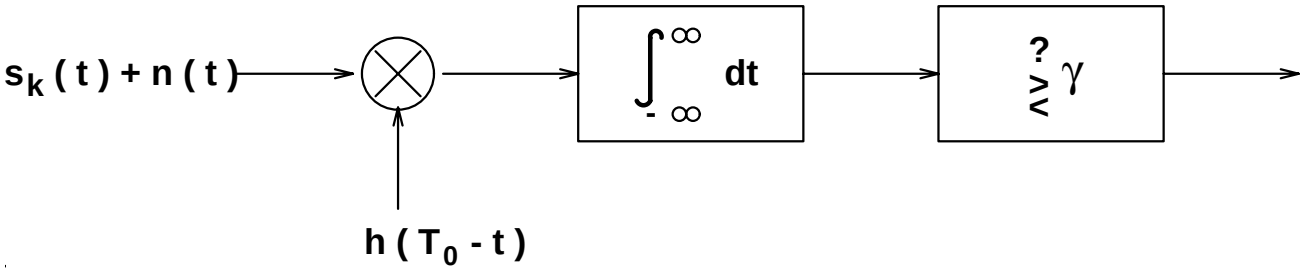

Figure 2.3: Correlation receiver

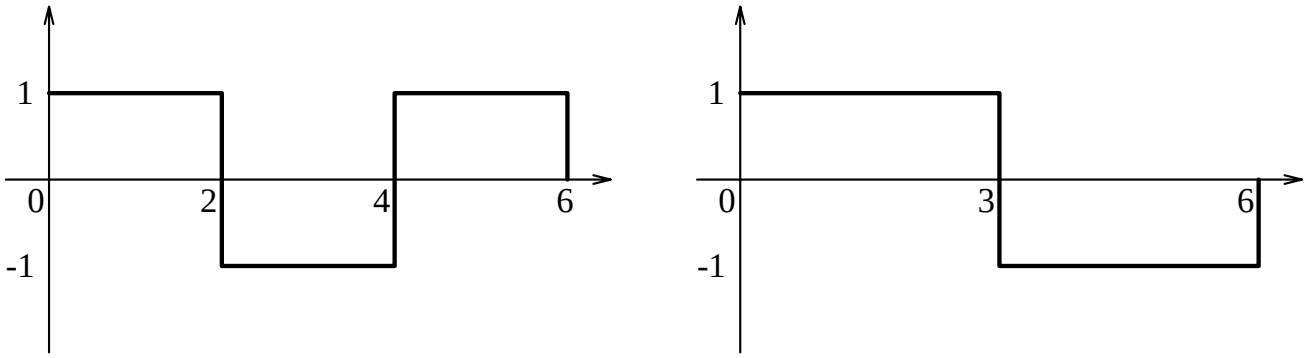

Figure 2.4: Two sample signals for a binary communication system

2.1.5 Correlation receiver

Instead of passing the received signal $s_k(t) + n(t)$ through a £lter and sampling the output at T_0, we can obtain the decision statistic $z_k(T_0)$ using the equivalent implementation in Figure 2.3. When the matched £lter is employed, the correlation function in Figure 2.3 becomes

$$\begin{aligned} h(T_0 - t) &= s_0(T_0 - (T_0 - t)) - s_1(T_0 - (T_0 - t)) \\ &= s_0(t) - s_1(t). \end{aligned} \tag{2.33}$$

This implementation of the matched £lter is called the *correlation receiver*.

2.1.6 Example

Consider a binary communication system where the two probable signals with probabilities p_0 and p_1 are shown in Figure 2.4 The communication channel is contaminated by AWGN with two-sided noise power spectral density of $N_0/2$.

1. Given an LTI £lter $h(t)$, a sampling time and a threshold, £nd the average probability of error.

2. Given an LTI £lter $h(t)$ and a sampling time, £nd the minimax threshold and the minimum P_b threshold.

3. Given an LTI £lter $h(t)$ and a threshold, £nd the best sampling time.

4. Find the matched £lter.

5. Find the minimax threshold and the minimum P_b threshold using the matched £lter.

6. Find the average bit error probability of error using the matched £lter.

2.2 Radio Frequency Communications

Very often, we do not directly transmit lowpass baseband signals as described in Section 2.1. Instead, we mix (modulate) the baseband signal with a carrier up to a certain frequency, which matches the electromagnetic propagation characteristic of the channel. As a result, the actual transmitted signal is a bandpass signal. The mixing process is accomplished by multiplying the information carrying signal with a high frequency carrier. In frequency domain, the effect is to translate the frequency spectrum of the information signal. Let $v(t)$ be the information signal and f_c be the carrier frequency. Then the transmitted (*radio frequency (RF)*) signal is $v(t)\cos(2\pi f_c t)$. Taking Fourier transform,

$$v(t)\cos(2\pi f_c t) \longleftrightarrow \frac{1}{2}[V(f-f_c)+V(f+f_c)]. \tag{2.34}$$

The spectrum of a typical RF signal is shown in Fig. 2.5.

The baseband AWGN model considered in Section 2.1 is inadequate for a RF communication channel. Here, we consider a simple extension of the AWGN model for RF communication channels—the *non-dispersive* channel. We model the received signal as

$$r(t) = Av(t)\cos(2\pi f_c t+\theta)+n(t), \tag{2.35}$$

where $A > 0$ represents the channel gain (attenuation), θ represents the carrier phase shift due to propagation delay, local oscillator mismatch, and *etc.*, and $n(t)$ is AWGN with autocorrelation function $R_n(\tau) = \frac{N_0}{2}\delta(\tau)$. Sometimes, a non-dispersive channel is also referred to as an AWGN channel in RF communication systems.

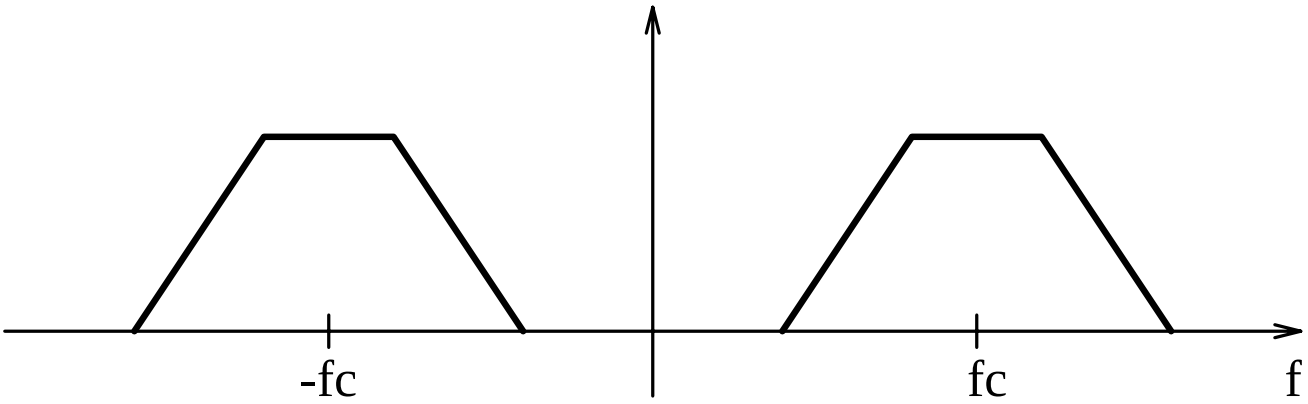

Figure 2.5: Spectrum of a typical RF signal

2.2.1 Coherent Demodulation

If the receiver knows the values of A and θ, the situation reduces to the one in Section 2.1. All our previous results on baseband binary communications hold by letting, for $k = 0,$ and 1,

$$s_0(t) = Av_0(t)\cos(2\pi f_c t + \theta) \tag{2.36}$$

$$s_1(t) = Av_1(t)\cos(2\pi f_c t + \theta), \tag{2.37}$$

where $v_0(t)$ and $v_1(t)$ are the baseband signals representing the values "0" and "1", respectively. Particularly, we can employ the matched £lter

$$\begin{aligned} h(t) &= s_0(T_0 - t) - s_1(T_0 - t) \\ &= [v_0(T_0 - t) - v_1(T_0 - t)]\cos(2\pi f_c(T_0 - t) + \theta) \end{aligned} \tag{2.38}$$

to demodulate the received signal. In summary, this approach, known as *coherent demodulation*, makes use of the phase and magnitude information of the channel to demodulate the received signal. In practice, the receiver has to estimate the phase and magnitude responses of the channel from the received signal.

As an illustration, let us consider a RF binary communication system employing a pair of equally probable antipodal signals, i.e., $v_0(t) = -v_1(t) = v(t)$ in (2.36) and (2.37). Then the matched £lter is

$$h(t) = v(T_0 - t)\cos(2\pi f_c(T_0 - t) + \theta). \tag{2.39}$$

The minimax threshold is $\gamma = 0$[2]. The average bit error probability is $P_b = Q(\sqrt{2E_b/N_0})$, where E_b

[2]For antipodal signals, the channel magnitude is not needed.

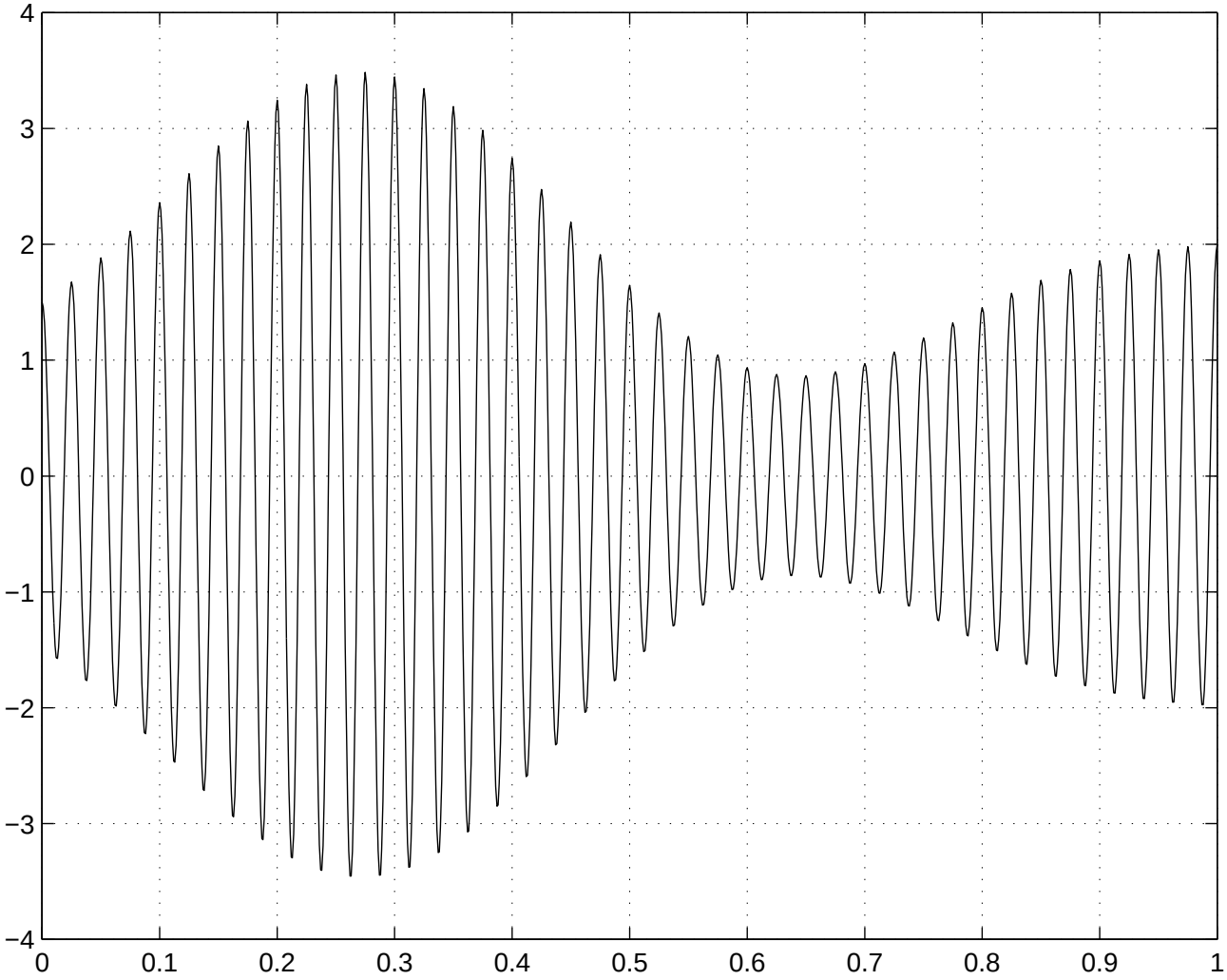

Figure 2.6: Carrier modulated (RF) signal in time domain

is the (received) energy per bit given by

$$\begin{aligned} E_b &= \int_{-\infty}^{\infty} A^2 v^2(t) \cos^2(2\pi f_c t + \theta) dt \\ &= \frac{1}{2}\int_{-\infty}^{\infty} A^2 v^2(t) dt + \frac{1}{2}\int_{-\infty}^{\infty} A^2 v^2(t) \cos(2\pi 2 f_c t + 2\theta) dt \\ &\approx \frac{A^2}{2}\int_{-\infty}^{\infty} v^2(t) dt. \end{aligned} \tag{2.40}$$

The double frequency term is neglected in the last approximation in (2.40) because the carrier frequency is usually high compared with frequency content of the information signal $v(t)$. A typical situation is shown in Fig. 2.6. When a signal with low frequency content is multiplied by a high fre-

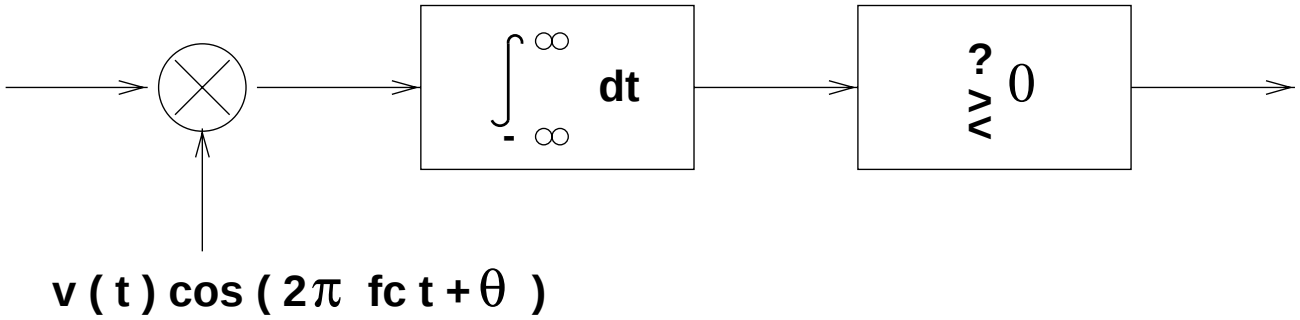

Figure 2.7: Correlation receiver for antipodal RF signals

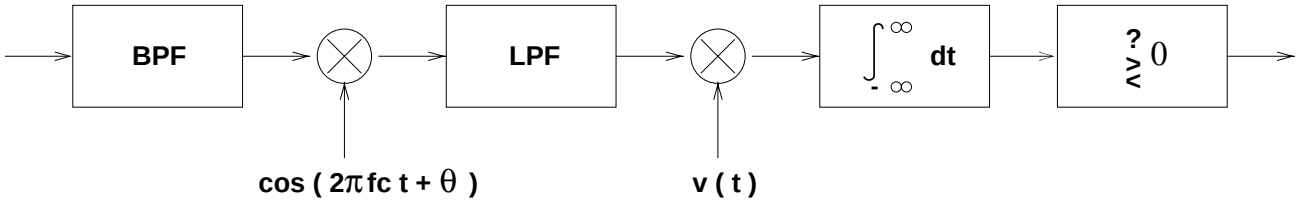

Figure 2.8: Correlation receiver with frequency translation

quency carrier, the integral of the resulting signal is approximately zero. More precisely, if $v(t)$ is bandlimited to f_c, i.e.,

$$V(f) = 0 \quad \text{for} \quad |f| \geq f_c \tag{2.41}$$

then the approximation becomes exact.

Just as before, instead of the matched £lter, we can use the correlation receiver in Fig. 2.7 to demodulate the received signal (of course, with the same P_b). In particular, the output of the integrator, due to the signal, is given by

$$\pm \int_{-\infty}^{\infty} Av^2(t)\cos^2(2\pi f_c t + \theta)dt \approx \pm\frac{A}{2}\int_{-\infty}^{\infty} v^2(t)dt. \tag{2.42}$$

Again, in most cases, the frequency content of the signal is low compared with the carrier frequency, and the double frequency term can be neglected. Equivalently, we can have the implementation in Fig. 2.8. It has the interpretation that the signal is translated back to baseband before detection.

For a pair of general binary RF signals, the corresponding coherent demodulating scheme using the matched £lter can be developed in exactly the same way as above. For conciseness, we do not repeat the process. Instead, we give an important result which facilitates such a development. Suppose

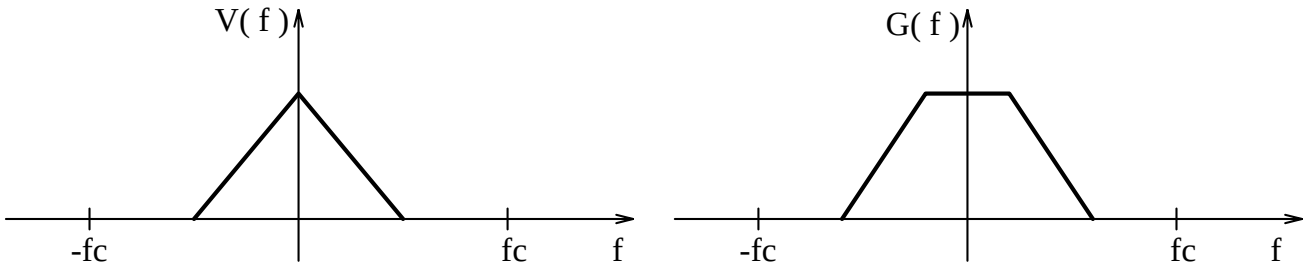

Figure 2.9: Spectra of lowpass signal and £lter

that

$$s(t) = v(t)\cos(2\pi f_c t + \alpha) \tag{2.43}$$

$$h(t) = g(t)\cos(2\pi f_c t + \beta), \tag{2.44}$$

where $v(t)$ and $g(t)$ are bandlimited to f_c, i.e., $V(f)$ and $G(f)$ are as shown in Fig. 2.9[3]. Consider the output of the signal $s(t)$ passing through the £lter $h(t)$. In frequency domain,

$$S(f) = \frac{1}{2}[V(f-f_c)e^{j\alpha} + V(f+f_c)e^{-j\alpha}] \tag{2.45}$$

$$H(f) = \frac{1}{2}[G(f-f_c)e^{j\beta} + G(f+f_c)e^{-j\beta}] \tag{2.46}$$

which are shown in Fig. 2.10. The Fourier transform of the output

$$\begin{aligned}\hat{S}(f) &= S(f)H(f) \\ &= \frac{1}{4}[V(f-f_c)G(f-f_c)e^{j(\alpha+\beta)} + V(f+f_c)G(f+f_c)e^{-j(\alpha+\beta)}].\end{aligned} \tag{2.47}$$

Therefore, the output

$$\hat{s}(t) = \frac{1}{2}[v * g(t)]\cos(2\pi f_c t + \alpha + \beta). \tag{2.48}$$

Although in practice the bandlimited condition might not be exactly satis£ed, this result of £ltering a bandlimited signal is often used as an approximation.

2.2.2 Noncoherent Demodulation

For coherent demodulation, we need to estimate the phase and magnitude responses of the channel. This estimation can sometimes be hard to perform, and inaccurate estimation will signi£cantly degrade the performance of the coherent demodulator. To illustrate this effect, let us reconsider the RF

[3]Note that $h(t)$ does not need to be the matched £lter.

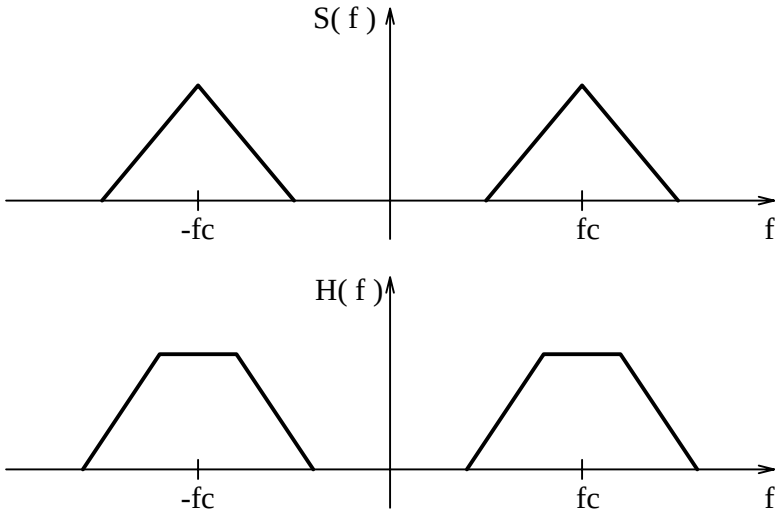

Figure 2.10: Spectra of bandpass signal and £lter

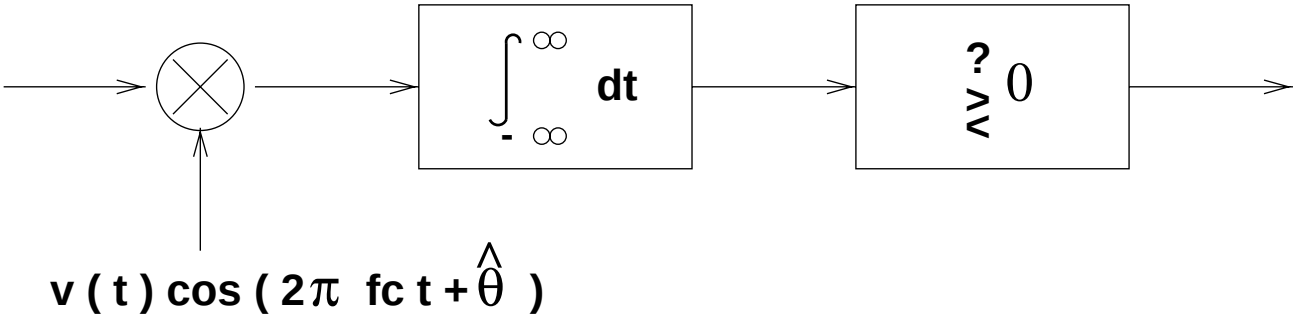

Figure 2.11: Correlation receiver for antipodal RF signals based on estimated phase response

binary communication system employing a pair of equally probable antipodal signals described in Section 2.2.1. Without the exact knowledge of the channel phase θ, we now need to estimate it. Let the estimate we obtain be $\hat{\theta}$. Then we perform coherent demodulation on the received signal based on the phase estimate $\hat{\theta}$. The resulting receiver is shown in Figure 2.11. It is straightforward to show that the average bit error probability is given by, for $|\theta - \hat{\theta}| < \pi/2$,

$$P_b = Q\left(\sqrt{\frac{2E_b}{N_0}}\cos(\theta - \hat{\theta})\right), \tag{2.49}$$

where E_b is given by (2.40). From (2.49), we see that the phase estimation error can cause a signi£cant degradation on P_b. For example, we have a 3dB loss in performance when the phase error $\theta - \hat{\theta}$ is $\pi/4$.

One alternative to overcome the dif£culty in estimating the channel phase response is to avoid using the phase and magnitude information in the demodulation process. Such an approach is referred

to as *noncoherent demodulation*, which is best described by the following example.

Consider a binary RF communication system employing the following pair of equally probable signals:

$$s_0(t) = Ap_T(t)\cos(2\pi f_0 t + \theta), \tag{2.50}$$

$$s_1(t) = Ap_T(t)\cos(2\pi f_1 t + \theta), \tag{2.51}$$

where $f_0 = f_c + \frac{\Delta f}{2}$, $f_1 = f_c - \frac{\Delta f}{2}$, and $p_T(t) = 1$ for $0 \le t < T$ and $p_T(t) = 0$ otherwise. This pair of signals correspond to the modulation scheme known as *frequency shift keying (FSK)* (see Section 2.2.3). The constants A and θ can be interpreted as the channel magnitude and phase responses, respectively. Moreover, we also assume that

$$\Delta f = \frac{k}{T} \tag{2.52}$$

for some integer k so that the signals $s_0(t)$ and $s_1(t)$ are orthogonal [4], i.e.,

$$\int_{-\infty}^{\infty} s_0(t)s_1(t)dt = 0.^5 \tag{2.53}$$

The received signal is modeled by

$$r(t) = s_k(t) + n(t), \tag{2.54}$$

where $n(t)$ is AWGN with two-sided noise spectral density $N_0/2$. In (2.54), $k = 0$ or 1 depending on whether the input bit value is "0" or "1". Instead of demodulating the received signal coherently, we consider the demodulator shown in Figure 2.12. The demodulator decides that a "0" is sent if $R_0 > R_1$. Otherwise, it decides that a "1" is sent.

Suppose that $s_0(t)$ is sent. First, we notice that at point (1) in Figure 2.12, the signal contribution is

$$\begin{aligned}\int_0^T A\cos(2\pi f_0 t + \theta)\cos(2\pi f_0 t)dt &= \int_0^T \frac{A}{2}[\cos\theta + \cos(2\pi 2 f_0 t + \theta)]dt \\ &= \frac{AT}{2}\cos\theta.\end{aligned} \tag{2.55}$$

[4] In practice, we usually have $\Delta f \gg 1/T$ and hence the two signals are approximately orthogonal

[5] The equality here is actually an approximation due to the existence of the double frequency term which we neglect. Throughout this section, all equalities involving double frequency terms should be interpreted in this way.

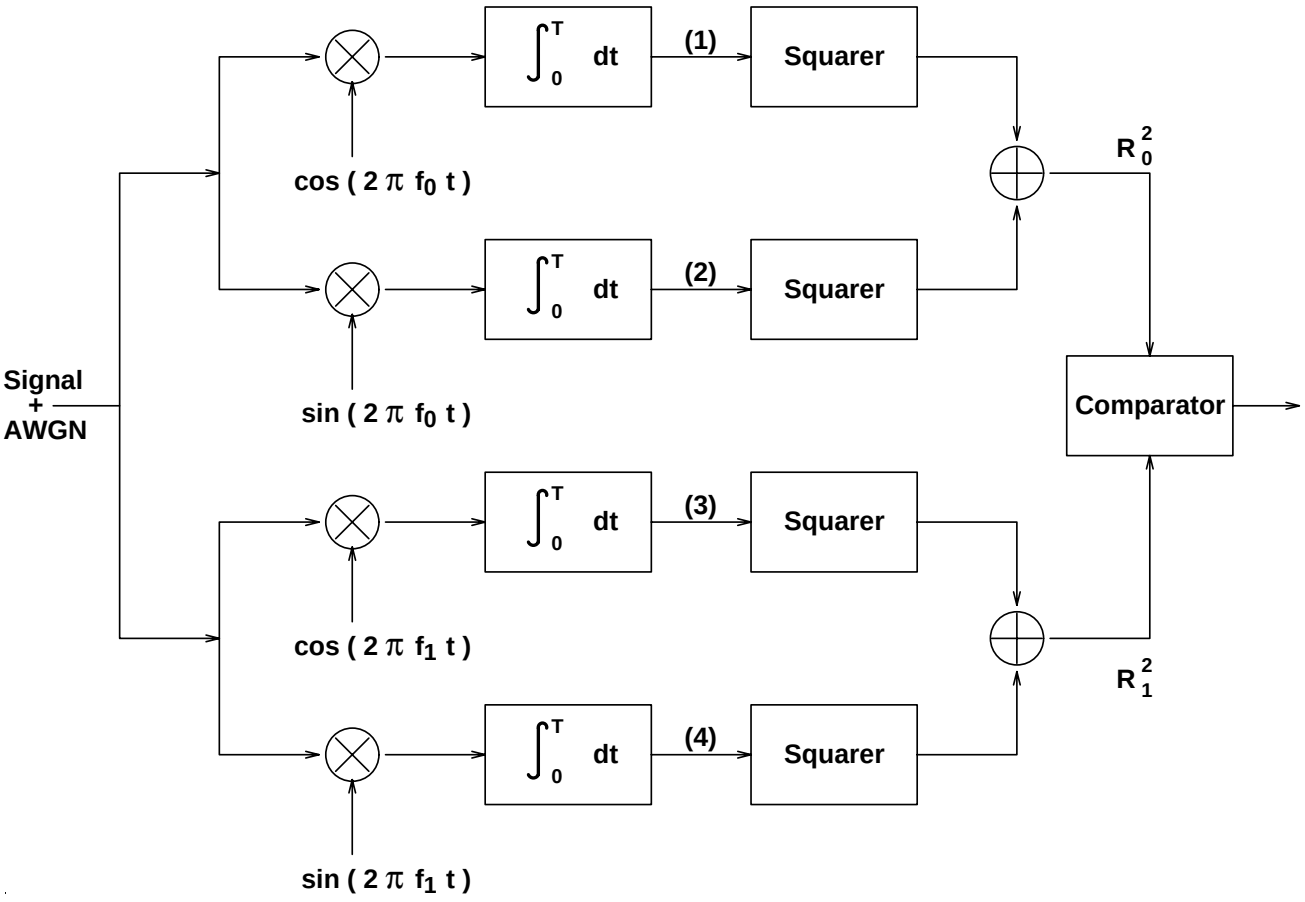

Figure 2.12: Noncoherent demodulator for binary FSK

Similarly, the signal contributions at points (2), (3) and (4) are $-\frac{AT}{2}\sin\theta$, 0, and 0 respectively. We notice that to obtain the results for points (3) and (4), the assumption $\Delta f = k/T$ is used.

Next, we look at the noise contributions due to $n(t)$. Let the noise contributions at points (1), (2), (3) and (4) be n_1, n_2, n_3, and n_4, respectively. Then n_1, n_2, n_3 and n_4 are jointly Gaussian random variables with zero means since they are all derived from the AWGN. Direct calculations show that they all have the same variance $N_0T/4$. For example,

$$\begin{aligned} \mathrm{E}[n_1^2] &= \mathrm{E}\left[\int_0^T n(t)\cos(2\pi f_0 t)dt \cdot \int_0^T n(s)\cos(2\pi f_0 s)ds\right] \\ &= \frac{N_0}{2}\int_0^T \cos^2(2\pi f_0 t)dt \\ &= \frac{N_0 T}{4}. \end{aligned} \tag{2.56}$$

Moreover, they are all uncorrelated. For example,

$$\begin{aligned} \mathrm{E}[n_1 n_2] &= \mathrm{E}\left[\int_0^T n(t)\cos(2\pi f_0 t)dt \cdot \int_0^T n(s)\sin(2\pi f_0 s)ds\right] \\ &= \frac{N_0}{2}\int_0^T \sin(2\pi f_0 t)\cos(2\pi f_0 t)dt \\ &= 0. \end{aligned} \tag{2.57}$$

Since they are also jointly Gaussian, they are independent.

The decision statistic R_1 is given by

$$R_1 = \sqrt{n_3^2 + n_4^2}. \tag{2.58}$$

Since n_3 and n_4 are independent zero-mean Gaussian random variables, R_1 is Rayleigh distributed. Its density is given by

$$f_{R_1}(r) = \begin{cases} \frac{r}{\sigma^2}\exp\left(-\frac{r^2}{2\sigma^2}\right) & \text{for} \quad r \geq 0, \\ 0 & \text{for} \quad r < 0, \end{cases} \tag{2.59}$$

where $\sigma^2 = N_0T/4$. Similarly, the statistic R_0 is given by

$$R_0 = \sqrt{\left(\frac{AT}{2}\cos\theta + n_1\right)^2 + \left(-\frac{AT}{2}\sin\theta + n_2\right)^2}. \tag{2.60}$$

For convenience, we consider the transformation

$$\begin{aligned} n_1' &= n_1\cos\theta - n_2\sin\theta, \\ n_2' &= n_1\sin\theta + n_2\cos\theta. \end{aligned} \tag{2.61}$$

Using the results in Chapter 1, we conclude that n_1' and n_2' are jointly Gaussian random variables with means equal to zero and variances equal to $N_0T/4$. It is also straightforward to check that they are uncorrelated. Hence, they are also independent. Using n_1' and n_2', R_0 can be expressed as

$$R_0 = \sqrt{\left(\frac{AT}{2} + n_1'\right)^2 + {n_2'}^2}. \tag{2.62}$$

It is the square root of the sum of the squares of two independent Gaussian random variables, one with zero mean and one with non-zero mean, with the same variance. Therefore, R_0 is Rician distributed. Its density is given by

$$f_{R_0}(r) = \begin{cases} \dfrac{r}{\sigma^2} \exp\left(-\dfrac{r^2 + \frac{A^2T^2}{4}}{2\sigma^2}\right) I_0\left(\dfrac{ATr}{2\sigma^2}\right) & \text{for} \quad r \geq 0, \\ 0 & \text{for} \quad r < 0, \end{cases} \tag{2.63}$$

where $\sigma^2 = N_0T/4$. Moreover, since n_1 and n_2 are independent of n_3 and n_4, R_0 and R_1 are independent.

Using the results above, the conditional error probability is given by

$$\begin{aligned} P_{b,0} &= \Pr(R_0 \leq R_1) \\ &= \int_0^\infty \int_{r_0}^\infty f_{R_0,R_1}(r_0, r_1) dr_1 dr_0 \\ &= \int_0^\infty f_{R_0}(r_0) \left[\int_{r_0}^\infty f_{R_1}(r_1) dr_1\right] dr_0 \\ &= \frac{1}{2} \exp\left(-\frac{A^2T^2}{16\sigma^2}\right) \\ &= \frac{1}{2} \exp\left(-\frac{E_b}{2N_0}\right), \end{aligned} \tag{2.64}$$

where the energy per bit $E_b = A^2T/2$. Similarly, if $s_1(t)$ is sent, we have

$$P_{b,1} = \frac{1}{2} \exp\left(-\frac{E_b}{2N_0}\right). \tag{2.65}$$

Therefore, the average bit error probably $P_b = P_{b,0} = P_{b,1}$. We note that the demodulator in Figure 2.12 does not use the channel phase information and the average bit error probability obtained by this noncoherent demodulator does not depend on the channel phase.

To summarize this example, we compare the result above to the average bit error probability obtained when coherent demodulation (using the matched £lter) is employed given that the channel phase

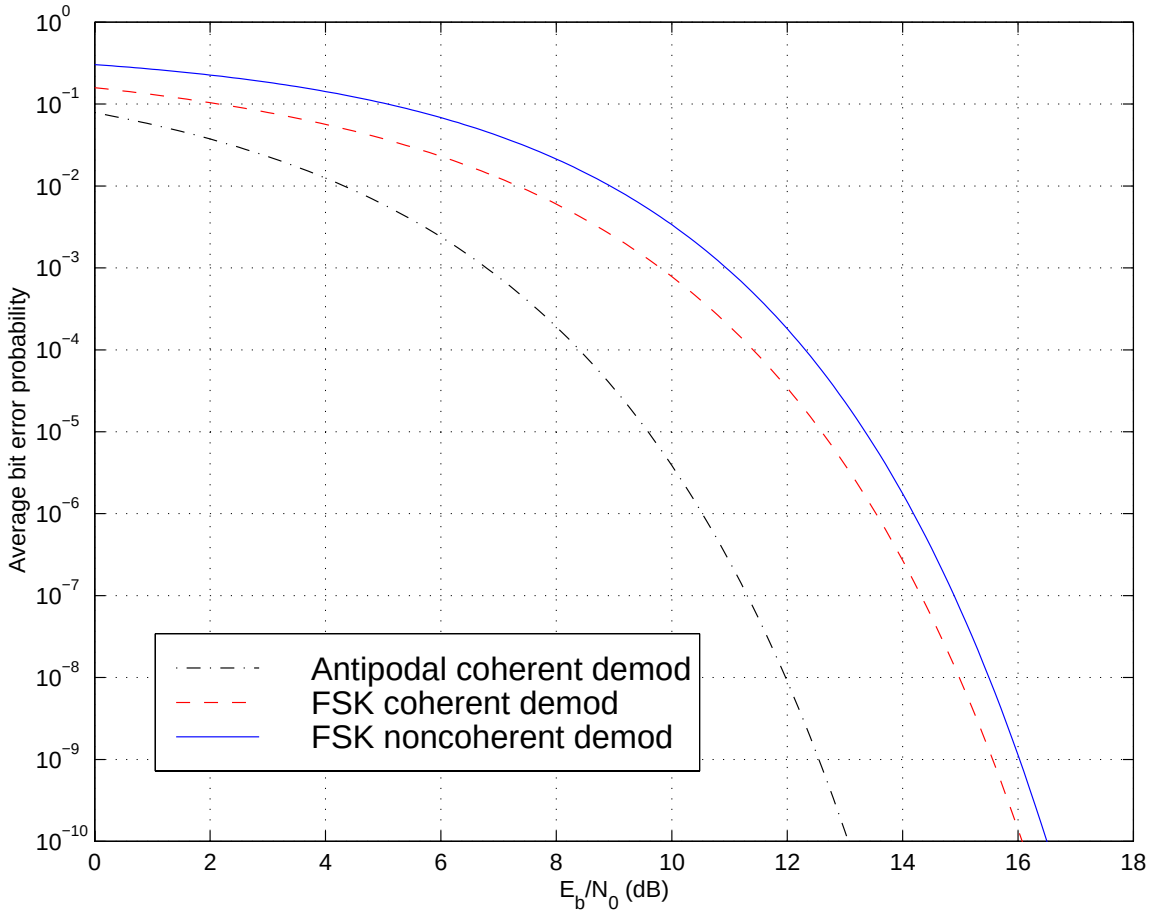

Figure 2.13: Average bit error probability for binary FSK

is known. It is easy to see that with the matched £lter, the average bit error probability is given by (2.25). The correlation coef£cient r of the two signals is 0 since they are orthogonal. Hence the average bit error probability with coherent demodulation is $Q(\sqrt{E_b/N_0})$. Figure 2.13 compares the average bit error probabilities obtained by different demodulation schemes for the binary FSK signals. From the £gure, we see that the loss from performing noncoherent demodulation on the binary FSK signals is small compared to coherent demodulation. Therefore, we would be better off to opt for noncoherent demodulation when accurate channel phase estimates are hard to obtain. However, if we employ coherent demodulation on a pair of antipodal signals[6] with the same E_b as the binary FSK signals, then we suffer a 3dB loss (when E_b/N_0 is large) by opting for noncoherent demodulation with the binary FSK signals.

[6]The demodulator in Figure 2.12 cannot be employed to demodulate antipodal signals. Why?

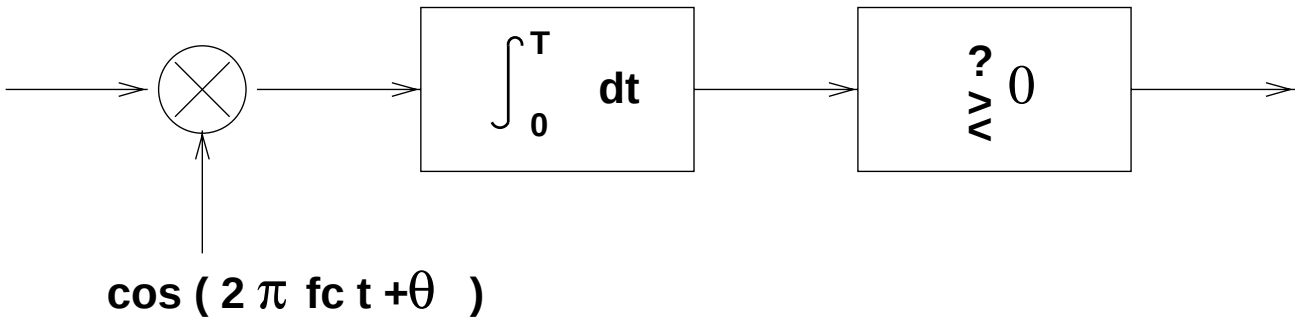

Figure 2.14: Correlation receiver for BPSK

2.2.3 Common modulation methods

Binary Phase Shift Keying (BPSK)

In BPSK, "0" and "1" are represented by

$$s_0(t) = Ap_T(t)\cos(2\pi f_c t + \theta) \tag{2.66}$$

$$s_1(t) = -Ap_T(t)\cos(2\pi f_c t + \theta). \tag{2.67}$$

Equivalently, we can write

$$s_0(t) = Ap_T(t)\cos(2\pi f_c t + \theta) \tag{2.68}$$

$$s_1(t) = Ap_T(t)\cos(2\pi f_c t + \theta + \pi). \tag{2.69}$$

In this representation, we see that the information is carried by the phase of the carrier, hence, the name *phase shift keying*. Coherent demodulation can be performed by the matched £lter or the correlation receiver in Figure 2.14. The average bit error probability (for equally probable binary signals) is

$$P_b = Q\left(\sqrt{2E_b/N_0}\right). \tag{2.70}$$

To coherently demodulate BPSK signals, we need to know the timing of the pulse and the frequency of the carrier as well as the channel phase response[7].

Differential Binary Phase Shift Keying (DBPSK)

Due to the fact that BPSK uses the phase of the carrier to carry information, the noncoherent approach described in Section 2.2.2 cannot be applied to demodulate BPSK signals. This dif£culty can partially

[7]Our convention here is to include the original phase of the carrier in the channel phase response θ.

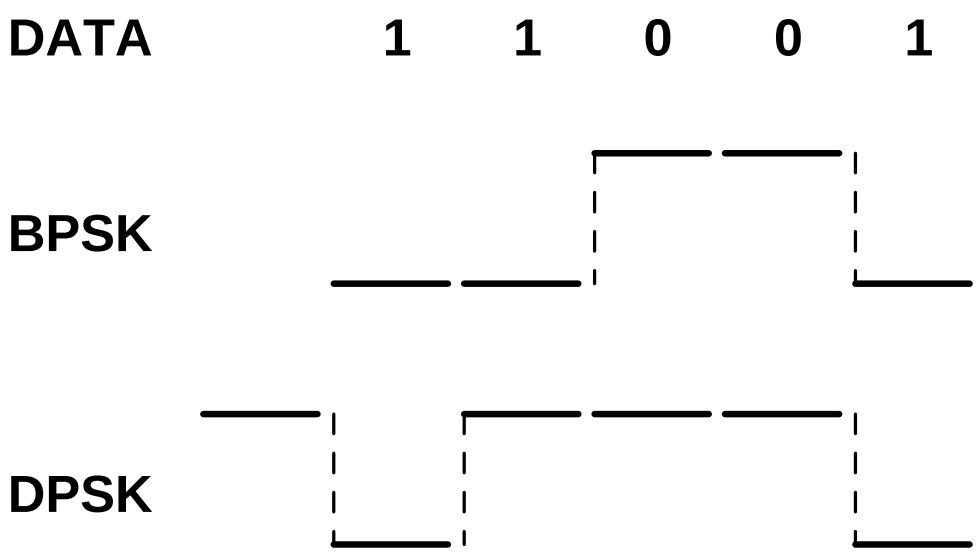

Figure 2.15: DBPSK signal

circumvented by a modi£ed version of BPSK called *differential binary phase shift keying (DBPSK)*. With DBPSK, it is possible to demodulate the received signal without knowing the absolute phase, but just relative phases.

Instead of modulating the binary data onto the phase of the carrier as in BPSK, we modulate the data onto the phase change of the carrier in DBPSK. A phase change of π across adjacent symbol intervals represents the bit value "1" while no phase change across adjacent symbol intervals represents "0". The situation is depicted in Figure 2.15. Alternatively, we can view DBPSK as a two-step process. First, the data sequence is *differentially encoded*. Then the resulting coded sequence is modulated with BPSK. Given a data sequence $\{b_j\}$ consisting of 0's and 1's, we obtain the differentially encoded sequence $\{c_j\}$ according to the following rule:

$$c_j = b_j \oplus c_{j-1} \tag{2.71}$$

where $\oplus$ represents modulo 2 addition (or the XOR operation). Consider Figure 2.15 in which we (arbitrarily) set the initial output symbol to be "0". Since the input sequence is $\{1, 1, 0, 0, 1\}$, the output sequence is $\{0, 1, 0, 0, 0, 1\}$. Modulating the coded sequence with the usual BPSK, we have the DBPSK signal.

To demodulate DBPSK signals, we notice that the value of the bit (in the time interval $[0, T)$) is

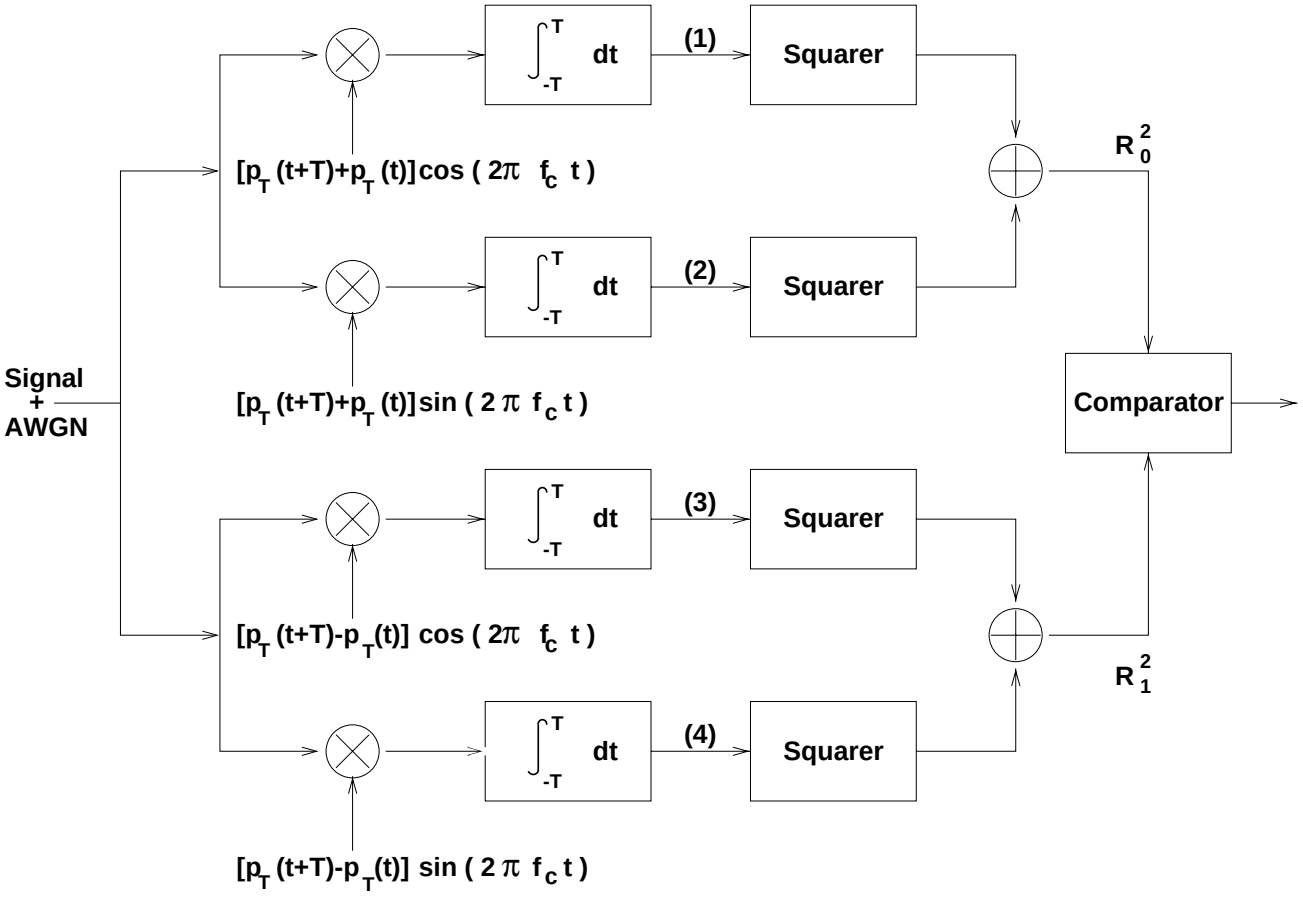

Figure 2.16: Noncoherent demodulator for DBPSK

represented by one of the following signals:

$$s_0(t) = A[p_T(t+T) + p_T(t)]\cos(2\pi f_c t + \theta + \alpha) \tag{2.72}$$

$$s_1(t) = A[p_T(t+T) - p_T(t)]\cos(2\pi f_c t + \theta + \alpha) \tag{2.73}$$

where $\alpha \in \{0, \pi\}$ depends on the values of the previous bits. Since the two signals are orthogonal, we can employ a noncoherent demodulator similar to the one in Figure 2.12 to differentiate the two signals without using the knowledge of θ and α. The demodulator for the DBPSK signal is shown in Figure 2.16. It decides that a "0" is sent if $R_0 > R_1$. Otherwise, it decides that a "1" is sent. Following a similar analysis as in Section 2.2.2, we can show that the average bit error probability for DBPSK based on this demodulator is given by

$$P_b = \frac{1}{2}\exp\left(-\frac{E_b}{N_0}\right) \tag{2.74}$$

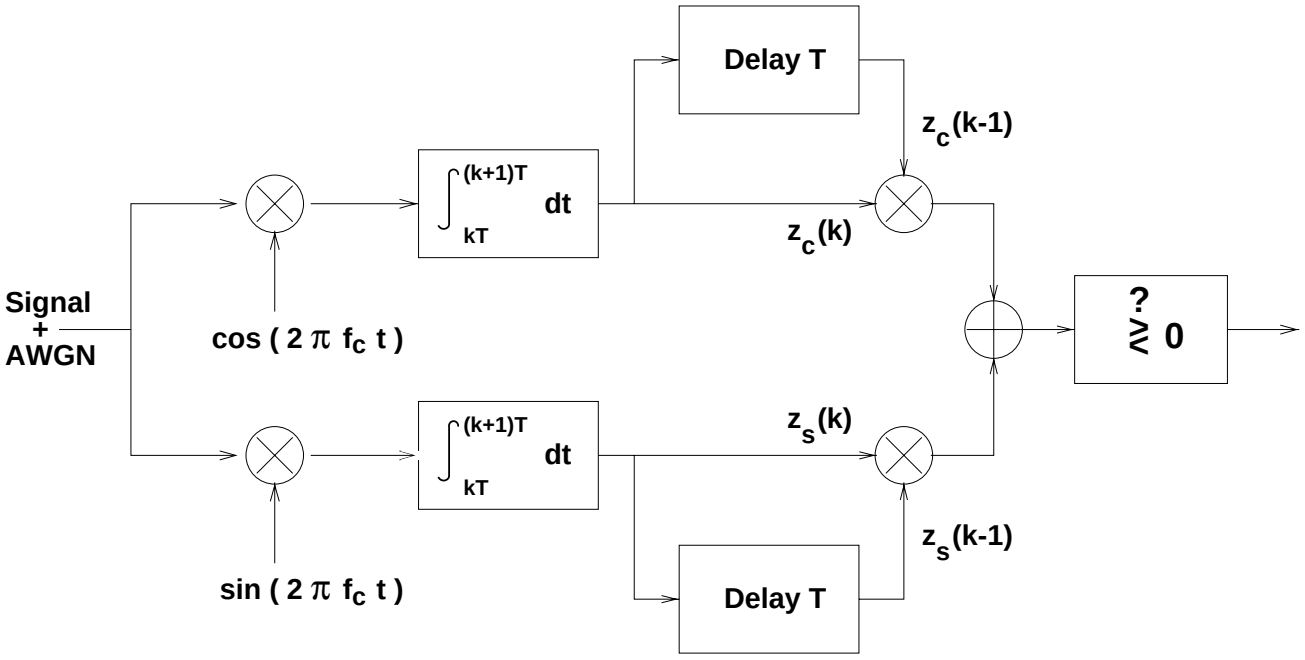

Figure 2.17: Differentially coherent demodulator for DBPSK

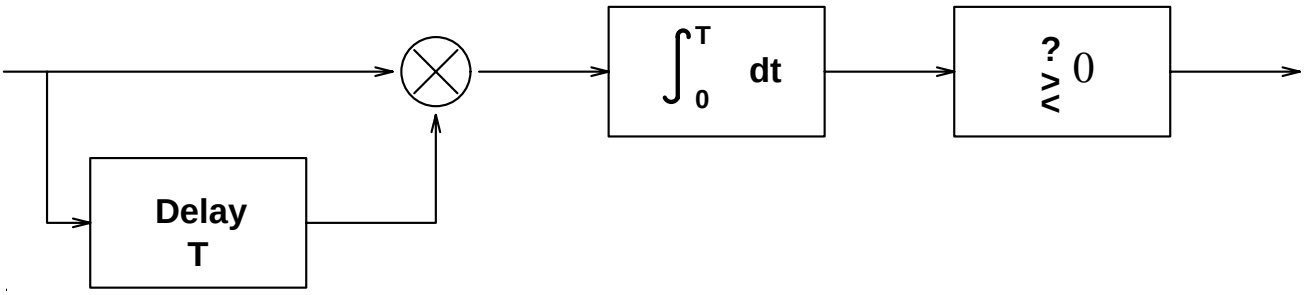

Figure 2.18: Delay-and-multiply demodulator for DBPSK

which is slightly inferior to BPSK with coherent demodulation. We note that noncoherent receiver in Figure 2.16 can also be implemented as shown in Figure 2.17. Because this equivalent implementation effectively compares the relative phases of two consecutive symbols, the noncoherent demodulation scheme for DBPSK is usually referred to as *differentially coherent demodulation*. Finally, we point out that yet another way to demodulate the DBPSK signal is to first delay and multiply the received signal as shown in Figure 2.18. However this demodulator is suboptimal, i.e., gives a higher P_b, compared to the differentially coherent demodulator in Figure 2.17.

Frequency Shift Keying (FSK)

In FSK, "0" and "1" are represented by different frequencies

$$s_0(t) = Ap_T(t)\cos\left[2\pi\left(f_c + \frac{\Delta f}{2}\right)t + \theta\right] \tag{2.75}$$

$$s_1(t) = Ap_T(t)\cos\left[2\pi\left(f_c - \frac{\Delta f}{2}\right)t + \theta\right]. \tag{2.76}$$

We notice that these signals are not antipodal.

FSK modulators can be built with two oscillators — one at frequency $f_0 = f + \frac{\Delta f}{2}$ and one at frequency $f_1 = f - \frac{\Delta f}{2}$. Alternatively, it can be built with a pulse modulator followed by an FM modulator.

Usually the frequency deviation Δf is much smaller than the carrier frequency f_c. Neglecting double frequency terms, the energies of the signals are given by $E_b = E_0 = E_1 = A^2T/2$. The correlation coef£cient r is given by

$$\begin{aligned} r &= \frac{1}{E_b}\int_0^T A^2\cos\left[2\pi\left(f_c + \frac{\Delta f}{2}\right)t + \theta\right]\cos\left[2\pi\left(f_c - \frac{\Delta f}{2}\right)t + \theta\right]dt \\ &\approx \frac{1}{T}\int_0^T \cos(2\pi\Delta f t)dt \\ &= \text{sinc}(2\pi\Delta f T). \end{aligned} \tag{2.77}$$

If Δf is chosen to be $\frac{k}{2T}$ where k is a positive integer, then $r = 0$, i.e., the signals are orthogonal. The minimum frequency deviation for orthogonality is achieved when k = 1 or $\Delta f = \frac{1}{2T}$. If, in addition, phase continuity is maintained, the resulting modulation is called *minimum shift keying (MSK)*.

Coherent demodulation can be achieved by the matched £lter or the correlation receiver. The average bit error probability is

$$P_b = Q\left(\sqrt{\frac{E_b}{N_0}(1-r)}\right). \tag{2.78}$$

However, FSK signals are often demodulated with the noncoherent demodulation approach described in Section 2.2.2. Beside the implementation shown in Figure 2.12, other implementations are possible as shown in Figures 2.19 and 2.20. For orthogonal signals ($r = 0$), the average bit error probability achieved by noncoherent demodulation is given by

$$P_b = \frac{1}{2}\exp\left(-\frac{E_b}{2N_0}\right) \tag{2.79}$$

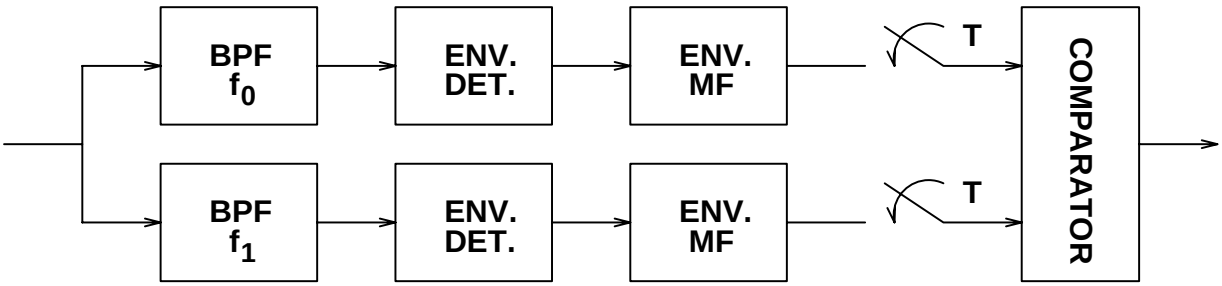

Figure 2.19: Alternative nonocoherent demodulator for FSK

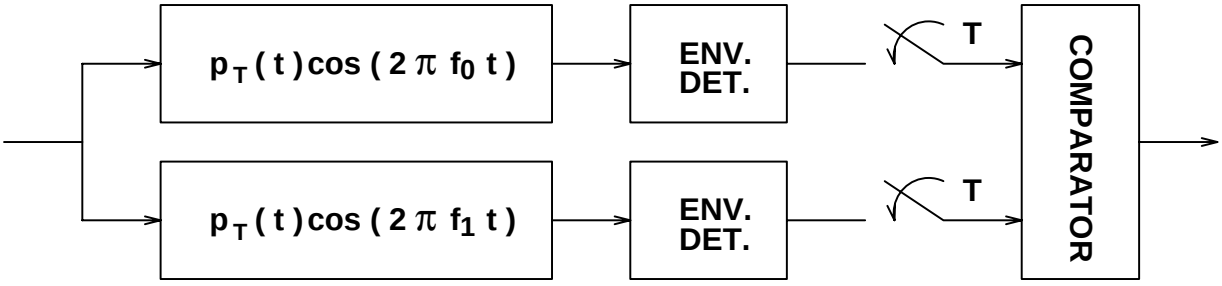

Figure 2.20: Alternative nonocoherent demodulator for FSK

and is slightly inferior to coherent demodulation. A comparison of the probabilities of error for BPSK, DBPSK, and FSK is given in Figure 2.21.

Quadrature Phase Shift Keying (QPSK)

Just as we can perform quadrature carrier multiplexing in analog communications, we can also perform quadrature carrier multiplexing in digital communications. Consider the following situation, we modulate the BPSK signal with $\sin(2\pi f_c t)$ instead of $\cos(2\pi f_c t)$.

$$s_0(t) = Ap_T(t)\sin(2\pi f_c t + \theta) \tag{2.80}$$

$$s_1(t) = -Ap_T(t)\sin(2\pi f_c t + \theta) \tag{2.81}$$

If it is passed through the correlation receiver in Figure 2.14 (or the equivalent matched £lter), the output due to the signal is given by

$$\begin{aligned} \pm\int_0^T A\sin(2\pi f_c t + \theta)\cos(2\pi f_c t + \theta)dt &= \pm\frac{A}{2}\int_0^T \sin(2\pi 2 f_c t + 2\theta)dt \\ &\approx 0. \end{aligned} \tag{2.82}$$

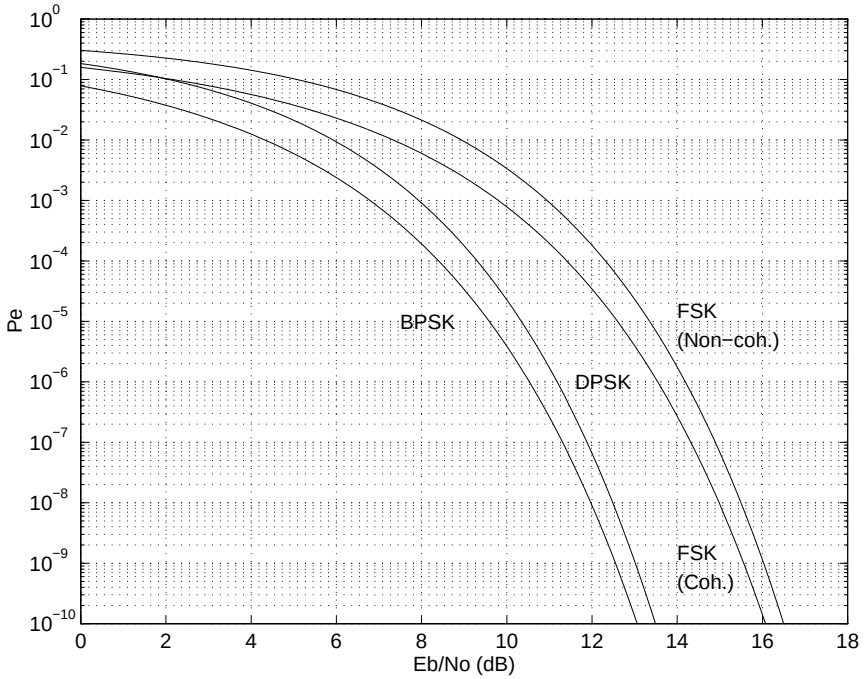

Figure 2.21: P_b for BPSK, DBPSK, and FSK

Of course, we would have normal detection if the received signal is multiplied by $\sin(2\pi f_c t+\theta)$ instead of $\cos(2\pi f_c t + \theta)$ in Figure 2.14. Hence, we see that it is possible to separate the sine carrier and the cosine carrier, and, therefore, to transmit information simultaneously through them. The cosine carrier is often called the *in-phase* channel, and the sine carrier is often called the *quadrature* channel.

In QPSK, both the in-phase and the quadrature channels are used. Each channel carries a BSPK component. The transmitted signal is of the form

$$s(t) = Ab_I p_T(t)\cos(2\pi f_c t + \theta) - Ab_Q p_T(t)\sin(2\pi f_c t + \theta) \tag{2.83}$$

where b_I and b_Q are the information bits on the in-phase and the quadrature channel respectively. Each of them can be $+1$ or -1 according to the information to be sent. The transmitted signal can also be expressed as

$$s(t) = \sqrt{2}Ap_T(t)\cos\left(2\pi f_c t + \theta + \tan^{-1}\frac{b_Q}{b_I}\right). \tag{2.84}$$

This representation clearly shows that QPSK is a kind of phase shift keying. (More precisely, $\tan^{-1}\frac{b_Q}{b_I}$ here should be written as $\tan^{-1}(b_Q, b_I)$ and interpreted as a double argument function.)

Coherent demodulation can be performed on the two channels separately using the receiver in

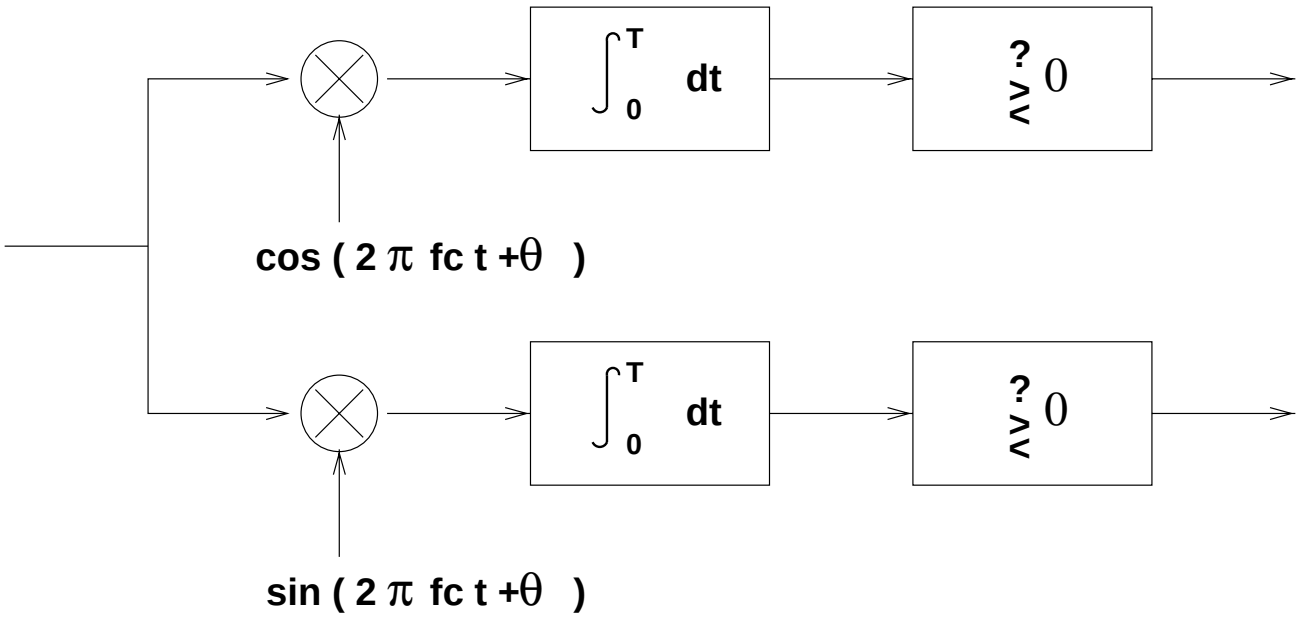

Figure 2.22: Receiver for QPSK

Figure 2.22. The probability of *bit* error remains the same as BPSK if the energy per bit E_b and the noise power spectral density N_0 are the same.

Next, let us consider the transmission of a sequence of symbols in QPSK format

$$\begin{aligned} s(t) &= A\left[\sum_n b_{I,n}p_T(t-nT)\right]\cos(2\pi f_c t+\theta) - A\left[\sum_n b_{Q,n}p_T(t-nT)\right]\sin(2\pi f_c t+\theta) \\ &= \sqrt{2}A\sum_n p_T(t-nT)\cos\left(2\pi f_c t+\theta+\tan^{-1}\frac{b_{Q,n}}{b_{I,n}}\right). \end{aligned} \tag{2.85}$$

A typical QPSK signal is shown in Figure 2.23. We notice that a phase change may occur during the transition from one symbol interval to another. If both the in-phase bit and the quadrature bit change, the phase change is π. This large phase change is undesirable when the signal goes through non-linear filtering.

A variation of QPSK that performs better under non-linear filtering is called the *offset QPSK (OQPSK)*. In OQPSK, the transmitted signal is

$$s(t) = A\left[\sum_n b_{I,n}p_T\left(t-\frac{T}{2}-nT\right)\right]\cos(2\pi f_c t+\theta) - A\left[\sum_n b_{Q,n}p_T(t-nT)\right]\sin(2\pi f_c t+\theta). \tag{2.86}$$

The information stream on the in-phase channel is delayed by a half symbol interval as shown in

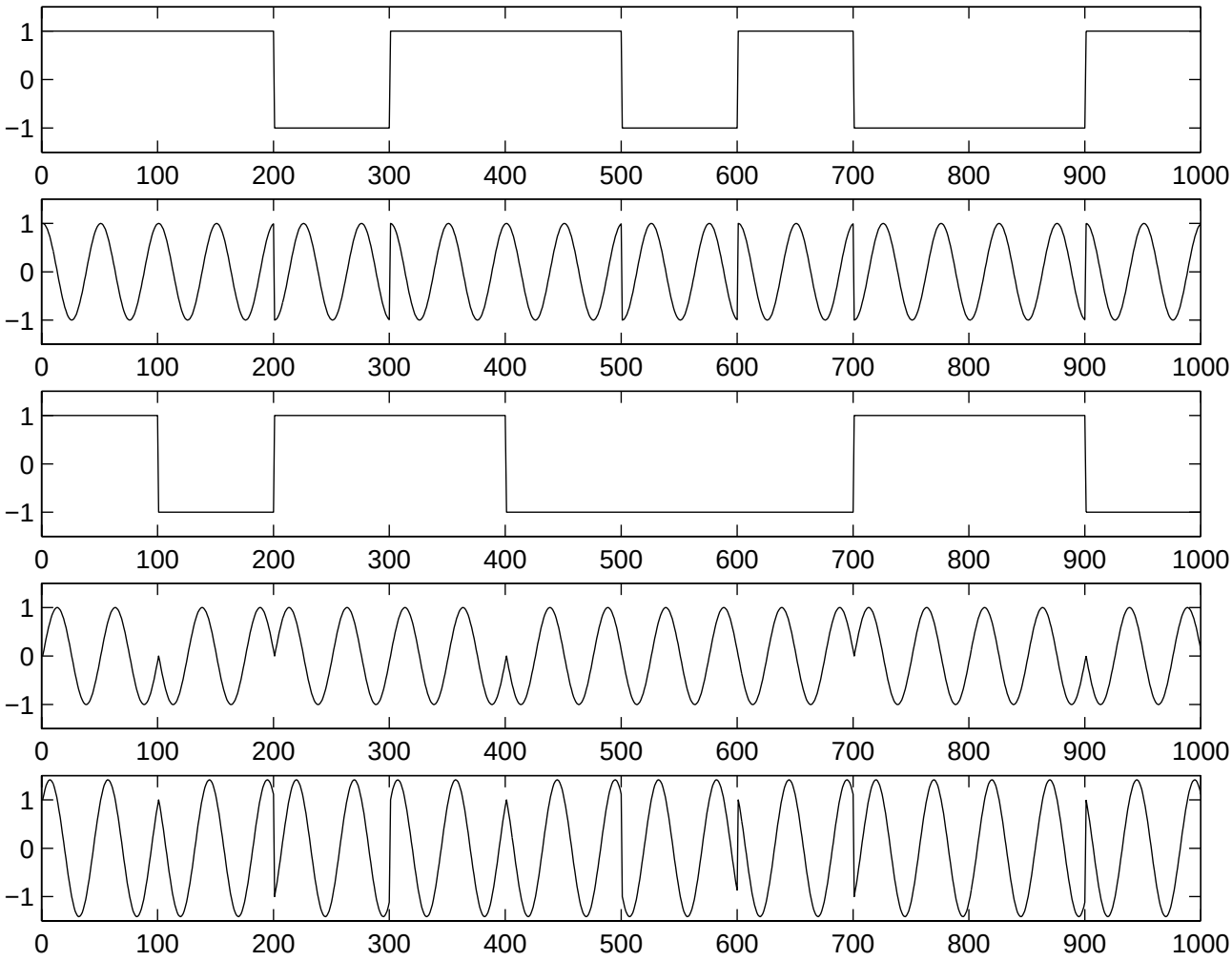

Figure 2.23: Typical QPSK signal

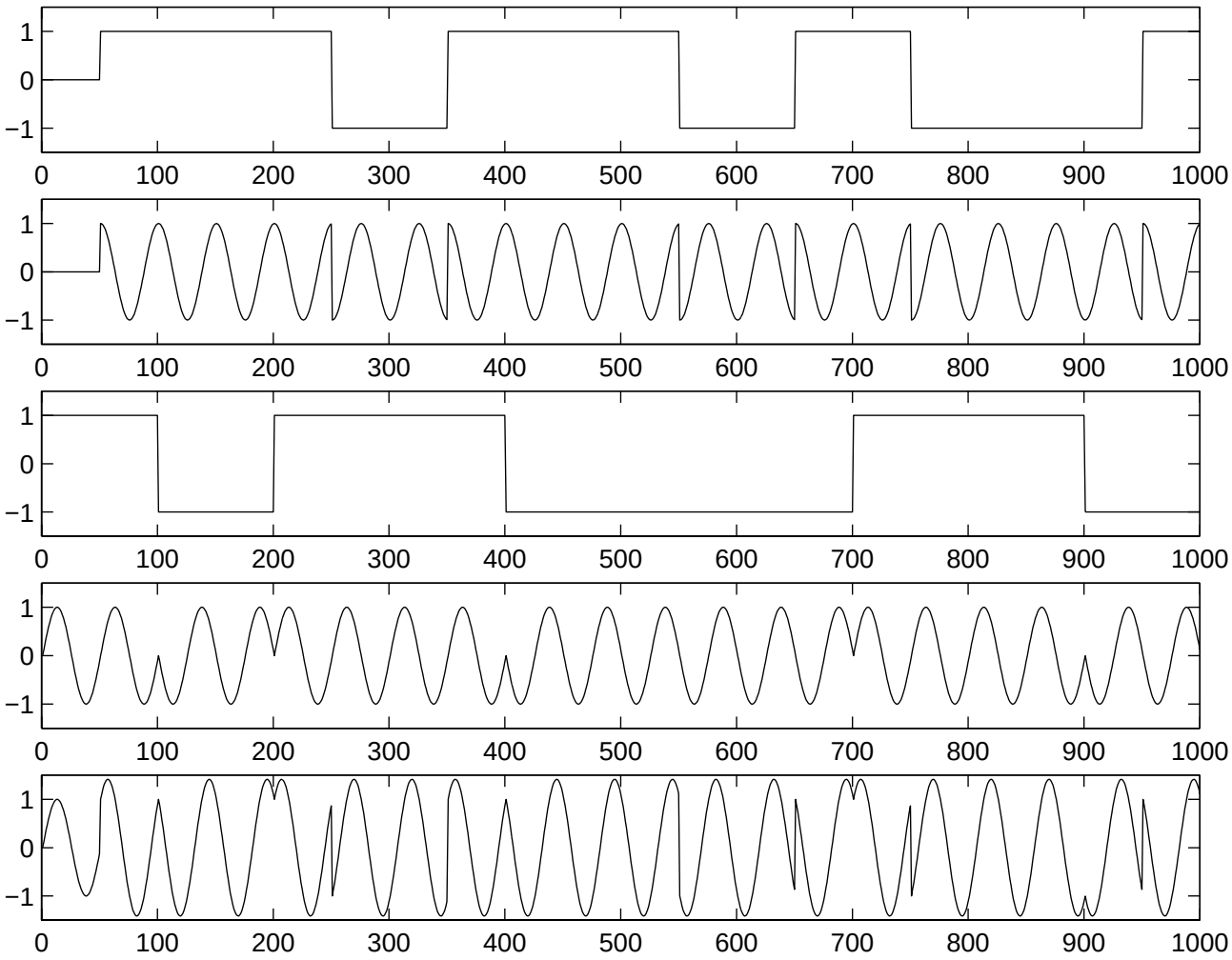

Figure 2.24: Typical OQPSK signal

Figure 2.24. W note that at time instants nT, only the quadrature bit may change while at time instants $nT + T/2$, only the in-phase bit may change. Therefore, at any time, the maximum phase change is $\pi/2$.

A further variation is by modifying the pulse shape of OQPSK. If we use the half-sine pulse $\sin(\pi t/T)p_T(t)$, i.e., the transmitted signal is of the form

$$\begin{aligned} s(t) &= A\left[\sum_n b_{I,n}\sin\left(\frac{\pi(t-T/2-nT)}{T}\right)p_T\left(t-\frac{T}{2}-nT\right)\right]\cos(2\pi f_c t+\theta) \\ &\quad -A\left[\sum_n b_{Q,n}\sin\left(\frac{\pi(t-nT)}{T}\right)p_T(t-nT)\right]\sin(2\pi f_c t+\theta), \end{aligned} \tag{2.87}$$

then it turns out that we have an MSK signal. Phase continuity is maintained during symbol transitions

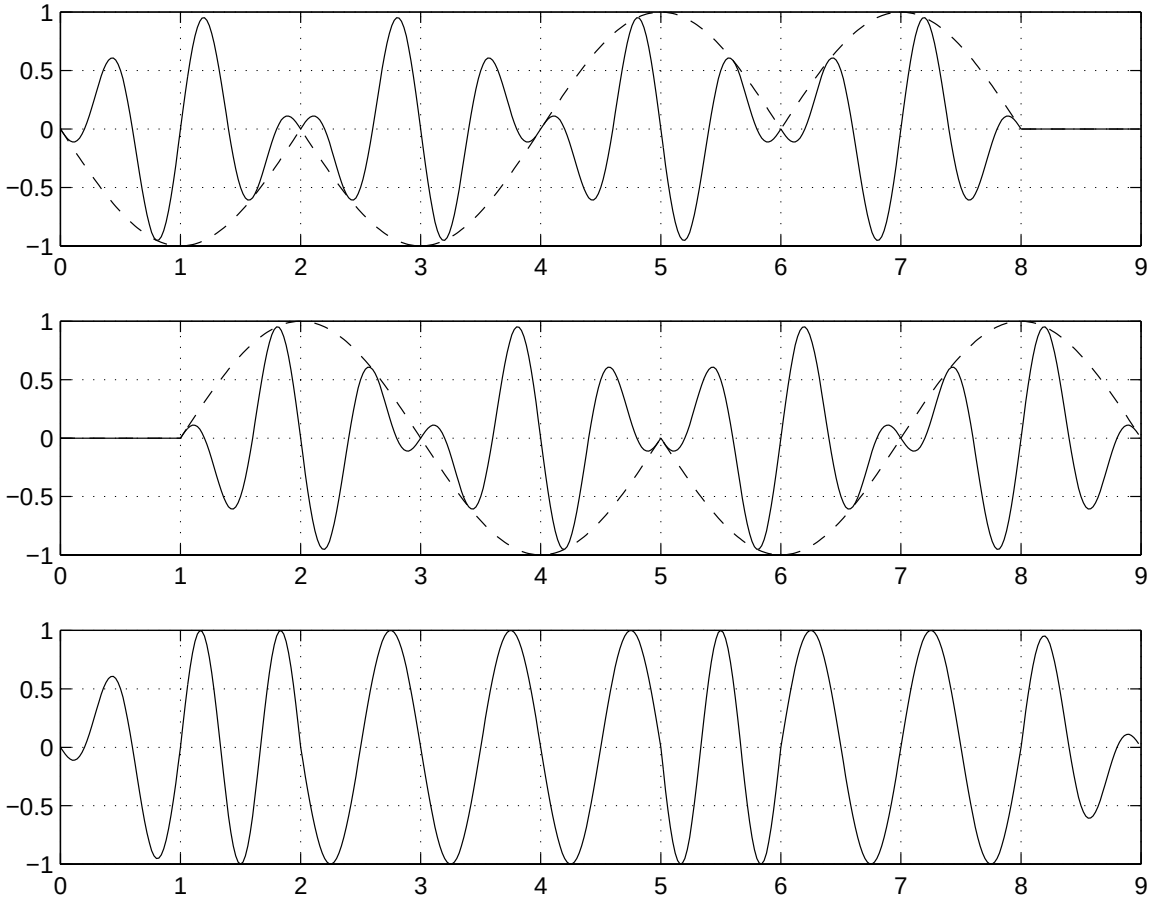

Figure 2.25: Typical MSK signal

for an MSK signal as shown in Figure 2.25. We notice that the encoding rules of the information bits in the two different representations of MSK we have so far are different. Actually, MSK can also be represented in yet another way as a special case of *continuous phase modulation (CPM)*.

2.2.4 Signal Bandwidths

Besides the average symbol error probability, another important consideration in the design of a digital communication system is the bandwidth requirement. Before we can discuss the bandwidth requirement, we need to characterize the bandwidth of a system. This is usually done by considering the power spectral density of the transmitted signal.

Consider the transmission of a data stream at the baseband. The baseband transmitted signal is of

the form

$$v(t) = \sum_{n=-\infty}^{\infty} b_n \psi(t - T_d - nT) \tag{2.88}$$

where b_n's are the information symbols, $\psi(\cdot)$ is the pulse waveform, T_d is the delay and T is the length of a symbol interval. We assume that b_n's are uncorrelated random variables with zero mean and unit variance. We also assume that the delay T_d is a random variable uniformly distributed on $[0, T)$ and independent of b_n's. Hence, the transmitted signal is modeled as a random process and its autocorrelation function $R_v(t+\tau, t)$ is given by

$$\begin{aligned}
R_v(t+\tau, t) &= \mathrm{E}[v(t+\tau)v(t)] \\
&= \mathrm{E}\left[\sum_{n=-\infty}^{\infty} b_n \psi(t+\tau-T_d-nT) \sum_{m=-\infty}^{\infty} b_m \psi(t-T_d-mT)\right] \\
&= \sum_{n=-\infty}^{\infty}\sum_{m=-\infty}^{\infty} \mathrm{E}[b_n b_m]\mathrm{E}[\psi(t+\tau-T_d-nT)\psi(t-T_d-mT)] \\
&= \sum_{n=-\infty}^{\infty} \mathrm{E}[\psi(t+\tau-T_d-nT)\psi(t-T_d-nT)] \\
&= \sum_{n=-\infty}^{\infty} \frac{1}{T}\int_0^T \psi(t+\tau-u-nT)\psi(t-u-nT)du \\
&= \sum_{n=-\infty}^{\infty} \frac{1}{T}\int_{nT}^{(n+1)T} \psi(t+\tau-u)\psi(t-u)du \\
&= \frac{1}{T}\int_{-\infty}^{\infty} \psi(t+\tau-u)\psi(t-u)du \\
&= \frac{1}{T}\int_{-\infty}^{\infty} \psi(w)\psi(w-\tau)dw \\
&= \frac{1}{T}\psi * \tilde{\psi}(\tau).
\end{aligned} \tag{2.89}$$

Therefore, the random process $v(t)$ is WSS (we can write $R_v(\tau)$) and its power spectral density (PSD) is given by

$$\Phi_v(f) = \frac{1}{T}|\Psi(f)|^2, \tag{2.90}$$

where $\Psi(f)$ is the Fourier transform of the pulse waveform $\psi(t)$. For example, if $\psi(t) = p_T(t)$, then

$$\Phi_v(f) = T\mathrm{sinc}^2(\pi f T). \tag{2.91}$$

When the data signal is modulated onto a (RF) carrier, the transmitted signal is of the form

$$s(t) = \sqrt{2}v(t)\cos(2\pi f_c t + \theta) \tag{2.92}$$

where θ is a phase shift. We assume that θ is a random variable uniformly distributed on $[0, 2\pi)$, and independent of other random variables. The autocorrelation function $R_s(t+\tau, t)$ is given by

$$\begin{aligned} R_s(t+\tau,t) &= \mathrm{E}[s(t+\tau)s(t)] \\ &= \mathrm{E}\left[2v(t+\tau)\cos(2\pi f_c(t+\tau)+\theta)v(t)\cos(2\pi f_c t+\theta)\right] \\ &= R_v(\tau)\mathrm{E}\left[\cos(2\pi 2 f_c t + 2\pi f_c \tau + 2\theta) + \cos(2\pi f_c \tau)\right] \\ &= R_v(\tau)\cos(2\pi f_c \tau). \end{aligned} \tag{2.93}$$

Again $s(t)$ is WSS and its PSD is given by

$$\Phi_s(f) = \frac{1}{2}\left[\Phi_v(f-f_c) + \Phi_v(f+f_c)\right]. \tag{2.94}$$

we notice that it is just a translation of the baseband spectrum to the carrier frequency. Hence, we can determine the spectral properties by just considering the baseband spectrum.

When two data signals are modulated onto the in-phase and the quadrature carriers, the (RF) transmitted signal is of the form

$$s(t) = \sqrt{2}v_I(t)\cos(2\pi f_c t + \theta) + \sqrt{2}v_Q(t)\sin(2\pi f_c t + \theta) \tag{2.95}$$

where $v_I(t)$ and $v_Q(t)$ are of the form of $v(t)$ as before (although it is allowed that one of them is offset by a half symbol interval). We assume that the data symbols in $v_I(t)$ and $v_Q(t)$ are uncorrelated. Then

$$\mathrm{E}[v_I(t+\tau)v_Q(t)] = \mathrm{E}[v_Q(t+\tau)v_I(t)] = 0. \tag{2.96}$$

It is then straightforward to show that $s(t)$ is WSS with autocorrelation function

$$R_s(\tau) = [R_{v_I}(\tau) + R_{v_Q}(\tau)]\cos(2\pi f_c \tau). \tag{2.97}$$

Therefore, the PSD is

$$\Phi_s(f) = \frac{1}{2}\left[\Phi_{v_I}(f-f_c) + \Phi_{v_Q}(f-f_c) + \Phi_{v_I}(f+f_c) + \Phi_{v_Q}(f+f_c)\right]. \tag{2.98}$$

It is the sum of the PSD's of the signals on the two channels.

Now, let us look at the PSD's of the modulation formats discussed in Section 2.2.3. For BPSK, the waveform $\psi(t)$ is the rectangular pulse $p_T(t)$. Therefore, the PSD is given by

$$\Phi_s(f) = \frac{T}{2}\left\{\text{sinc}^2[\pi(f-f_c)T] + \text{sinc}^2[\pi(f+f_c)T]\right\}. \tag{2.99}$$

For QPSK or OQPSK, again the waveform $\psi(t)$ is the rectangular pulse $p_T(t)$. Therefore the PSD is the sum of two BPSK spectra. However, the important point is that it does not occupy a wider spectrum. Therefore, it is possible to transmit data at twice the rate of BPSK, with the same bandwidth, using QPSK or OQPSK. For comparison purpose, it is often convenient to express the PSD in terms of the *average bit interval* T_b. For BPSK, $T_b = T$. For QPSK or OQPSK, $T_b = T/2$. For MSK, the waveform $\psi(t)$ is the half-sine pulse $\sin(\pi t/T)p_T(t)$. Therefore, the corresponding baseband PSD is

$$\Phi_s(f) = \frac{4T}{\pi^2}\left\{\left[\frac{\cos\pi(f-f_c)T}{1-4(f-f_c)^2T^2}\right]^2 + \left[\frac{\cos\pi(f+f_c)T}{1-4(f+f_c)^2T^2}\right]^2\right\}. \tag{2.100}$$

We note that while the spectra for BPSK, QPSK and OQPSK decay roughly as $1/f^2$, the spectrum for MSK decays roughly as $1/f^4$. This is one of the desirable properties of MSK. A comparison of the PSD's of QPSK and MSK is shown in Figure 2.26.

Given the PSD of the transmitted signal, there are many different ways we can de£ne bandwidth. All of them are based on some properties of the PSD. Depending on the property of interest and the practical situation, we select one of the de£nitions to characterize the bandwidth requirement of the system.

Null-to-null bandwidth

It is de£ned by the width of the main lobe of the PSD, and is obtained by solving for the zeros of the PSD.

For BPSK with bit interval of T_b, the £rst zeros occur at $\pm 1/T_b$. Therefore, the null-to-null bandwidth is $2/T_b$, i.e., twice the bit rate. For QPSK, the £rst zeros of the PSD occurs at $\pm 0.5/T_b$. Therefore, the null-to-null bandwidth for QPSK is $1/T_b$, i.e., the bit rate. For MSK, the £rst zeros of the PSD occur at $\pm 0.75/T_b$. Therefore, the null-to-null bandwidth for MSK is $1.5/T_b$, i.e., 1.5 $\times$ the bit rate.

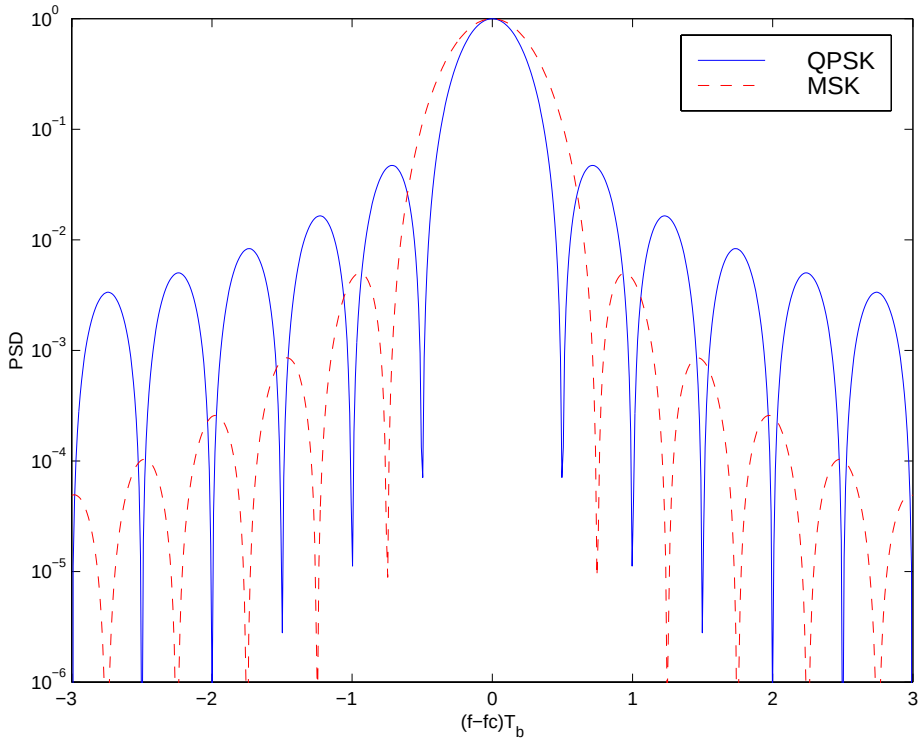

Figure 2.26: PSD's of QPSK and MSK

Half-power bandwidth

It is the interval between frequencies at which the PSD drops to half power, or 3dB below the peak value.

The half-power bandwidth for BPSK, QPSK and MSK are $0.88/T_b$, $0.44/T_b$ and $0.59/T_b$, respectively.

Noise equivalent bandwidth

It is the bandwidth of an ideal bandpass signal having the same power. More precisely, the noise equivalent bandwidth is given by

$$B_n = \frac{1}{\Phi_{s,max}} \int_0^\infty \Phi_s(f) df \tag{2.101}$$

where $\Phi_{s,max} = \max_f \Phi_s(f)$.

The noise equivalent bandwidth for BPSK, QPSK and MSK are $1.0/T_b$, $0.5/T_b$ and $0.62/T_b$, respectively.

35dB bandwidth

It is the width of the frequency band outside which the PSD has fallen 35dB below the value at the band center.

The 35dB bandwidth for BPSK, QPSK and MSK are $35.12/T_b$, $17.56/T_b$ and $3.24/T_b$, respectively.

99% power containment bandwidth

It is the width of the frequency band that contains 99% of the power of the signal.

The 99% power containment bandwidth for BPSK, QPSK and MSK are $20.56/T_b$, $10.28/T_b$ and $1.18/T_b$, respectively.

2.3 Representations of Communication Signals

In Section 2.2.1, we make use of the similarity between RF and baseband communications to develop the coherent demodulator for a binary RF communication system. It turns out that we can reduce most RF design problems into their baseband counterparts if we choose the right way to represent RF signals. With such an uni£ed approach, we only need to consider a particular problem once in the baseband (independent of the carrier frequency). The RF solutions can be obtained by translating the baseband results to the carrier frequency. The signal representation allows us to employ such an approach is the *complex baseband (complex envelope) representation*. Another common way to represent communication signals is the *signal space representation* which provides a geometric representation for a set of continuous-time signals. It turns out that this geometric viewpoint greatly facilitates the understanding and analysis of many (non-binary) modulation schemes. We study these two useful representations in this section.

2.3.1 Hilbert Transform

The *Hilbert transform* of a function $s(t)$ is de£ned by

$$\hat{s}(t) = s(t) * \frac{1}{\pi t} = \frac{1}{\pi} \int_{-\infty}^{\infty} \frac{s(\tau)}{t-\tau} d\tau. \tag{2.102}$$

We note that the Hilbert transform is a continuous-time £lter (or system). Taking Fourier transform, we have

$$\hat{S}(f) = -\text{jsgn}(f)S(f). \tag{2.103}$$

Therefore, the result of the Hilbert transform is to increase the phase of the negative frequencies by $\pi/2$ and to decrease the phase of the positive frequencies by $\pi/2$. For example, the Hilbert transform of $\cos(2\pi f_c t)$ is $\sin(2\pi f_c t)$. Obviously, the inverse Hilbert transform in frequency domain is given by

$$S(f) = \text{jsgn}(f)\hat{S}(f). \tag{2.104}$$

In time domain, we have

$$s(t) = \hat{s}(t) * \frac{-1}{\pi t} = -\frac{1}{\pi}\int_{-\infty}^{\infty} \frac{\hat{s}(\tau)}{t-\tau} d\tau. \tag{2.105}$$

Hence, we obtain the following two properties of the Hilbert transform:

1. $|S(f)| = |\hat{S}(f)|$,
2. $\hat{\hat{s}}(t) = -s(t)$.

2.3.2 Representations of Bandpass Deterministic Signals

A (real) signal $s(t)$ is called *bandpass* or *narrowband* if its frequency content concentrates around f_c. More precisely, $s(t)$ is bandpass if its Fourier transform satis£es

$$S(f) = 0 \qquad \text{for } |f| \le f_c - W \text{ and } f_c + W \le |f|, \tag{2.106}$$

where $W \le f_c$. Recall the Fourier transform property that for any signal $s(t)$ (real or complex),

$$s^*(t) \quad \longleftrightarrow \quad S^*(-f). \tag{2.107}$$

The signal $s(t)$ is real if and only if

$$s(t) = s^*(t), \tag{2.108}$$

if and only if

$$S(f) = S^*(-f). \tag{2.109}$$

Therefore, the Fourier transform on positive frequencies of a real bandpass signal completely speci£es the signal itself. This result is depicted in Figure 2.27.

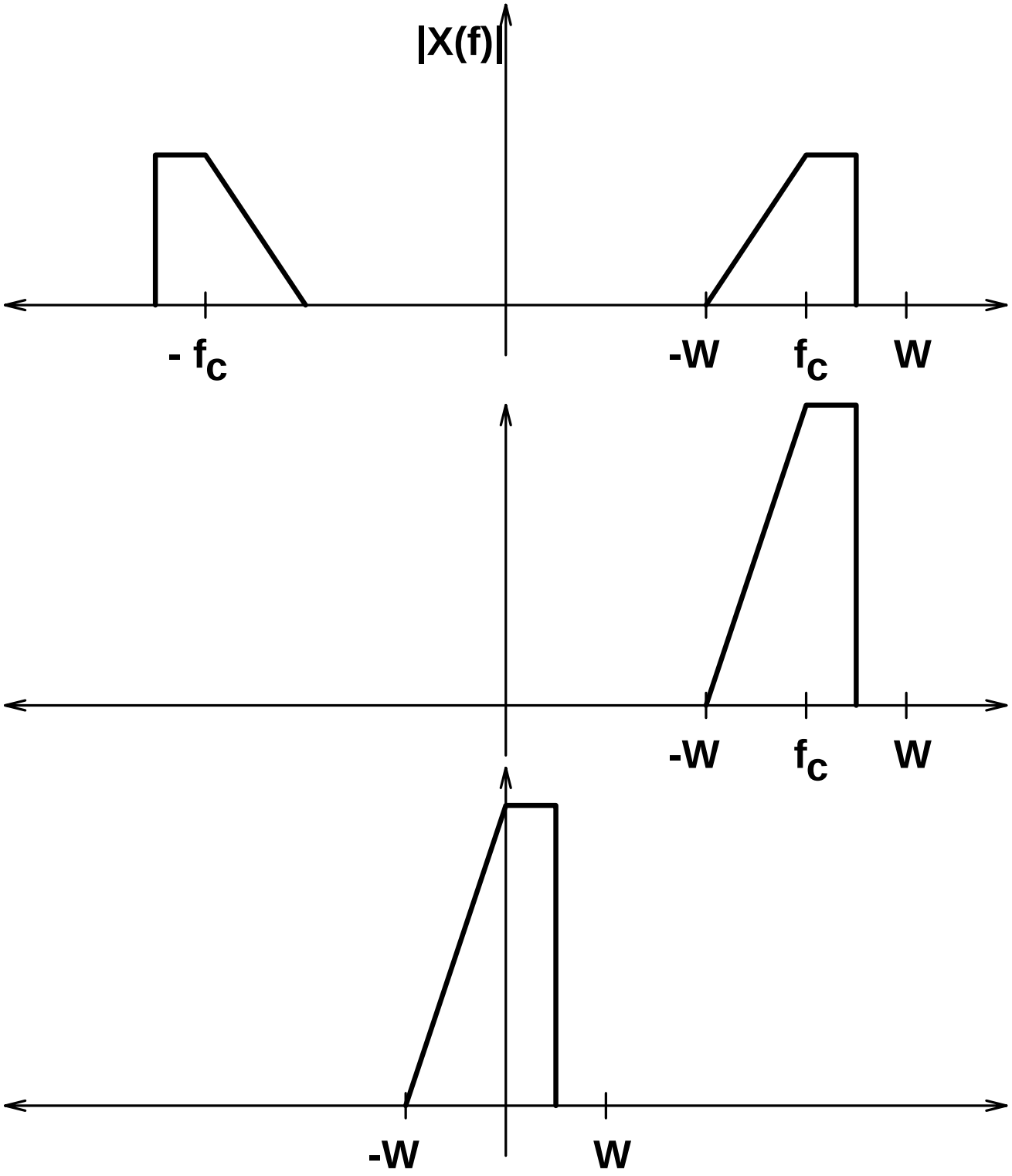

Figure 2.27: Fourier transforms of a bandpass signal, its complex analytic representation, and its complex envelope

Complex analytic representation

Since the bandpass signal $s(t)$ is real, it is unique determined by $S(f)$ for $f > 0$. We de£ne $S_+(f)$ by

$$\begin{aligned} S_+(f) &= \begin{cases} 2S(f) & \text{for} \quad f > 0, \\ 0 & \text{for} \quad f \leq 0, \end{cases} \\ &= S(f) + \mathrm{j}\hat{S}(f). \end{aligned} \tag{2.110}$$

The corresponding time domain signal $s_+(t)$ is the *complex analytic representation* of $s(t)$. Taking inverse Fourier transform of (2.110), we have

$$s_+(t) = s(t) + \mathrm{j}\hat{s}(t). \tag{2.111}$$

Conversely,

$$s(t) = \mathrm{Re}[s_+(t)], \tag{2.112}$$

and

$$S(f) = \frac{1}{2}\left[S_+(f) + S_+^*(-f)\right]. \tag{2.113}$$

Complex baseband representation

If the carrier frequency f_c is known, one can translate $s_+(t)$ to baseband to obtain the *complex baseband representation* or *complex envelope* de£ned by

$$\tilde{s}(t) = s_+(t)e^{-\mathrm{j}2\pi f_c t}. \tag{2.114}$$

Taking Fourier transform, we have

$$\tilde{S}(f) = S_+(f + f_c). \tag{2.115}$$

Notice that the complex envelope $\tilde{s}(t)$ is bandlimited to W, i.e., $\tilde{S}(f) = 0$ for $|f| > W$. Conversely,

$$s_+(t) = \tilde{s}(t)e^{\mathrm{j}2\pi f_c t}, \tag{2.116}$$

and

$$S_+(f) = \tilde{S}(f - f_c). \tag{2.117}$$

To get back $s(t)$ and $S(f)$, one can use

$$s(t) = \mathrm{Re}\left[\tilde{s}(t)e^{\mathrm{j}2\pi f_c t}\right] \tag{2.118}$$

and

$$S(f) = \frac{1}{2}\left[\tilde{S}(f - f_c) + \tilde{S}^*(-f - f_c)\right]. \tag{2.119}$$

Bandpass representation

Let $s_I(t)$ and $s_Q(t)$ be the real and the imaginary parts of $\tilde{s}(t)$, i.e.,

$$\tilde{s}(t) = s_I(t) + \mathrm{j}s_Q(t). \tag{2.120}$$

Then

$$s(t) = s_I(t)\cos(2\pi f_c t) - s_Q(t)\sin(2\pi f_c t), \tag{2.121}$$

and, in frequency domain,

$$S(f) = \frac{1}{2}\left[S_I(f - f_c) + S_I(f + f_c)\right] + \frac{\mathrm{j}}{2}\left[S_Q(f - f_c) - S_Q(f + f_c)\right]. \tag{2.122}$$

This is the *bandpass representation* of $s(t)$. Notice that

$$s_I(t) = \frac{1}{2}\left[\tilde{s}(t) + \tilde{s}^*(t)\right], \tag{2.123}$$

and, hence,

$$S_I(f) = \frac{1}{2}\left[\tilde{S}(f) + \tilde{S}^*(-f)\right]. \tag{2.124}$$

Therefore, $s_I(t)$ is also bandlimited to W. Similarly,

$$s_Q(t) = \frac{1}{2\mathrm{j}}\left[\tilde{s}(t) - \tilde{s}^*(t)\right], \tag{2.125}$$

and

$$S_Q(f) = \frac{1}{2\mathrm{j}}\left[\tilde{S}(f) - \tilde{S}^*(-f)\right], \tag{2.126}$$

and $s_Q(t)$ is also bandlimited to W. Therefore, the bandpass representation expresses $s(t)$ in terms of a pair of baseband signals modulated onto quadrature carriers. The baseband signal can be obtained directly from the bandpass signal via the following relationships

$$S_I(f) = \mathrm{LPF}_{f_c}\left[S(f - f_c) + S(f + f_c)\right] \tag{2.127}$$

and

$$S_Q(f) = \mathrm{jLPF}_{f_c}\left[S(f - f_c) - S(f + f_c)\right] \tag{2.128}$$

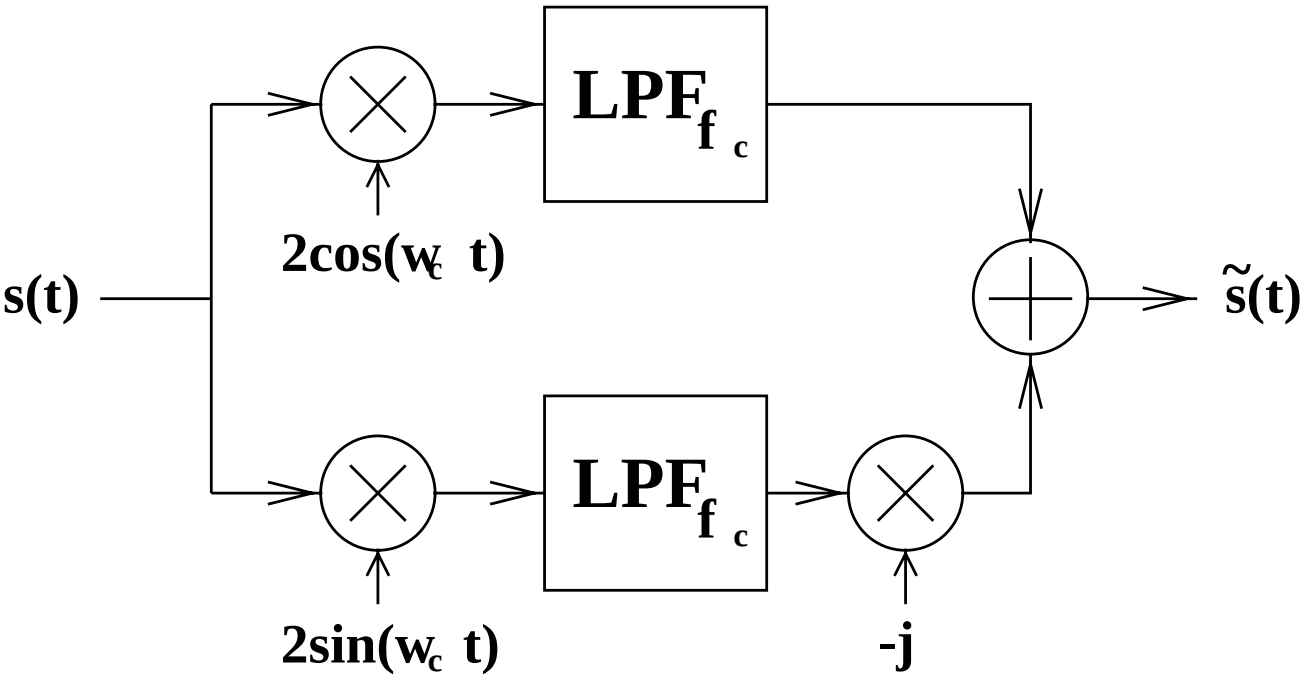

Figure 2.28: Complex envelope conversion circuit

where $\text{LPF}_{f_c}[\cdot]$ represents ideal lowpass filtering with cut-off at f_c. In time domain, we have

$$s_I(t) = \text{LPF}_{f_c}\left[2s(t)\cos(2\pi f_c t)\right] \tag{2.129}$$

and

$$s_Q(t) = -\text{LPF}_{f_c}\left[2s(t)\sin(2\pi f_c t)\right]. \tag{2.130}$$

Therefore, we can use the circuit shown in Figure 2.28 to convert a real bandpass signal to its complex envelope. Since the complex envelope is a (complex) baseband signal which uniquely represents the real bandpass signal, we can perform all the previous developments of the RF communication system in baseband by treating the complex envelope as our baseband signal.

Examples

Consider that $s(t) = \cos(2\pi(f_c + \Delta f)t)$ where $\Delta f < f_c$. Then

$$\begin{aligned} s_+(t) &= e^{\text{j}2\pi(f_c+\Delta f)t} \\ \tilde{s}(t) &= e^{\text{j}2\pi(\Delta f)t} \end{aligned}$$

$$\begin{aligned} s_I(t) &= \cos(2\pi(\Delta f)t) \\ s_Q(t) &= \sin(2\pi(\Delta f)t). \end{aligned}$$

Therefore,

$$s(t) = \cos(2\pi(\Delta f)t)\cos(2\pi f_c t) - \sin(2\pi(\Delta f)t)\sin(2\pi f_c t) \tag{2.131}$$

which is the obvious result.

Very often, $s(t)$ is not strictly bandlimited to some $W < f_c$. However, if most of its energy is contained in a neighborhood of the carrier frequency, we would still use these representations.

Consider that $s(t) = p_T(t)\cos(2\pi f_c t) - p_T(t)\sin(2\pi f_c t)$. Notice that $s(t)$ is not bandlimited. Suppose that $f_c >> 1/T$. Then

$$\begin{aligned} s_+(t) &= [p_T(t) + \mathrm{j}p_T(t)]e^{\mathrm{j}2\pi f_c t} \\ \tilde{s}(t) &= p_T(t) + \mathrm{j}p_T(t) \\ s_I(t) &= p_T(t) \\ s_Q(t) &= p_T(t). \end{aligned}$$

We note that these are approximations. Some of the relationships between these signals no longer hold exactly, but only approximately.

2.3.3 Representation of Bandpass Random Processes

Suppose $n(t)$ is a wide-sense stationary (WSS) process with zero mean and power spectral density $\Phi_n(f)$. If $\Phi_n(f)$ satis£es the narrowband assumption in (2.106), i.e.,

$$\Phi_n(f) = 0 \qquad \text{for } |f| \le f_c - W \text{ and } f_c + W \le |f|, \tag{2.132}$$

where $W \le f_c$, then $n(t)$ is called a *bandpass (narrowband) process*. It turns out that $n(t)$ also has the bandpass representation:

$$n(t) = n_I(t)\cos(2\pi f_c t) - n_Q(t)\sin(2\pi f_c t), \tag{2.133}$$

where $n_I(t)$ and $n_Q(t)$ are zero-mean jointly WSS processes. Moreover, if $n(t)$ is Gaussian, $n_I(t)$ and $n_Q(t)$ are jointly Gaussian. By employing the stationarity of the random processes involved, we can

show that

$$R_{n_I}(\tau) = R_{n_Q}(\tau), \tag{2.134}$$

$$R_{n_I n_Q}(\tau) = -R_{n_Q n_I}(\tau), \tag{2.135}$$

$$R_n(\tau) = R_{n_I}(\tau)\cos(2\pi f_c\tau) - R_{n_Q n_I}(\tau)\sin(2\pi f_c\tau), \tag{2.136}$$

where $R_n(\tau) \triangleq E[n(t+\tau)n(t)]$ is the autocorrelation function of the random process $n(t)$, $R_{n_I}(\tau) \triangleq E[n_I(t+\tau)n_I(t)]$ and $R_{n_Q}(\tau) \triangleq E[n_Q(t+\tau)n_Q(t)]$ are, respectively, the autocorrelation functions of the processes $n_I(t)$ and $n_Q(t)$, and $R_{n_I n_Q}(\tau) \triangleq E[n_I(t+\tau)n_Q(t)]$ and $R_{n_Q n_I}(\tau) \triangleq E[n_Q(t+\tau)n_I(t)]$ are the cross-correlation functions. Now, let us de£ne the complex envelope $\tilde{n}(t)$ of the random process $n(t)$,

$$\tilde{n}(t) \triangleq n_I(t) + \mathrm{j}n_Q(t). \tag{2.137}$$

Obviously, $\tilde{n}(t)$ is a zero-mean WSS complex random process with autocorrelation function

$$\begin{aligned} R_{\tilde{n}}(\tau) &\triangleq \frac{1}{2}\mathrm{E}\left[\tilde{n}(t+\tau)\tilde{n}^*(t)\right] \\ &= \frac{1}{2}\mathrm{E}\left[(n_I(t+\tau)+\mathrm{j}n_Q(t+\tau))(n_I(t)-\mathrm{j}n_Q(t))\right] \\ &= \frac{1}{2}R_{n_I}(\tau) + \frac{1}{2}R_{n_Q}(\tau) - \frac{\mathrm{j}}{2}R_{n_I n_Q}(\tau) + \frac{\mathrm{j}}{2}R_{n_Q n_I}(\tau) \\ &= R_{n_I}(\tau) + \mathrm{j}R_{n_Q n_I}(\tau). \end{aligned} \tag{2.138}$$

Now compare (2.136) with (2.121) and (2.138) with (2.120). If we treat the autocorrelation function $R_n(\tau)$ as a bandpass signal (by de£nition, it satis£es the narrowband assumption since $n(t)$ is a narrowband process), then $R_{\tilde{n}}(\tau)$ is its complex envelope. Hence, we can use the results in the previous section to convert between $R_n(\tau)$ and $R_{\tilde{n}}(\tau)$. For example, the frequency domain equivalent of (2.136) is

$$\Phi_n(f) = \frac{1}{2}\left[\Phi_{n_I}(f-f_c) + \Phi_{n_I}(f+f_c)\right] + \frac{\mathrm{j}}{2}\left[\Phi_{n_Q n_I}(f-f_c) - \Phi_{n_Q n_I}(f+f_c)\right]. \tag{2.139}$$

To obtain $\Phi_{n_I}(f)$ and $\Phi_{n_Q n_I}(f)$ from $\Phi_n(f)$, we can do

$$\Phi_{n_I}(f) = \mathrm{LPF}_{f_c}\left[\Phi_n(f-f_c) + \Phi_n(f+f_c)\right] \tag{2.140}$$

$$\Phi_{n_Q n_I}(f) = \mathrm{jLPF}_{f_c}\left[\Phi_n(f-f_c) - \Phi_n(f+f_c)\right]. \tag{2.141}$$

Bandpass additive Gaussian noise

A common example of narrowband process is the bandpass additive Gaussian noise $n(t)$ with zero mean and power spectral density $\Phi_n(f) = N_0/2$ for $|f| < 2f_c$ and $\Phi_n(f) = 0$ otherwise. Since $\Phi_n(f)$ satisfies the narrowband assumption, $n(t)$ can be written as

$$n(t) = n_I(t)\cos(2\pi f_c t) - n_Q(t)\sin(2\pi f_c t), \tag{2.142}$$

where $n_I(t)$ and $n_Q(t)$ are zero-mean jointly WSS Gaussian processes. The complex envelope of $n(t)$ is given by

$$\tilde{n}(t) = n_I(t) + \mathrm{j}n_Q(t). \tag{2.143}$$

Using the result above, the power spectral density $\Phi_{\tilde{n}}(f)$ of the complex envelope $\tilde{n}(t)$ is given by

$$\begin{aligned} \Phi_{\tilde{n}}(\omega) &= \Phi_{n_I}(f) + \mathrm{j}\Phi_{n_Q n_I}(f) \\ &= \Phi_{n_I}(f) \\ &= \begin{cases} N_0 & \text{if } |f| < f_c, \\ 0 & \text{otherwise}, \end{cases} \end{aligned} \tag{2.144}$$

because $\Phi_{n_Q n_I}(f) = 0$. Taking inverse Fourier transform, we get

$$R_{\tilde{n}}(\tau) = N_0 \left[2f_c \frac{\sin(2\pi f_c \tau)}{2\pi f_c \tau} \right], \tag{2.145}$$

Since $\Phi_{n_Q n_I}(f) = 0$, the processes $n_I(t)$ and $n_Q(t)$ are uncorrelated. Moreover, we have $R_{n_Q}(\tau) = R_{n_I}(\tau) = R_{\tilde{n}}(\tau)$. For the case where bandpass transmitted signals are sent through a channel corrupted by $n(t)$ and the bandwidths of the transmitted signals are much smaller than the carrier frequency f_c, we approximate $R_{\tilde{n}}(\tau)$ in (2.145) by $N_0\delta(\tau)$. This means that the lowpass equivalent of the additive bandpass Gaussian noise looks white to the lowpass equivalents of the transmitted signals. In this way, we are back to the communication model of transmitting baseband signals over an AWGN channel as in Section 2.1. Of course, all the signal are complex instead of real now.

Recall in Section 2.2, we employ the non-dispersive model to describe the RF communication channel. In the non-dispersive model, the thermal noise is modeled by an AWGN component. Since every RF communication system is inherently bandpass, we should have used the additive bandpass Gaussian noise instead of the AWGN component in the non-dispersive model. However, the effect

of replacing the AWGN by the additive bandpass Gaussian noise is minimal when the bandwidths of the transmitted signals are much smaller than the carrier frequency f_c. Hence, we do not make a distinction between the two noise models in Section 2.2. Similarly, we can also approximate the complex envelope of the additive bandpass Gaussian noise by AWGN as above. In summary, we only need to consider AWGN (for the case where the bandwidths of the transmitted signals are much smaller than the carrier frequency f_c) whether we use the complex baseband representation or not.

2.3.4 Bandpass Filter

To complete the development in complex baseband representation, let us work out the input-output relationship when a bandpass signal or a bandpass process is entered into a bandpass £lter. First, we can use the complex envelope to represent the impulse response $h(t)$ of a bandpass £lter given that $h(t)$ satis£es the narrowband assumption stated in (2.106). Hence, if $\tilde{h}(t)$ is the complex envelope of $h(t)$, then

$$h(t) = \text{Re}[\tilde{h}(t)e^{\text{j}2\pi f_c t}]. \tag{2.146}$$

Now, if a bandpass signal $s_i(t)$ is the input to the bandpass £lter $h(t)$, then the output from the £lter $s_o(t)$ is also a bandpass signal and

$$s_o(t) = h(t) * s_i(t), \tag{2.147}$$

where $*$ denotes the convolution operator. In the frequency domain,

$$S_o(f) = H(f)S_i(f), \tag{2.148}$$

where $S_o(f)$, $H(f)$, and $S_i(f)$ are the Fourier transforms of $s_o(t)$, $h(t)$, and $s_i(t)$, respectively. From (2.115), the Fourier transform of the complex envelope, $\tilde{s}_o(t)$, of $s_o(t)$ is given by

$$\begin{aligned} \tilde{S}_o(f) &= S_{o+}(f + f_c) \\ &= \frac{1}{2}H_+(f + f_c)S_{i+}(f + f_c) \\ &= \frac{1}{2}\tilde{H}(f)\tilde{S}_i(f), \end{aligned} \tag{2.149}$$

where $S_{o+}(f)$, $H_+(f)$, and $S_{i+}(f)$ are the Fourier transforms of the complex analytic representations of $s_o(t)$, $h(t)$, and $s_i(t)$, respectively. Also, $\tilde{H}(f)$ and $\tilde{S}_i(f)$ are the Fourier transforms of the complex

envelopes, $\tilde{h}(t)$ and $\tilde{s}_i(t)$, of $h(t)$ and $s_i(t)$, respectively. The second equality in (2.149) is due to the fact that both $h(t)$ and $s_i(t)$ share the same passband. By taking inverse Fourier transform on both sides of (2.149), we obtain

$$\tilde{s}_o(t) = \frac{1}{2}\tilde{h}(t) * \tilde{s}_i(t). \tag{2.150}$$

Hence, we can convolute the complex envelopes of $h(t)$ and $s_o(t)$ and then convert the result back to obtain the output bandpass signal. We note that (2.150) is a generalization of (2.48).

Similarly, if a bandpass process $n_i(t)$ is the input to the bandpass £lter $h(t)$, then the output from the £lter $n_o(t)$ is also a bandpass process and its power spectral density is given by

$$\Phi_{n_o}(f) = |H(f)|^2 \Phi_{n_i}(f), \tag{2.151}$$

where $\Phi_{n_i}(f)$ and $\Phi_{n_o}(f)$ are the power spectral densities of the input and output processes, respectively. Again, from (2.115), the power spectral density of the complex envelope $\tilde{n}_o(t)$ of $n_o(t)$ is

$$\begin{aligned} \Phi_{\tilde{n}_o}(f) &= \Phi_{n_o+}(f + f_c) \\ &= \frac{1}{4}|H_+(f + f_c)|^2 \Phi_{n_i+}(f + f_c) \\ &= \frac{1}{4}|\tilde{H}(f)|^2 \Phi_{\tilde{n}_i}(f), \end{aligned} \tag{2.152}$$

where $\Phi_{n_o+}(f)$ and $\Phi_{n_i+}(f)$ are the complex analytic representations of $\Phi_{n_o}(f)$ and $\Phi_{n_i}(f)$, respectively. Also, $\Phi_{\tilde{n}_o}(f)$ and $\Phi_{\tilde{n}_i}(f)$ are the power spectral densities of the complex envelopes $\tilde{n}_o(t)$ and $\tilde{n}_i(t)$, respectively.

2.3.5 Complex Baseband Matched Filter

All the results in Section 2.2 can be obtained based on the complex baseband representation. As an illustration, we re-derive the matched £lter here.

Let us consider that the pair of RF signals in (2.36) and (2.37) are transmitted with equal probabilities. In complex baseband representation, the two signals are

$$\tilde{s}_0(t) = Ae^{\mathrm{j}\theta} v_0(t), \tag{2.153}$$

$$\tilde{s}_1(t) = Ae^{\mathrm{j}\theta} v_1(t). \tag{2.154}$$

As in Section 2.1.2, we choose the minimax threshold

$$\gamma = \frac{\hat{s}_0(T_0) + \hat{s}_1(T_0)}{2} \tag{2.155}$$

to give the average bit error probability

$$P_b = Q\left(\frac{\hat{s}_0(T_0) - \hat{s}_1(T_0)}{2\sqrt{R_{\hat{n}}(0)}}\right), \tag{2.156}$$

where, now,

$$\hat{s}_0(t) = \text{Re}\left[\frac{1}{2}\tilde{s}_0 * \tilde{h}(t)e^{\text{j}2\pi f_c t}\right], \tag{2.157}$$

$$\hat{s}_1(t) = \text{Re}\left[\frac{1}{2}\tilde{s}_1 * \tilde{h}(t)e^{\text{j}2\pi f_c t}\right], \tag{2.158}$$

and the complex envelope of $\hat{n}(t)$ is the output process, $\tilde{\hat{n}}(t)$, of the £lter $\tilde{h}(t)$ due to the input process $\tilde{n}(t)$, where $\tilde{n}(t)$ is complex AWGN with autocorrelation function $R_{\tilde{n}}(\tau) = N_0\delta(\tau)$ as described in Section 2.3.3. Using (2.152), we have

$$\begin{aligned} R_{\tilde{\hat{n}}}(0) &= \frac{1}{4}\int_{-\infty}^{\infty} |\tilde{H}(f)|^2 \Phi_{\tilde{n}}(f) df \\ &= \frac{N_0}{4}\int_{-\infty}^{\infty} |\tilde{H}(f)|^2 df \\ &= \frac{N_0}{4}\int_{-\infty}^{\infty} |\tilde{h}(t)|^2 dt \\ &= \frac{N_0}{4}\|\tilde{h}\|^2. \end{aligned} \tag{2.159}$$

Since $R_{\tilde{\hat{n}}}(0)$ is real,

$$R_{\hat{n}}(0) = R_{\tilde{\hat{n}}}(0) = \frac{N_0}{4}\|\tilde{h}\|^2. \tag{2.160}$$

Moreover,

$$\hat{s}_0(T_0) - \hat{s}_1(T_0) = \text{Re}\left[\int_{-\infty}^{\infty} \frac{1}{2}e^{\text{j}2\pi f_c T_0}(\tilde{s}_0(T_0 - t) - \tilde{s}_1(T_0 - t))\tilde{h}(t)dt\right]. \tag{2.161}$$

Again, using the Cauchy-Schwartz inequality[8],

$$\begin{aligned} \hat{s}_0(T_0) - \hat{s}_1(T_0) &\leq \left|\int_{-\infty}^{\infty} \frac{1}{2}e^{\text{j}2\pi f_c T_0}(\tilde{s}_0(T_0 - t) - \tilde{s}_1(T_0 - t))\tilde{h}(t)dt\right| \\ &\leq \frac{1}{2}\|\tilde{s}_0 - \tilde{s}_1\|\|\tilde{h}\|. \end{aligned} \tag{2.162}$$

[8]The complex-valued version of the Cauchy-Schwartz inequality is that for any two complex-valued functions f and g such that $\|f\|, \|g\| < \infty$, $\left|\int_{-\infty}^{\infty} f(t)g^*(t)dt\right| \leq \|f\| \cdot \|g\|$ with equality only if $f(t) = \lambda g(t)$ where λ is a complex constant.

and $\hat{s}_0(T_0) - \hat{s}_1(T_0)$ is maximized with equality in (2.162) if we choose

$$\tilde{h}(t) = e^{-\mathrm{j}(2\pi f_c T_0 + \theta)} \left[v_0(T_0 - t) - v_1(T_0 - t) \right]. \tag{2.163}$$

This is the matched filter in complex baseband representation. Of course, the minimum average bit error probability is given by

$$P_b = Q\left(\sqrt{\frac{\bar{E}(1-r)}{N_0}} \right) \tag{2.164}$$

with

$$\bar{E} = \frac{1}{2}\left(\frac{\|\tilde{s}_0\|^2}{2} + \frac{\|\tilde{s}_1\|^2}{2} \right) = \frac{1}{2}\left(\|s_0\|^2 + \|s_1\|^2 \right) \tag{2.165}$$

$$r = \frac{1}{2\bar{E}} \int_{-\infty}^{\infty} \tilde{s}_0(t)\tilde{s}_1(t)dt = \frac{1}{\bar{E}} \int_{-\infty}^{\infty} s_0(t)s_1(t)dt. \tag{2.166}$$

We can convert $\tilde{h}(t)$ back to obtain the real bandpass matched filter

$$h(t) = \mathrm{Re}\left[\tilde{h}(t) e^{\mathrm{j}2\pi f_c t} \right] = \left[v_0(T_0 - t) - v_1(T_0 - t) \right] \cos(2\pi f_c (t - T_0) - \theta) \tag{2.167}$$

exactly as (2.37).

2.3.6 Signal Space Representation

We are going to generalize the idea of binary communications to M-ary communications in Section 2.4. This basically means that the transmitter selects one out of a set of M signals, instead of one out of a set of 2 signals, to send. Due to the increase in the size of the signal set, it would be convenient if we can have a simple way to represent the set of signals. A common approach is to obtain an orthonormal basis for the signal set and, then, to represent a signal by it coordinates with respect to the basis. In other words, we represent the set of signals by a set of vectors. This method provides us a geometric viewpoint for the set of signals, and is usually known as the *signal space representation*.

Examples

First, let us look at two examples.

1. Antipodal signals:

$$\begin{aligned} s_0(t) &= v(t) \\ s_1(t) &= -v(t). \end{aligned}$$

In this case, $M = 2$. Suppose the basic pulse shape $v(t)$ has unit norm (i.e., $\|v\| = 1$), we may choose it to be the basis of our signal set. Then we can just use the vector $[1]$ to represent $s_0(t)$ and $[-1]$ to represent $s_1(t)$.

2. QPSK:

In this case, $M = 4$. Consider the symbol interval $[0, T)$. The set of possible signals are

$$\begin{aligned} s_1(t) &= \sqrt{2P}\cos(2\pi f_c t + \pi/4)p_T(t), \\ s_2(t) &= \sqrt{2P}\cos(2\pi f_c t + 3\pi/4)p_T(t), \\ s_3(t) &= \sqrt{2P}\cos(2\pi f_c t + 5\pi/4)p_T(t), \\ s_4(t) &= \sqrt{2P}\cos(2\pi f_c t + 7\pi/4)p_T(t). \end{aligned}$$

By inspection, a simple basis[9] for this signal set is

$$\begin{aligned} \phi_1(t) &= \sqrt{\frac{2}{T}}\cos(2\pi f_c t)p_T(t), \\ \phi_2(t) &= -\sqrt{\frac{2}{T}}\sin(2\pi f_c t)p_T(t). \end{aligned}$$

For this basis, the corresponding signal vectors are

$$\begin{aligned} \mathbf{s}_1 &= \left[\sqrt{PT/2}, \sqrt{PT/2}\right]^T, \\ \mathbf{s}_2 &= \left[-\sqrt{PT/2}, \sqrt{PT/2}\right]^T, \\ \mathbf{s}_3 &= \left[-\sqrt{PT/2}, -\sqrt{PT/2}\right]^T, \\ \mathbf{s}_4 &= \left[\sqrt{PT/2}, -\sqrt{PT/2}\right]^T. \end{aligned}$$

The corresponding constellation diagram is drawn in Figure 2.29. If we choose to represent the

[9] Strictly speaking, the basis functions $\phi_1(t)$ and $\phi_2(t)$ are not orthogonal unless $f_c = n/T$ for some integer n. However, when $f_c \gg 1/T$, they are approximately orthogonal because of the fact the double frequency term is small. We will make this orthogonal approximation whenever we encounter RF signals.

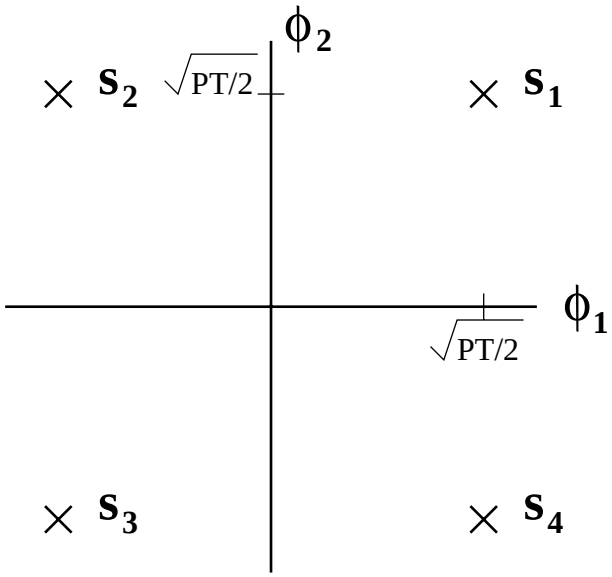

Figure 2.29: QPSK constellation

set of signals by the complex baseband representation, we have

$$\begin{aligned}
\tilde{s}_1(t) &= \sqrt{2P}e^{\mathrm{j}\pi/4}p_T(t), \\
\tilde{s}_2(t) &= \sqrt{2P}e^{\mathrm{j}3\pi/4}p_T(t), \\
\tilde{s}_3(t) &= \sqrt{2P}e^{\mathrm{j}5\pi/4}p_T(t), \\
\tilde{s}_4(t) &= \sqrt{2P}e^{\mathrm{j}7\pi/4}p_T(t).
\end{aligned}$$

A basis for this set of complex envelopes is then

$$\tilde{\phi}_1(t) = \sqrt{\frac{1}{T}}p_T(t),$$

For this basis, the corresponding signal vectors are

$$\begin{aligned}
\mathbf{s}_1 &= \left[\sqrt{PT} + \mathrm{j}\sqrt{PT}\right], \\
\mathbf{s}_2 &= \left[-\sqrt{PT} + \mathrm{j}\sqrt{PT}\right], \\
\mathbf{s}_3 &= \left[-\sqrt{PT} - \mathrm{j}\sqrt{PT}\right], \\
\mathbf{s}_4 &= \left[\sqrt{PT} - \mathrm{j}\sqrt{PT}\right].
\end{aligned}$$

Gram-Schmidt procedure

Before we can generalize the two examples considered in the previous section to any set of M signals, we need a way to obtain an orthonormal basis for the signal set. Recall an orthonormal basis is a set of unit-norm orthogonal signals which span the space formed by linear combinations of the M signals. Given a set of M £nite-energy signals $\{s_i(t)\}_{i=1}^M$, one way to determine a minimal orthonormal basis (i.e., an orthonormal basis with the fewest basis functions) $\{\phi_j(t)\}_{j=1}^N$, where $N \leq M$, is the *Gram-Schmidt procedure*:

1. Choose $\phi_1(t) = s_1(t)/\|s_1\|$.
2. For $j > 1$, £nd
$$v_j(t) = s_j(t) - (s_j, \phi_1)\phi_1(t) - \ldots - (s_j, \phi_{j-1})\phi_{j-1}(t).$$
Then choose $\phi_j(t) = v_j(t)/\|v_j\|$.
3. Continue until all M functions are expressed in terms of $\phi_j(t)$'s.

Several remarks are needed to explain the above procedure. First, the *inner product* (x, y) between two £nite-norm signals $x(t)$ and $y(t)$ is de£ned as

$$(x, y) = \int_{-\infty}^{\infty} x(t)y^*(t)dt. \tag{2.168}$$

Second, the procedure above assumed that the M signals are independent. If this is not the case, the norm of the signal $v_j(t)$ in the second step will be zero for some j. In this case, we can just skip that signal and move to the next one. Third, the proof that the procedure does give an orthonormal basis is straightforward by showing that the resulting set $\{\phi_j(t)\}$ is an orthonormal set.

For example, let us consider the set of three signals ($M = 3$) in Figure 2.30. Applying the Gram-Schmidt procedure, we £nd the basis signals (two of them, i.e., $N = 2$) in Figure 2.31. The vector representation for the signals are $\mathbf{s}_1 = [\sqrt{2}, 0]^T$, $\mathbf{s}_2 = [0, \sqrt{2}]^T$, and $\mathbf{s}_3 = [-1, 1]^T$. Alternatively, if we rearrange the order of the signals when we perform the Gram-Schmidt procedure (e.g., $s_3(t)$ £rst, then $s_2(t)$, then $s_1(t)$), then we obtain an alternative basis of signals as shown in Figure 2.32. The vector representation for the signals are $\mathbf{s}_1 = [-1, 1]^T$, $\mathbf{s}_2 = [1, 1]^T$, and $\mathbf{s}_3 = [\sqrt{2}, 0]^T$.

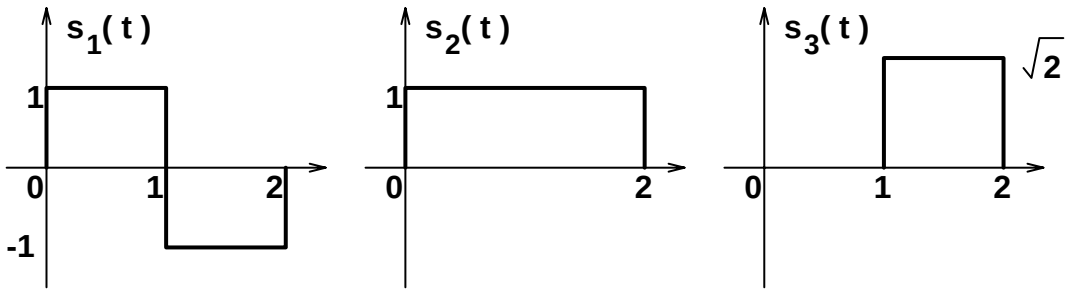

Figure 2.30: A set of 3 signals

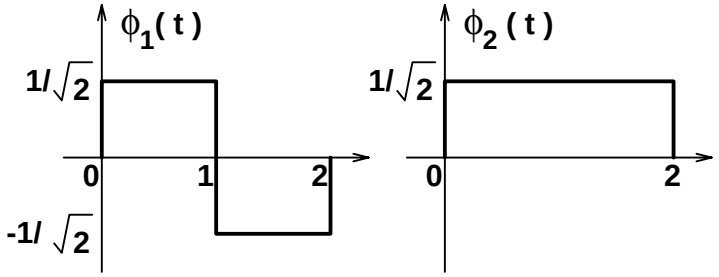

Figure 2.31: A basis for the set of 3 signals

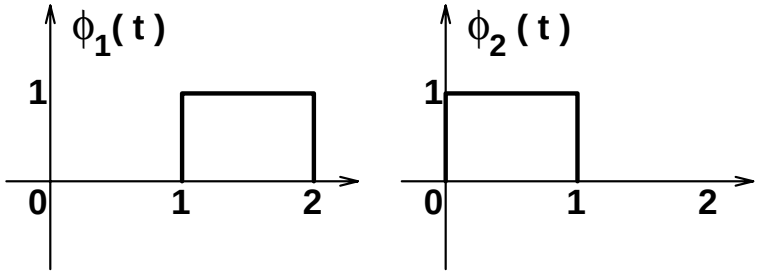

Figure 2.32: An alternative basis for the set of 3 signals

Orthogonal representation

Given a set of M £nite-energy signals $\{s_i(t)\}_{i=1}^M$, we can express each $s_i(t)$ as

$$s_i(t) = \sum_{j=1}^{N} s_{i,j}\phi_j(t) \tag{2.169}$$

where $N \leq M$ and $\{\phi_j(t)\}_{j=1}^N$ is an orthonormal basis for $\{s_i(t)\}_{i=1}^M$, i.e., $\{\phi_j(t)\}_{j=1}^N$ spans $\{s_i(t)\}_{i=1}^M$ and

$$(\phi_i, \phi_j) = \int_{-\infty}^{\infty} \phi_i(t)\phi_j^*(t)dt = \delta_{ij}. \tag{2.170}$$

With the knowledge of the basis, we can represent $s_i(t)$ simply by the N-dimensional vector

$$\mathbf{s}_i = [s_{i,1}, s_{i,2}, \ldots, s_{i,N}]^T, \tag{2.171}$$

where

$$s_{i,j} = (s_i, \phi_j) = \int_{-\infty}^{\infty} s_i(t)\phi_j^*(t)dt. \tag{2.172}$$

is the jth coordinate, for $j = 1, 2, \ldots, N$, of the signal $s_i(t)$ with respect to the basis $\{\phi_j(t)\}_{j=1}^N$. In this approach, we represent the signals by vectors. The resulting vector space is called the *signal space*. Given the basis, we can uniquely[10] determine the signal $s_i(t)$ from the vector $\mathbf{s}_i$ or vice versa. As a result, the vector representation provides a geometric viewpoint for the set of the signals. Since we are much more familiar with Euclidean geometry than function spaces, this geometric viewpoint allows us to visualize the underlying structure of the signal space easily.

With signal space representation, signals are represented by vectors. It turns out that many properties of the signals carry over to the corresponding properties of vectors in the signal space:

1. **Norm and length (energy and square of length)**

   Consider the norm of a signal

$$\begin{aligned} \|s_i\| &= \sqrt{\int_{-\infty}^{\infty} |s_i|^2(t)dt} \\ &= \sqrt{\int_{-\infty}^{\infty} \left[\sum_{k=1}^{N} s_{ik}\phi_k(t)\right]\left[\sum_{l=1}^{N} s_{il}\phi_l(t)\right] dt} \end{aligned}$$

[10] There can be many bases for the set of signals. Different bases give rise to different vector representations.

$$\begin{aligned} &= \sqrt{\sum_{k=1}^{N} |s_{i,k}|^2} \\ &= \|\mathbf{s}_i\|. \end{aligned} \tag{2.173}$$

Therefore, the norm of the signal is equal to the length of the corresponding vector in the signal space. Since the energy of the signal is the square of the norm, it is equal to the square of the length of the vector. Hence, the "longer" the vector, the larger is the energy of the signal.

2. **Inner products**

The inner product of two signal $s_i(t)$ and $s_j(t)$ is

$$\begin{aligned} (s_i, s_j) &= \int_{-\infty}^{\infty} s_i(t) s_j^*(t) dt \\ &= \int_{-\infty}^{\infty} \left[\sum_{k=1}^{N} s_{ik}\phi_k(t)\right] \left[\sum_{l=1}^{N} s_{jl}\phi_l(t)\right]^* dt \\ &= \sum_{k=1}^{N} s_{i,k} s_{j,k}^* \qquad (2.174) \\ &= \mathbf{s}_i \cdot \mathbf{s}_j. \qquad (2.175) \end{aligned}$$

Therefore, inner product of the two signals is equal to the inner product of the vectors $\mathbf{s}_i$ and $\mathbf{s}_j$.

3. **Norm of difference and distance**

Notice that

$$\|s_i - s_j\| = \sqrt{\int_{-\infty}^{\infty} |s_i(t) - s_j(t)|^2 dt} = \|\mathbf{s}_i - \mathbf{s}_j\| \triangleq d(\mathbf{s}_i, \mathbf{s}_j), \tag{2.176}$$

i.e., the norm of the difference is equal to the distance between $\mathbf{s}_i$ and $\mathbf{s}_j$.

2.4 M-ary Communications

We have considered binary communications in which we send one bit at a time using one of two possible signals. This idea can be extended to, say, sending two bits at a time by choosing one from four possible signals. In general, we can send $\log_2 M$ bits at a time using one of M possible signals. This is called *M-ary communications*.

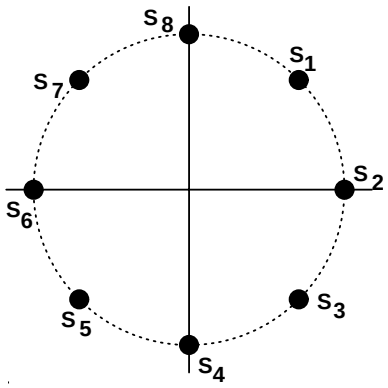

Figure 2.33: 8PSK constellation

2.4.1 Common M-ary modulation schemes

First, let us introduce some common M-ary modulation schemes.

MPSK

Consider the symbol interval $[0, T)$. For $i = 1, 2, \ldots, M$,

$$s_i(t) = A\cos\left(2\pi f_c t + \theta + \frac{2i\pi}{M}\right) p_T(t). \tag{2.177}$$

The signal space is 2-D. The basis functions can be

$$\phi_1(t) = \sqrt{\frac{2}{T}}\cos(2\pi f_c t + \theta) p_T(t) \tag{2.178}$$

$$\phi_2(t) = -\sqrt{\frac{2}{T}}\sin(2\pi f_c t + \theta) p_T(t). \tag{2.179}$$

With this basis, $s_i(t)$ can be represented by the 2-D vector

$$\mathbf{s}_i = \left[A\sqrt{T/2}\cos\left(\frac{2i\pi}{M}\right), A\sqrt{T/2}\sin\left(\frac{2i\pi}{M}\right)\right]^T. \tag{2.180}$$

As an example, an 8PSK constellation is shown in Figure 2.33.

Pulse amplitude modulation (PAM)

For example, let us consider PAM with four possible symbols. The symbols are given by $\pm A p_T(t)\cos(2\pi f_c t + \theta)$ and $\pm 3A p_T(t)\cos(2\pi f_c t + \theta)$. The signal space is 1-D. The basis consists of only one element, the function $\sqrt{\frac{2}{T}}\cos(2\pi f_c t + \theta) p_T(t)$. The constellation is shown in Figure 2.34.

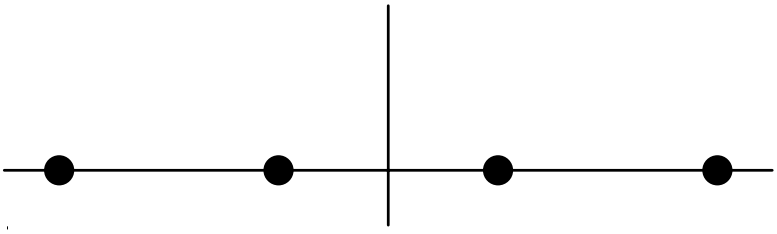

Figure 2.34: 4PAM constellation

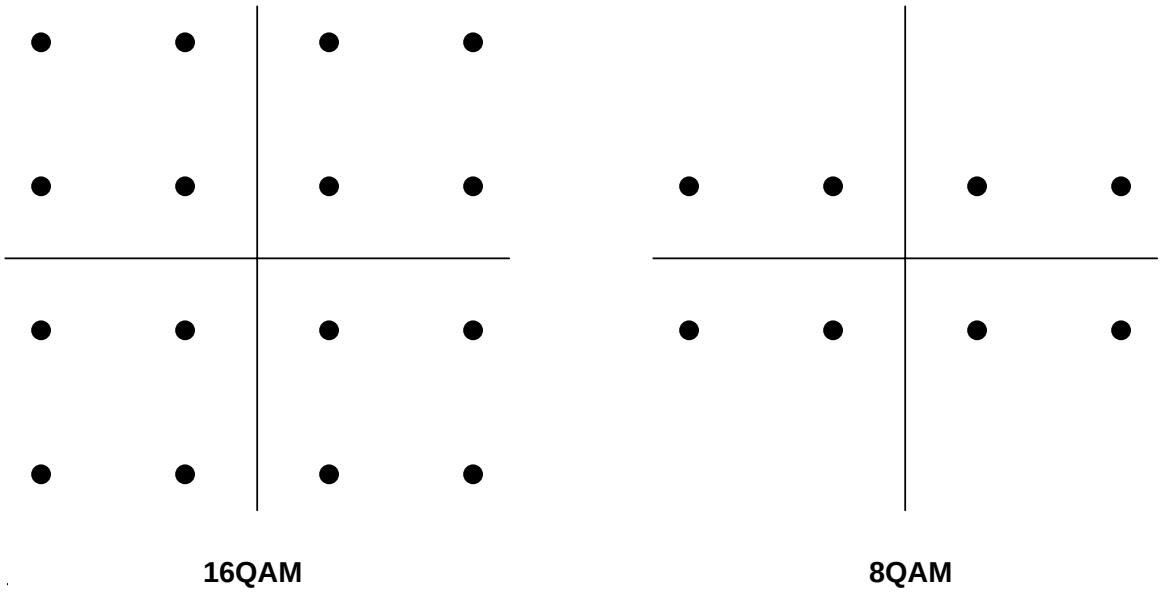

Figure 2.35: QAM constellations

Quadrature amplitude modulation (QAM)

In the simplest case of QAM, one data stream is modulated with PAM onto the in-phase carrier and another data stream is modulated with PAM onto the quadrature carrier. The signal space becomes 2-D. Some QAM constellations are shown in Figure 2.35.

Orthogonal signal set

A set of signals $\{s_i(t)\}$ is an orthogonal signal set over $[0, T)$ if

$$\int_0^T s_i(t)s_j^*(t)dt = 0 \quad \text{for all } i \neq j. \tag{2.181}$$

It is easy to see that an orthonormal set is an orthogonal set. Actually, an orthonormal set is an orthogonal set that is normalized in energy. Therefore, to obtain a basis, we just normalize each signal,

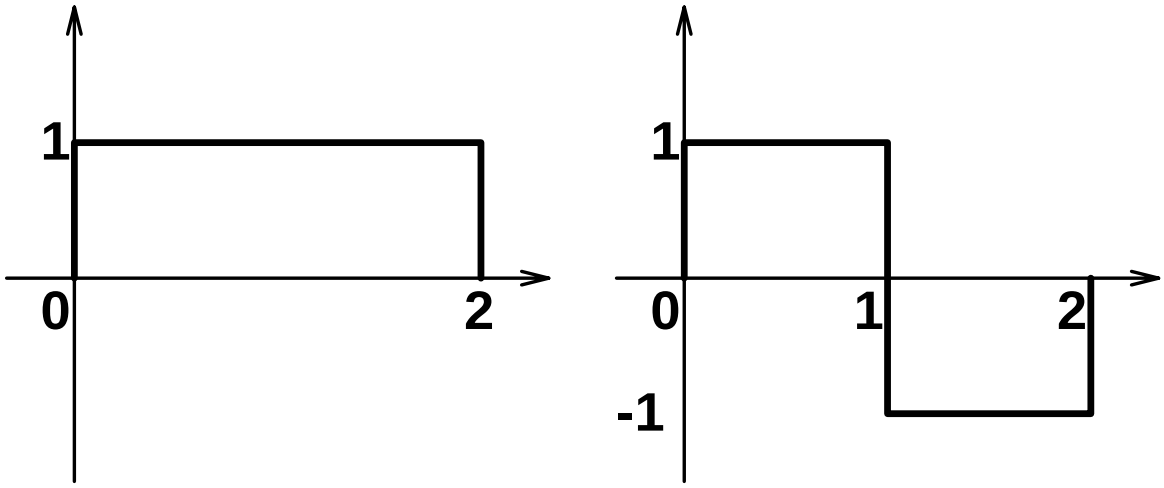

Figure 2.36: A pair of orthogonal signals

i.e., $\phi_j(t) = s_j(t)/||s_j||$. As an example, an orthogonal set of 2 signals is shown in Figure 2.36. There are many ways to generate orthogonal sets of signals. One way is by using the Hadamard matrices de£ned by

$$H_0 = [1] \tag{2.182}$$

and

$$H_n = \begin{bmatrix} H_{n-1} & H_{n-1} \\ H_{n-1} & -H_{n-1} \end{bmatrix} \tag{2.183}$$

for $n \geq 1$. Each row can be used to generate a signal. For example,

$$H_2 = \begin{bmatrix} 1 & 1 & 1 & 1 \\ 1 & -1 & 1 & -1 \\ 1 & 1 & -1 & -1 \\ 1 & -1 & -1 & 1 \end{bmatrix} \tag{2.184}$$

can be used to generate the signal set in Figure 2.37.

Biorthogonal signal set

Given an orthogonal set of signals $\{s_1(t), s_2(t), \ldots, s_M(t)\}$, the corresponding biorthogonal set is the set $\{s_1(t)$, $-s_1(t)$, $s_2(t)$, $-s_2(t)$, ..., $s_M(t)$, $-s_M(t)\}$, i.e., all the sign-reversed signals are also included. As an example, a biorthogonal set of four signals is shown in Figure 2.38.

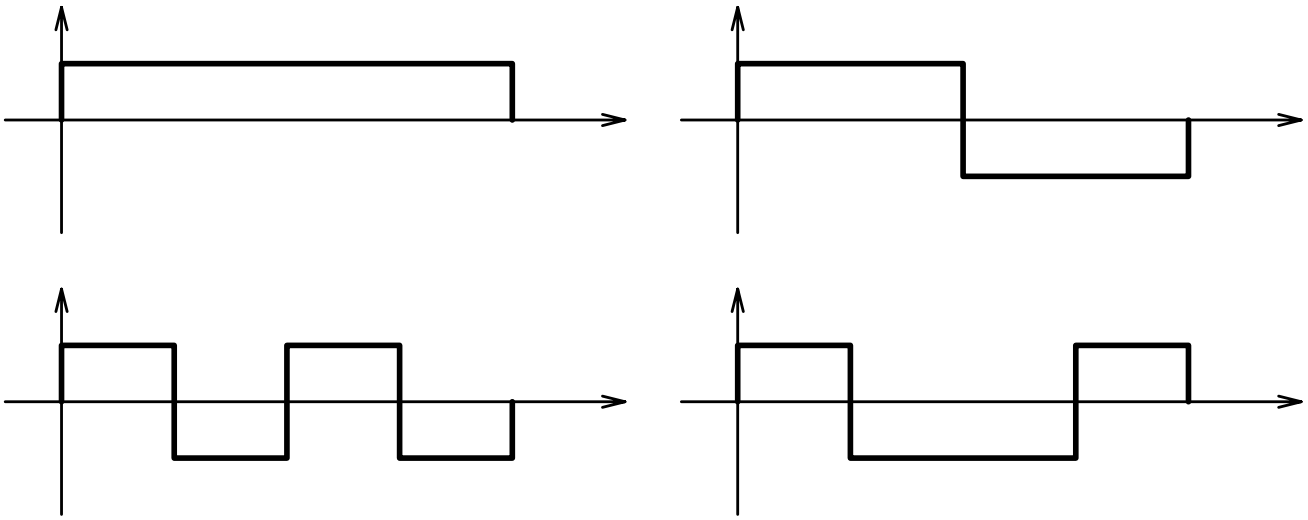

Figure 2.37: 4 orthogonal signals from H_2

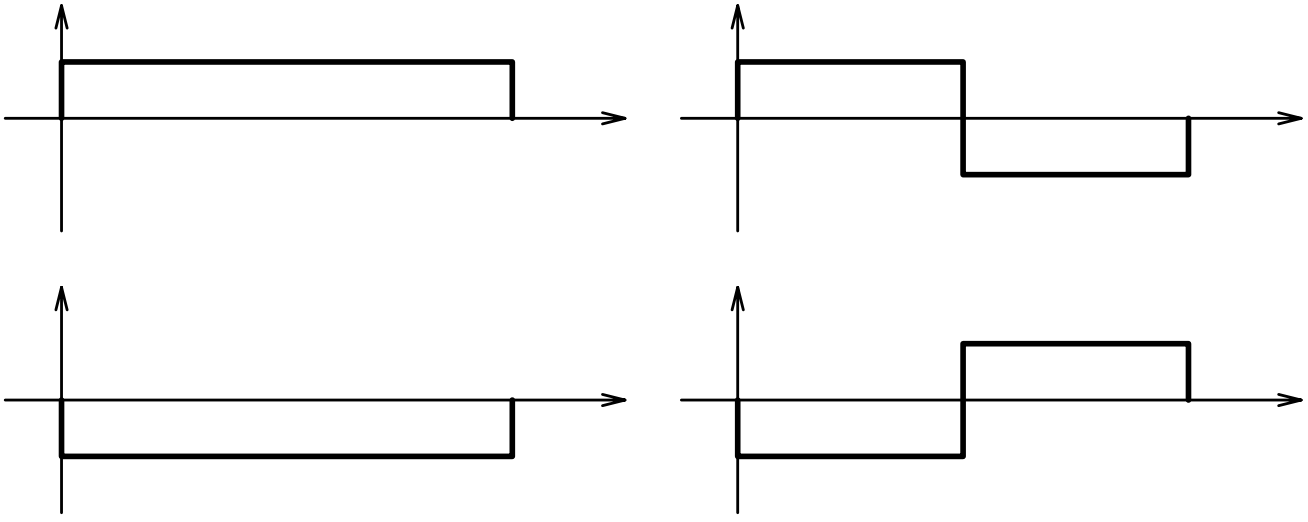

Figure 2.38: A biorthogonal signal set

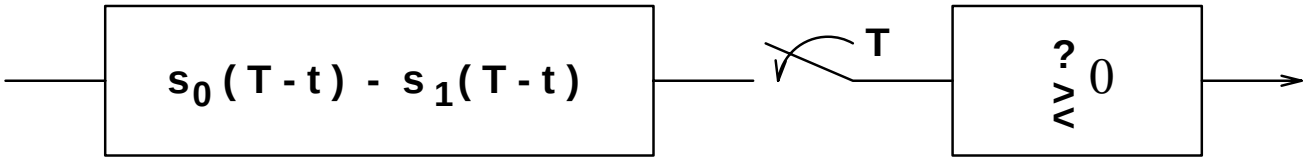

Figure 2.39: Matched £lter receiver for binary communications with equal-energy signals

2.4.2 Receivers for M-ary communication systems

In this section, we obtain receivers for M-ary communication systems through our intuition and our experience with binary communication systems. For simplicity, we assume that the signals are real, of equal energy, and supported only in the interval $[0, T)$. The general case will be considered in Section 2.5.

First, let us re-visit the matched £lter receiver for binary communications as shown in Figure 2.39. In words, the decision rule is to decide $s_0(t)$[11] if

$$\int_0^T r(t)[s_0(t) - s_1(t)]dt > 0 \tag{2.185}$$

and $s_1(t)$ otherwise. Equivalently, we decide $s_0(t)$ if

$$\int_0^T r(t)s_0(t)dt > \int_0^T r(t)s_1(t)dt \tag{2.186}$$

and $s_1(t)$ otherwise. As a result, the matched £lter receiver in Figure 2.39 can be re-drawn in the form shown in Figure 2.40. This form can be readily generalized for a M-ary communication system as shown in Figure 2.41. In words, the decision rule is to decide $s_j(t)$ with the largest inner product

$$\int_0^T r(t)s_j(t)dt. \tag{2.187}$$

Equivalent, we decide $s_j(t)$ with the minimum distance

$$\int_0^T [r(t) - s_j(t)]^2 dt. \tag{2.188}$$

As in the binary case, we can also have the correlator implementation as in Figure 2.42. In the ith

[11] Since the symbols are no longer bits for M-ary communication, we choose to say "decide $s_0(t)$ is sent" or "decide $s_1(t)$ is sent" instead of "decide '0' is sent" or "decide '1' is sent". The meaning of this notion should be apparent and can be easily generalized to the case the symbols are non-binary.

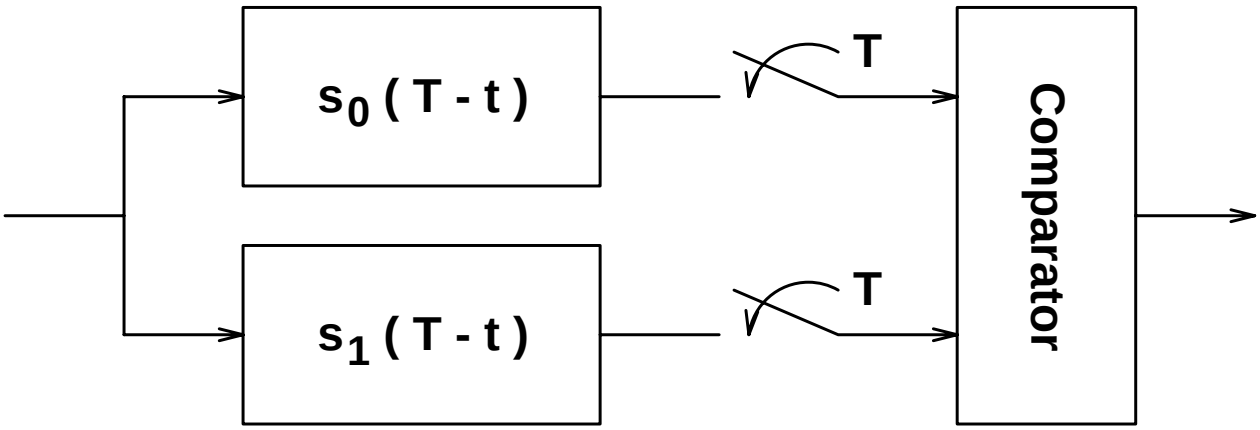

Figure 2.40: Alternative form of the matched £lter receiver

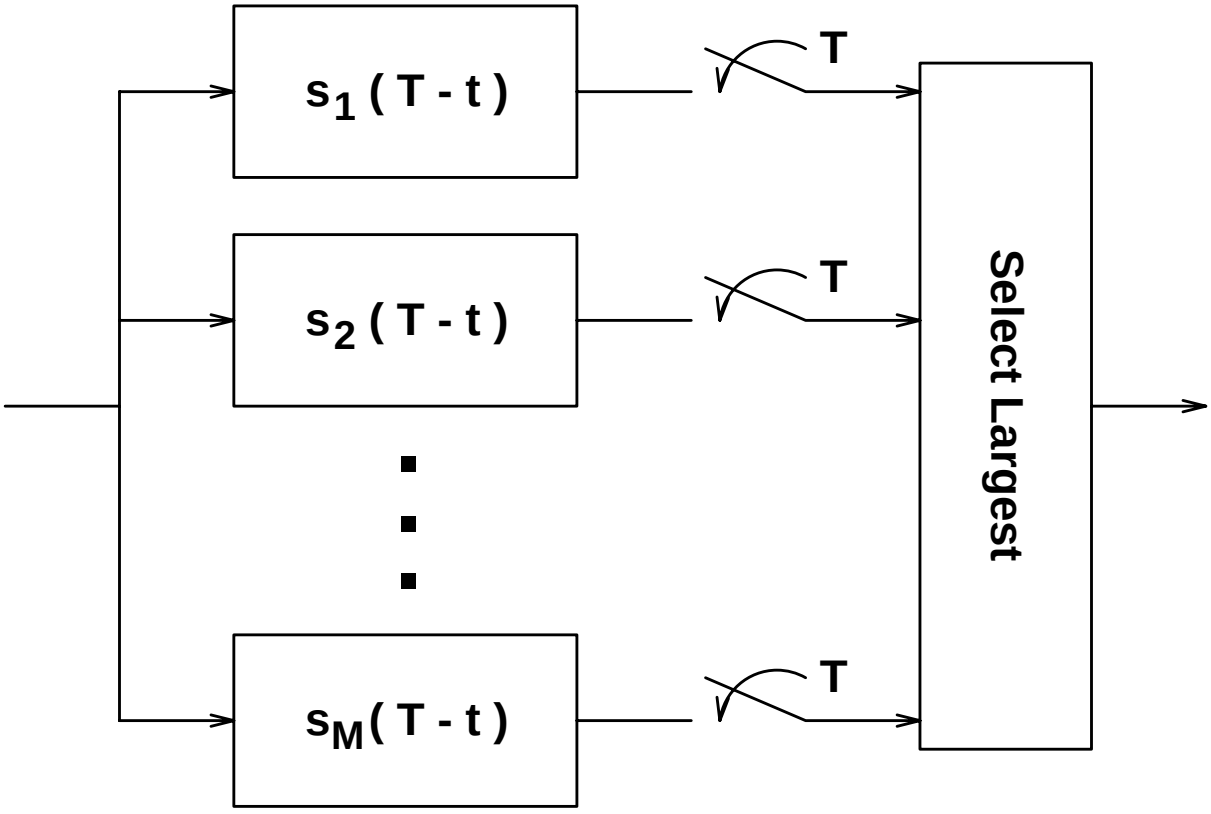

Figure 2.41: Matched £lter receiver for M-ary communications with equal-energy signals

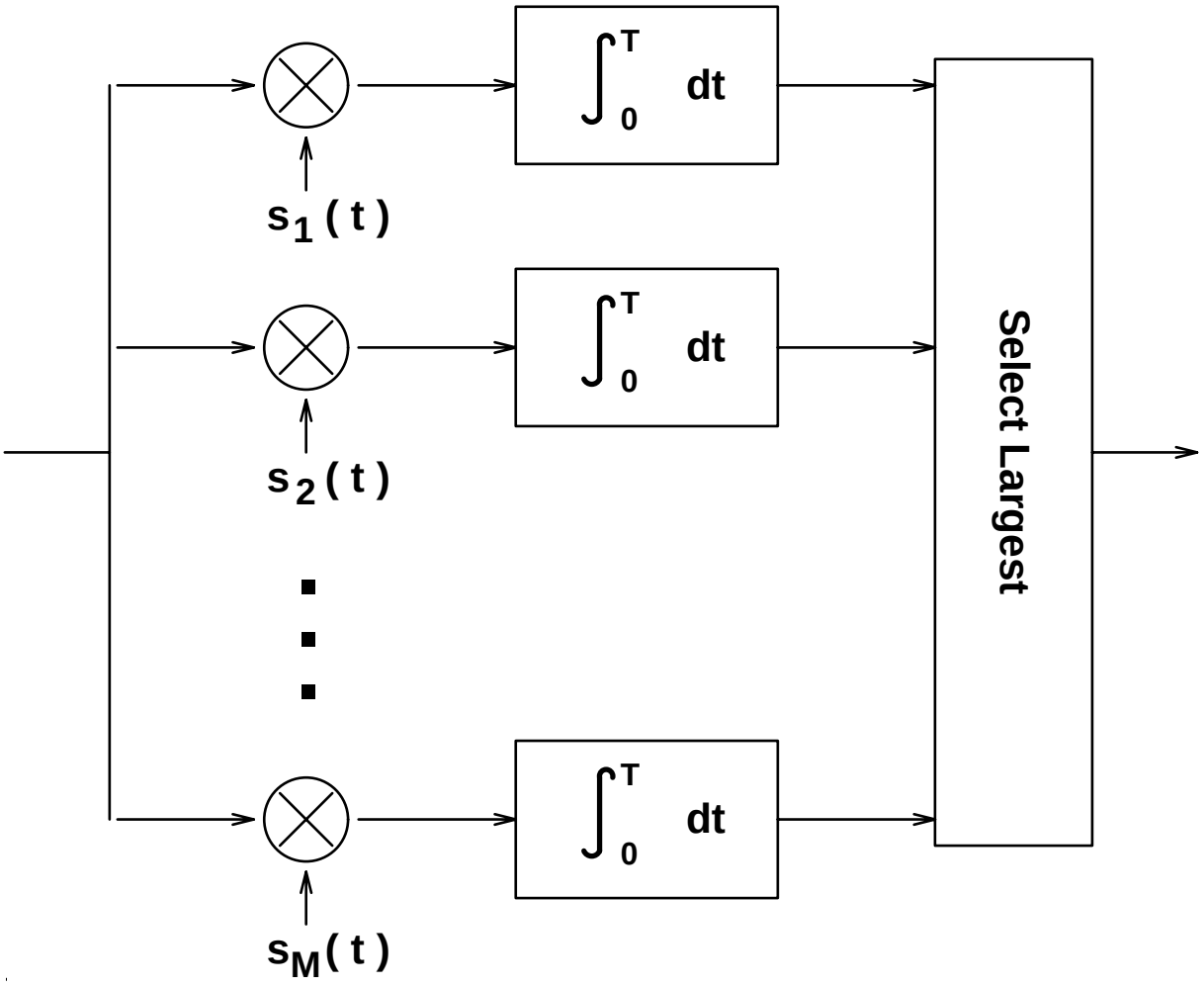

Figure 2.42: Correlator receiver for M-ary communications with equal-energy signals

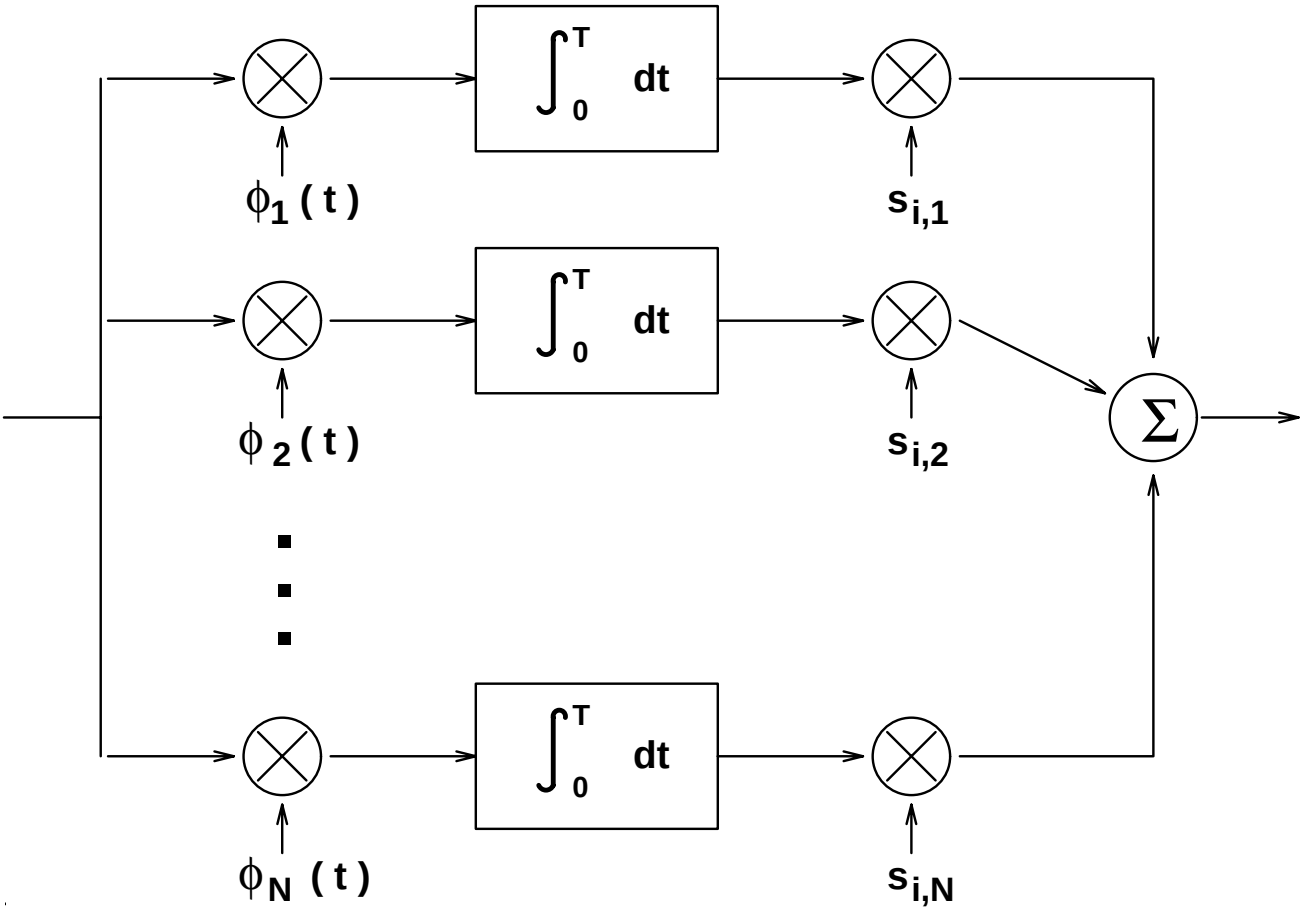

Figure 2.43: Alternative implementation for the ith correlator branch

branch of the correlator receiver in Figure 2.42, we correlate the received signal with $s_i(t)$. Equivalently, we can obtain the same output by correlating the received signal with each of the basis functions and adding the outputs with appropriate weighting since

$$\int_0^T r(t)s_i(t)dt = \sum_{k=1}^{N} s_{i,k} \int_0^T r(t)\phi_k(t)dt \tag{2.189}$$

as depicted in Figure 2.43. Since the output of every branch of the correlation receiver can be implemented this way, we can have the equivalent implementation for the correlator receiver in Figure 2.44. Finally, the form of correlator receiver in Figure 2.44 can also be implemented by matched £lters (matched to the basis functions) as shown in Figure 2.45. Notice that the implementations with basis functions may be preferable if the number of basis functions N is smaller than the number of possible signals M. For example, the receiver for MPSK is usually implemented in the from shown in Figure 2.46.

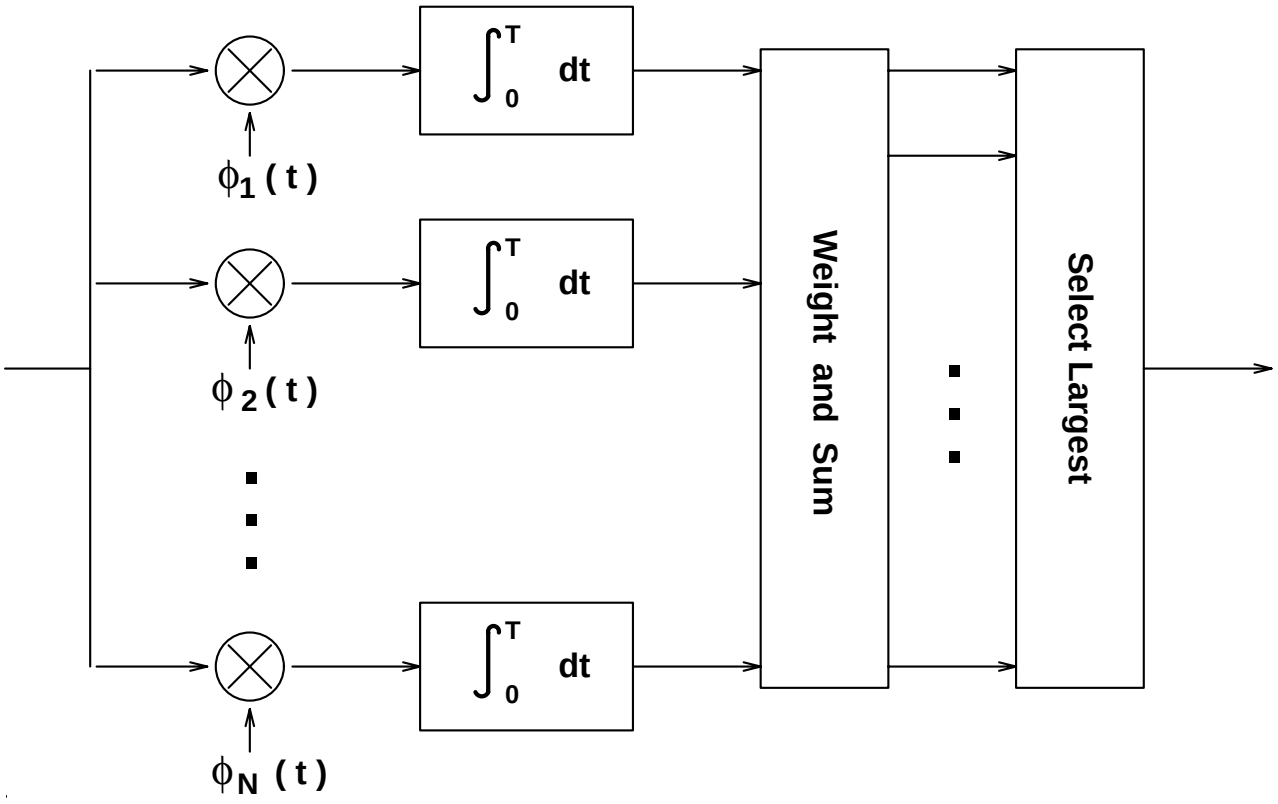

Figure 2.44: Alternative implementation for the correlator receiver

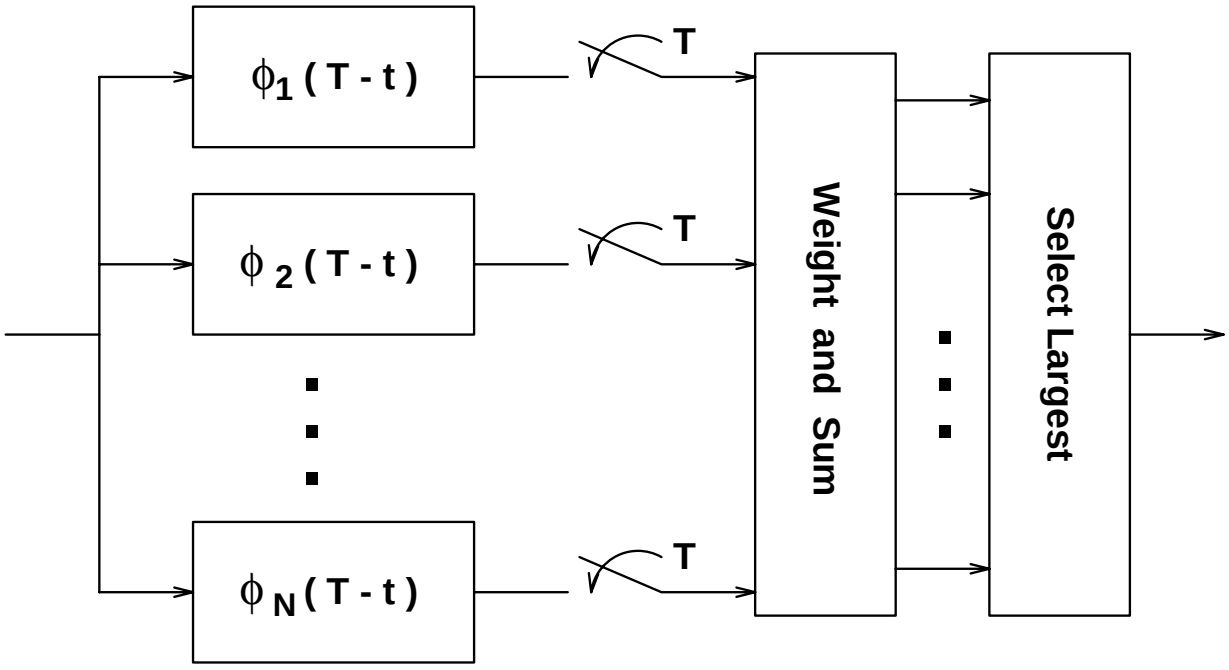

Figure 2.45: Alternative implementation for the matched £lter receiver

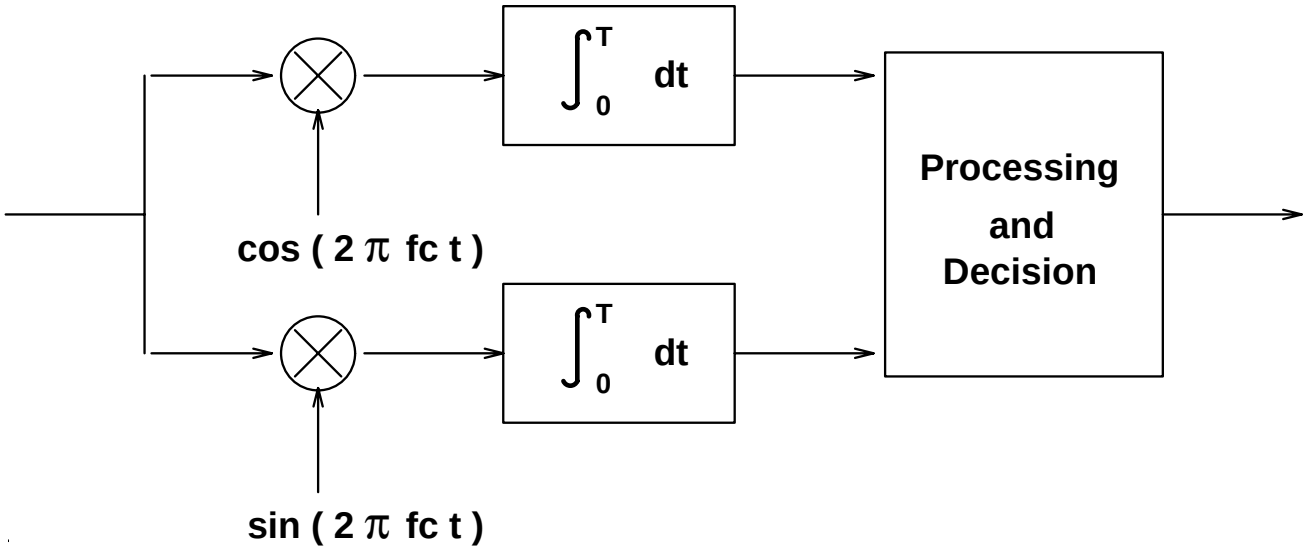

Figure 2.46: Alternative implementation for the matched £lter receiver

2.4.3 Performance — Union Bound

Now, let us investigate the performance of M-ary communications over the AWGN channel by evaluating average symbol error probability. For simplicity, again, we assume that the signals are real, equally probable, of equal energy, and supported only in the interval $[0, T)$. The noise spectral density of the AWGN is $N_0/2$.

Suppose that $s_i(t)$ is sent. Let Z_k be the output of the kth branch of the matched £lter receiver in Figure 2.41 or the correlator receiver in Figure 2.42. Then, it is obvious that the random vector $\mathbf{Z}$ formed by the decision statistics $Z_1, Z_2, \ldots, Z_M$ is Gaussian with mean

$$\mu_{\mathbf{Z}} = [\rho_{i1}, \rho_{i2}, \ldots, \rho_{iM}]^T \tag{2.190}$$

and covariance matrix $\mathbf{C_Z}$ whose (i, j)th element is $\frac{N_0}{2}\rho_{ij}$, where

$$\rho_{ij} = \int_0^T s_i(t) s_j(t) dt \tag{2.191}$$

is the inner product of the signals $s_i(t)$ and $s_j(t)$. The probability of correct decision is given by

$$\begin{aligned} &\Pr(\text{correct decision}) \\ &= \Pr\left(\bigcap_{\substack{k=1 \\ k \neq i}}^{M} \{Z_i > Z_k\} \right) \end{aligned}$$

$$= \int_{\bigcap_{\substack{k=1\\k\neq i}}^{M}\{Z_i>Z_k\}} \frac{1}{(2\pi)^{n/2}\sqrt{\det(\mathbf{C_Z})}} \exp\left[-\frac{1}{2}(\mathbf{z}-\mu_\mathbf{Z})^T {\mathbf{C_Z}}^{-1}(\mathbf{z}-\mu_\mathbf{Z})\right] d\mathbf{z}. \quad (2.192)$$

Given $s_i(t)$ is sent, the conditional symbol error probability equals

$$P_{s|i} = 1 - \Pr(\text{correct decision}). \quad (2.193)$$

Hence, the average symbol error probability is given by

$$P_s = \frac{1}{M}\sum_{i=1}^{M} P_{s|i}. \quad (2.194)$$

In general, it is dif£cult to calculate integrals like the one in (2.192). Therefore, it is dif£cult to obtain a closed form solution for the average symbol error probability. However, it is relatively easy to obtain an upper bound on this probability using the countable sub-additivity property of probabilities:

$$\Pr\left(\bigcup_k A_k\right) \leq \sum_k \Pr(A_k). \quad (2.195)$$

Using this result,

$$\begin{aligned} P_{s|i} &= \Pr\left(\bigcup_{\substack{k=1\\k\neq i}}^{M}\{Z_i \leq Z_k\}\right) \\ &\leq \sum_{\substack{k=1\\k\neq i}}^{M} \Pr(Z_i \leq Z_k). \end{aligned} \quad (2.196)$$

This is called the *union bound* of the conditional symbol error probability. When the energy per symbol to noise power spectral density ratio, E_s/N_0, is large, the union bound is often a good approximation to the true probability of error. We note that in (2.196), each term is the union bound considering the pair of signals $s_i(t)$ and $s_k(t)$ only, without regard to any other signals. Since, the matched £lter demodulator is employed for each pair of signals, for any $k \neq i$,

$$\begin{aligned} \Pr(Z_i \leq Z_k) &= Q\left(\sqrt{\frac{\|s_i - s_k\|^2}{2N_0}}\right) \\ &= Q\left(\frac{d(\mathbf{s}_i, \mathbf{s}_k)}{2\sigma_n}\right), \end{aligned} \quad (2.197)$$

where $\sigma_n^2 = N_0/2$, as in binary communications. With the union bound, we can bound probabilities of error in M-ary communications with results from binary communications:

$$P_{s|i} \leq \sum_{\substack{k=1 \\ k \neq i}}^{M} Q\left(\frac{d(\mathbf{s}_i, \mathbf{s}_k)}{2\sigma_n}\right). \tag{2.198}$$

For example, let us consider the 8PSK constellation in Figure 2.33. Suppose that $s_1(t)$ is sent. Then the union bound on the conditional symbol error probability is

$$\begin{aligned} P_{s|1} &\leq \sum_{k=2}^{8} Q\left(\frac{d(\mathbf{s}_1, \mathbf{s}_k)}{\sqrt{2N_0}}\right) \\ &= 2Q\left(\sqrt{\frac{E_s}{N_0}\left(1 - \frac{1}{\sqrt{2}}\right)}\right) + 2Q\left(\sqrt{\frac{E_s}{N_0}}\right) \\ &\quad + 2Q\left(\sqrt{\frac{E_s}{N_0}\left(1 + \frac{1}{\sqrt{2}}\right)}\right) + Q\left(\sqrt{\frac{2E_s}{N_0}}\right), \end{aligned} \tag{2.199}$$

where $E_s = A^2T/2$ is the energy per symbol. When E_s/N_0 is large, the £rst term above (due to $s_2(t)$ and $s_8(t)$) dominates the other terms. Hence, the union bound is mainly accounted for by the two signals $s_2(t)$ and $s_8(t)$, which are called the *nearest neighbors* of $s_1(t)$. In general, we may obtain a good approximation to the union bound by considering only the nearest neighbors.

2.5 Optimal Detection

Up to now, all the receivers we consider process the received signal by linear £ltering it. One may wonder if there is any reason behind the linear £ltering step. Or can we do better by employing something other than linear £ltering? We are going to answer these questions by developing the *optimal* (in the sense of giving smallest average symbol error probability) receiver structure for the non-dispersive channel model. Throughout the section, we employ the complex baseband representation. All the signals are complex and should be interpreted as complex envelopes of real RF signals.

2.5.1 Channel model and signal representation

We consider a general M-ary communication system, in which the transmitter sends a signal chosen from the set of M £nite-energy signals $s_1(t), s_2(t), \ldots, s_M(t)$, according to the *a priori* probabilities

$p_1, p_2, \ldots, p_M$, respectively. We note that $\sum_{m=1}^{M} p_m = 1$. The channel is contaminated by AWGN $n(t)$ with noise power spectral density N_0. The channel also changes the amplitude and phase of the transmitted signal. Hence, the received signal becomes

$$r(t) = Ae^{\mathrm{j}\theta} s_m(t) + n(t), \tag{2.200}$$

for some $m \in \{0, 1, \ldots, M-1\}$, where A and θ are the amplitude and phase responses of the channel.

First, we try to represent the signals in a more convenient form. By employing the Gram-Schmidt procedure, we can construct a set of N ($N \leq M$) orthonormal functions $\{\phi_n(t)\}_{n=1}^{N}$ which spans the signal space formed by $\{s_m(t)\}_{m=0}^{M-1}$. We augment this set of functions by another set of orthonormal functions $\{\phi_n(t)\}_{n=N+1}^{\infty}$ so that the augmented set $\{\phi_n(t)\}_{n=1}^{\infty}$ forms an *orthonormal basis* for the space of £nite-energy (square-integrable) signals, i.e., for every £nite-energy signal $s(t)$,

$$s(t) = \sum_{n=1}^{\infty} (s, \phi_n)\phi_n(t). \tag{2.201}$$

Employing this basis, any £nite-energy signal can be represented by a vector whose elements are coordinates with respect to the basis functions $\{\phi_n(t)\}_{n=1}^{\infty}$. Based on this representation, we can rewrite (2.200) as

$$\mathbf{r} = Ae^{\mathrm{j}\theta}\mathbf{s}_m + \mathbf{n}, \tag{2.202}$$

where

$$\begin{aligned} \mathbf{r} &= [r_1, r_2, \ldots, r_N, \ldots]^T, \\ \mathbf{s}_m &= [s_{m1}, s_{m2}, \ldots, s_{mN}, \ldots]^T \quad \text{for } m = 0, 1, \ldots, M-1, \\ \mathbf{n} &= [n_1, n_2, \ldots, n_N, \ldots]^T, \end{aligned}$$

are the vectors representing $r(t)$, $s_m(t)$, and $n(t)$[12], respectively. The coordinates are, respectively, given by, for $k = 1, 2, \ldots$,

$$r_k = \int_{-\infty}^{\infty} r(t)\phi_k^*(t)dt, \tag{2.203}$$

[12]For a zero-mean WSS process with £nite variance, we have a similar expansion as in (2.201). The only difference is how the equality in (2.201) is interpreted. Also, strictly speaking, the AWGN does not have £nite energy and hence does not have such an expansion. However, since the AWGN model is an approximation to the bandpass additive Gaussian noise, we abuse the mathematics a little bit and assume that there is an expansion like (2.201) for the AWGN we consider here.

$$s_{mk} = \int_{-\infty}^{\infty} s_m(t)\phi_k^*(t)dt \quad \text{for } m = 1, 2, \ldots, M, \tag{2.204}$$

$$n_k = \int_{-\infty}^{\infty} n(t)\phi_k^*(t)dt. \tag{2.205}$$

From now on, we use this representation and assume that we observe the vector $\mathbf{r}$.

2.5.2 Decision criteria

To employ a minimum amount of mathematical machinery, let us truncate the in£nite dimensional observation vector $\mathbf{r}$ to the K-dimensional vector $\mathbf{r}_K = [r_1, r_2, \ldots, r_K]^T$ and work with this truncated vector instead of the original observation vector $\mathbf{r}$. Because of (2.201), the effect of this truncation gets smaller and smaller when K increases. In fact, we will show later that it is suf£cient to choose $K = N$, where N is the dimension of the signal set.

Now, with observation $\mathbf{r}_K$, our goal is to decide which signal is sent, i.e., we want to pick a number $m \in \{1, 2, \ldots, M\}$. Since we can interpret $\mathbf{r}_K$ as a point in the K-dimensional complex space $\mathbb{C}^K$, this is to say that we have to determine a unique number $m \in \{1, 2, \ldots, M\}$ given a point $\mathbf{r}_K$ in $\mathbb{C}^K$. In other words, we have to partition $\mathbb{C}^K$ into M regions, say, $\mathcal{R}_1, \mathcal{R}_2, \ldots, \mathcal{R}_M$, and associate each region (uniquely) with one of the M signals. Without loss of generality, we can associate $\mathcal{R}_m$ with $s_m(t)$. If the received vector $\mathbf{r}_K$ falls in $\mathcal{R}_m$, then the receiver decides that $s_m(t)$ is sent.

Based on the discussion above, the optimal detection strategy is the one that partitions $\mathbb{C}^K$ into M decision regions, $\mathcal{R}_1, \mathcal{R}_2, \ldots, \mathcal{R}_M$, in such a way that the average symbol error probability is minimized. The average symbol error probability is given by

$$\begin{aligned} P_s &= 1 - \Pr(\text{correct detection}) \\ &= 1 - \sum_{m=1}^{M} p_m \int_{\mathcal{R}_m} f(\mathbf{r}'|m)d\mathbf{r}', \end{aligned} \tag{2.206}$$

where $f(\mathbf{r}'|m)$ is the conditional density function of the received vector $\mathbf{r}_K$ given the signal $s_m(t)$ is transmitted. It is obvious from (2.206) that P_s is minimized by the following partition rule:
For each $\mathbf{r}' \in \mathbb{C}^K$, assign it to the region $\mathcal{R}_{m_*}$, where

$$m_* = \arg\max_{m \in \{1,2,\ldots,M\}} p_m f(\mathbf{r}'|m). \tag{2.207}$$

Now with the partition above, for a £xed K and the corresponding observation vector $\mathbf{r}_K$, the optimal decision rule is:

$$m_* = \arg\max_{m\in\{1,2,\ldots,M\}} p_m f(\mathbf{r}_K|m). \tag{2.208}$$

Moreover, since the conditional (*a posteriori*) probability

$$\Pr(m|\mathbf{r}_K) = \frac{p_m f(\mathbf{r}_K|m)}{f(\mathbf{r}_K)} \tag{2.209}$$

and $f(\mathbf{r}_K)$ is independent of m, we can also rewrite the optimal decision rule in the form:

$$m_* = \arg\max_{m\in\{1,2,\ldots,M\}} \Pr(m|\mathbf{r}_K). \tag{2.210}$$

Because of this equivalent form, the optimal decision rule is sometimes referred to as *maximum a posterior (MAP)* detection. Very often, the M signals are sent with equal probabilities of $1/M$. Then the decision rule simpli£es to

$$m_* = \arg\max_{m\in\{1,2,\ldots,M\}} f(\mathbf{r}_K|m). \tag{2.211}$$

The conditional density function $f(\mathbf{r}_K|m)$ is usually known as the *likelihood function* of $s_m(t)$. This simpli£ed decision rule of maximizing the likelihood function is called *maximum likelihood (ML)* detection. We will focus on ML detection in the followings and the MAP decision rule is just a trivial extension.

2.5.3 Maximum Likelihood Coherent Receiver

First, let us assume that we have perfect knowledge of the channel amplitude and phase responses, i.e., the values of A and θ are known. With this knowledge, we work out the *maximum likelihood (ML) coherent receiver* for the non-dispersive channel.

For any £xed $K \geq N$, the truncated observation vector $\mathbf{r}_K$ is given by

$$\mathbf{r}_K = Ae^{\mathrm{j}\theta}\mathbf{s}_{mK} + \mathbf{n}_K, \tag{2.212}$$

where $\mathbf{s}_{mK}$ and $\mathbf{n}_K$ are the K-dimensional truncations of $\mathbf{s}_m$ and $\mathbf{n}$, respectively. It is easy to see that

$$\mathbf{s}_{mK} = [s_{m1}, s_{m2}, \ldots, s_{mN}, \underbrace{0, \ldots, 0}_{K-N}]^T \tag{2.213}$$

and $\mathbf{n}_K$ is a zero-mean Gaussian random vector whose covariance matrix is $N_0\mathbf{I}$. Hence the likelihood function is

$$\begin{aligned} f(\mathbf{r}_K|m) &= \prod_{k=1}^{N} \frac{1}{2\pi N_0} \exp\left(-\frac{|r_k - Ae^{\mathrm{j}\theta}s_{mk}|^2}{2N_0}\right) \cdot \prod_{k=N+1}^{K} \frac{1}{2\pi N_0} \exp\left(-\frac{|r_k|^2}{2N_0}\right) \\ &= f(\mathbf{r}_N|m) \cdot \prod_{k=N+1}^{K} \frac{1}{2\pi N_0} \exp\left(-\frac{|r_k|^2}{2N_0}\right). \end{aligned} \tag{2.214}$$

The ML coherent receiver makes a decision (select $m \in \{0, 1, \ldots, M-1\}$) which maximizes the likelihood function above. Since the second product on the right hand side of (2.214) does not depend on m, $p(\mathbf{r}_K|m)$ is maximized by maximizing $p(\mathbf{r}_N|m)$. This means that no matter how many coef£cients of the received vector $\mathbf{r}$ we observe (as long as $K \geq N$), only the £rst N coef£cients are actually needed. In other words, the N-dimensional truncation, $\mathbf{r}_N$, of the the received vector $\mathbf{r}$ is suf£cient to for us to perform ML detection. Because of this, $\mathbf{r}_N$ is known as the *suf£cient statistic* for the detection of the transmitted signal.

From the discussion above, we can base our development on the truncated observation vector $\mathbf{r}_N$ without loss of generality. Since logarithm is a monotone increasing function, by taking logarithm of $p(\mathbf{r}_N|m)$, it is easy to see that the ML receiver picks $m \in \{0, 1, \ldots, M-1\}$ such that the squared Euclidean distance between the signal vector $Ae^{\mathrm{j}\theta}\mathbf{s}_{mN}$ and the receiver vector $\mathbf{r}_N$,

$$\begin{aligned} d^2(\mathbf{r}_N, Ae^{\mathrm{j}\theta}\mathbf{s}_{mN}) &= \sum_{k=1}^{N} \left|r_k - Ae^{\mathrm{j}\theta}s_{mk}\right|^2 \\ &= \|\mathbf{r}_N\|^2 - 2A\mathrm{Re}\left[e^{-\mathrm{j}\theta}\mathbf{s}_{mN}^H\mathbf{r}_N\right] + A^2\|\mathbf{s}_{mN}\|^2 \end{aligned} \tag{2.215}$$

is minimized. Moreover, since $\|\mathbf{r}_N\|^2$ is constant for all values of m, we have

$$\arg\min_{m\in\{1,2,\ldots,M\}} d^2(\mathbf{r}_N, Ae^{\mathrm{j}\theta}\mathbf{s}_{mN}) = \arg\max_{m\in\{1,2,\ldots,M\}} c(\mathbf{r}_N, Ae^{\mathrm{j}\theta}\mathbf{s}_{mN}) \tag{2.216}$$

where

$$\begin{aligned} c(\mathbf{r}_N, Ae^{\mathrm{j}\theta}\mathbf{s}_{mN}) &= \mathrm{Re}\left[e^{-\mathrm{j}\theta}\mathbf{s}_{mN}^H\mathbf{r}_N\right] - \frac{1}{2}A\|\mathbf{s}_{mN}\|^2, \\ &= \mathrm{Re}\left[e^{-\mathrm{j}\theta}\int_{-\infty}^{\infty} r(t)s_m^*(t)dt\right] - \frac{AE_m}{2}. \end{aligned} \tag{2.217}$$

In (2.217), $c(\mathbf{r}_N, Ae^{\mathrm{j}\theta}\mathbf{s}_{mN})$ is called the *correlation metric* between the received signal $r(t)$ and the transmitted signal $s_m(t)$, and

$$E_m = \int_{-\infty}^{\infty} |s_m(t)|^2 dt, \tag{2.218}$$

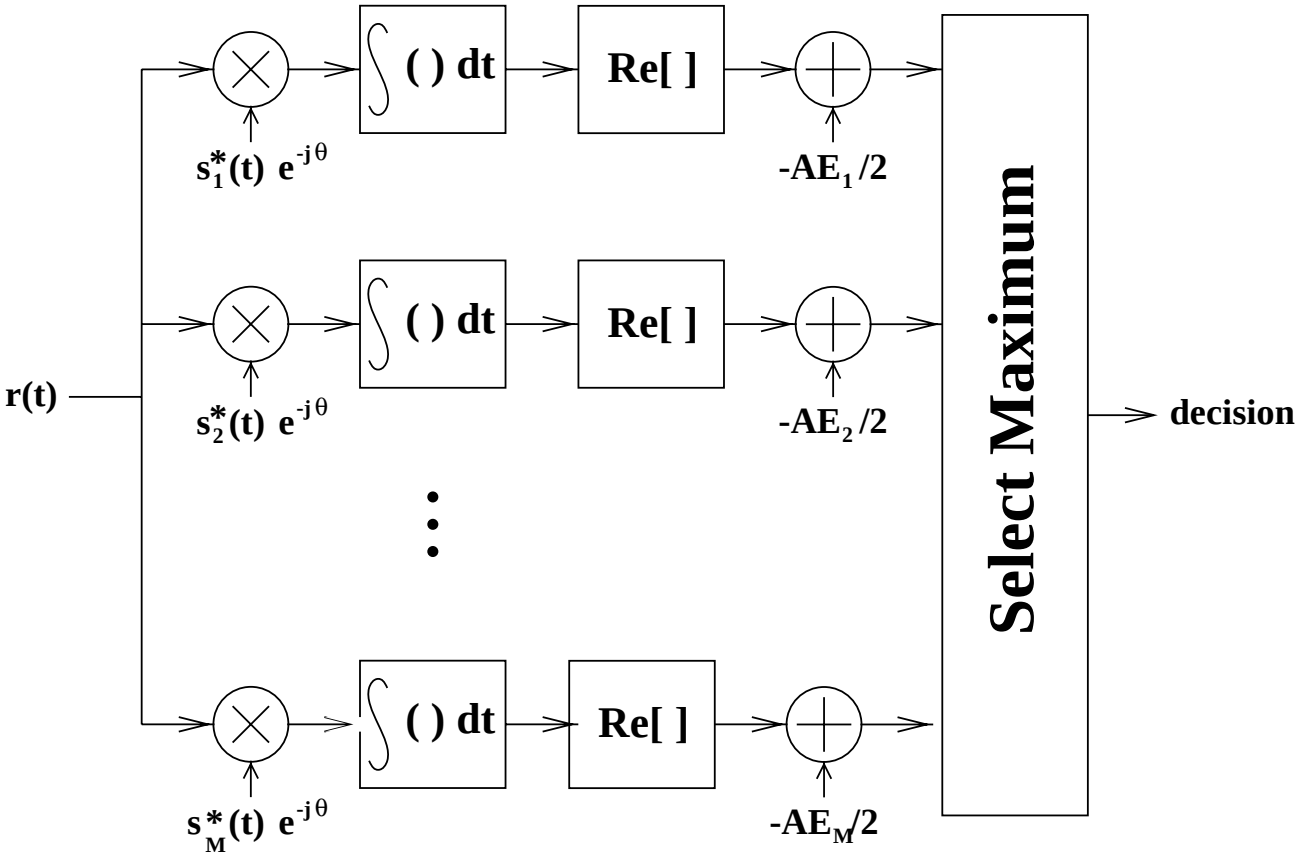

Figure 2.47: Maximum likelihood coherent receiver

is the energy of the transmitted signal $s_m(t)$. In summary, we can implement the ML coherent receiver as in the block diagram shown in Figure 2.47. We note that the ML coherent receiver reduces to the matched £lter for binary communications (when $M = 2$) and to the correlator receiver in Figure 2.42 when the M signals are real and of equal energy. Therefore, the linear coherent receivers we develop before are indeed optimal.

Now, we analyze the performance of the ML coherent receiver by evaluating the symbol error probability. To do this, let us £rst understand the geometric intuition of the ML decision rule. From (2.215), we know that the ML receiver decides that the mth signal is sent when the Euclidean distance $d(\mathbf{r}_N, Ae^{j\theta}\mathbf{s}_{mN})$ is the smallest among all the M signals. If we draw the signal vectors as points in the constellation diagram as shown in Figure 2.48, the geometric meaning of the ML decision rule is that the signal $\mathbf{s}_{mN}$ closest to the receiver vector $\mathbf{r}_N$ is selected. Equivalently, the decision region for each of the signal contains all the points in $\mathbb{C}^N$ which are closest to that signal. A diagram showing the signal

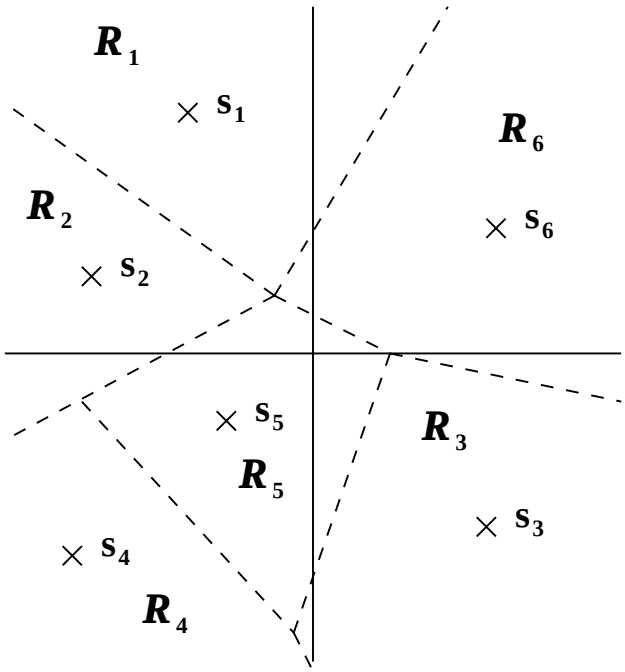

Figure 2.48: Voronoi diagram

points and their corresponding decision regions is known as the *Voronoi diagram* of a modulation scheme. With the Voronoi diagram, we can use (2.206) to obtain the average symbol error probability. We can rewrite (2.206) as

$$P_s = \sum_{m=1}^{M} p_m P_{s|m}, \tag{2.219}$$

where

$$\begin{aligned} P_{s|m} &= \int_{\mathbb{C}^N \setminus \mathcal{R}_m} f(\mathbf{r}'|m) d\mathbf{r}' \\ &= 1 - \int_{\mathcal{R}_m} f(\mathbf{r}'|m) d\mathbf{r}' \end{aligned} \tag{2.220}$$

is the conditional symbol error probability given that $s_m(t)$ is sent. The conditional density function in (2.220) is given by

$$f(\mathbf{r}'|m) = \prod_{k=1}^{N} \frac{1}{2\pi\sigma_n^2} \exp\left(-\frac{|r_k' - Ae^{j\theta} s_{mk}|^2}{2\sigma_n^2}\right), \tag{2.221}$$

where $\sigma_n^2 = N_0$. Although the expression in (2.220) looks simple, it is generally dif£cult to construct the Voronoi diagram and evaluate the integral in (2.220). However, for some special cases closed form solutions can be found. For example, we consider is the binary case ($M = 2$, $N \leq 2$) in which the

signal set contains two signals $s_0(t)$ and $s_1(t)$. It is intuitive that the decision regions for the signal points $\mathbf{s}_0$ and $\mathbf{s}_1$ are separated by the hyperplane half-way between the signal points and perpendicular to the line joining the two signal points. The next step is to evaluate the integral in (2.220). Suppose $s_0(t)$ is sent, we know that

$$\begin{aligned} P_{s|0} &= \int_{\mathcal{R}_1} f(\mathbf{r}'|0)d\mathbf{r}' \\ &= \int_{-\infty}^{0} \frac{1}{\sqrt{2\pi\sigma_n^2}} \exp\left[-\frac{(x - d(Ae^{\mathrm{j}\theta}\mathbf{s}_{0N}, Ae^{\mathrm{j}\theta}\mathbf{s}_{1N})/2)^2}{2\sigma_n^2}\right] dx \\ &= Q\left(\frac{d(Ae^{\mathrm{j}\theta}\mathbf{s}_{0N}, Ae^{\mathrm{j}\theta}\mathbf{s}_{1N})}{2\sigma_n}\right), \end{aligned} \tag{2.222}$$

We note that the second equality in (2.222) above is obtained by a change of variable which corresponds to a suitable rotation and translation of the axis. Clearly, $P_{s|1}$ can be calculated in the same way. Thus $P_s = Q(d(Ae^{\mathrm{j}\theta}\mathbf{s}_{0N}, Ae^{\mathrm{j}\theta}\mathbf{s}_{1N})/2\sigma_n)$. Moreover, it can be seen that the result in (2.222) reduces to $P_s = P_b = Q(\sqrt{2E_b/N_0})$ for BPSK.

When the exact symbol error probability is too dif£cult to evaluate, we can resort to the union bound. Suppose $s_1(t)$ is being transmitted, we know from the ML decision rule that

$$\begin{aligned} P_{s|1} &= \Pr\left[\bigcup_{m=2}^{M} \{d(Ae^{\mathrm{j}\theta}\mathbf{r}_N, Ae^{\mathrm{j}\theta}\mathbf{s}_{mN}) < d(Ae^{\mathrm{j}\theta}\mathbf{r}_N, Ae^{\mathrm{j}\theta}\mathbf{s}_{1N})\}\right] \\ &\leq \sum_{m=2}^{M} \Pr\left[\{d(Ae^{\mathrm{j}\theta}\mathbf{r}_N, Ae^{\mathrm{j}\theta}\mathbf{s}_{mN}) < d(Ae^{\mathrm{j}\theta}\mathbf{r}_N, Ae^{\mathrm{j}\theta}\mathbf{s}_{1N})\}\right]. \end{aligned} \tag{2.223}$$

We notice that the event $\{d(Ae^{\mathrm{j}\theta}\mathbf{r}_N, Ae^{\mathrm{j}\theta}\mathbf{s}_{mN}) < d(Ae^{\mathrm{j}\theta}\mathbf{r}_N, Ae^{\mathrm{j}\theta}\mathbf{s}_{1N})\}$ in (2.223) is exactly the same as the error event as if there were only two signals, $s_1(t)$ and $s_m(t)$ ($m \geq 2$), in the signal set. The probability of this event has been calculated in (2.222). Hence, we obtain the union bound of the conditional symbol error probability as

$$P_{s|1} \leq \sum_{m=2}^{M} Q\left(\frac{d(Ae^{\mathrm{j}\theta}\mathbf{s}_{1N}, Ae^{\mathrm{j}\theta}\mathbf{s}_{mN})}{2\sigma_n}\right), \tag{2.224}$$

where $\sigma_n^2 = N_0$. Similarly, we can £nd union bounds for the conditional error probabilities given that other signals are sent.

2.5.4 Maximum Likelihood Noncoherent Receiver

Now, suppose we have no knowledge of the channel phase response θ. We can only perform noncoherent demodulation. Since we do not know θ, a reasonable starting point is to model θ as a random variable uniformly distributed on the interval $[0, 2\pi)$. Again, we employ the vector representation in Section 2.5.1 and select the signal, which maximizes the likelihood function $f(\mathbf{r}_K|m)$, based on the observation vector $\mathbf{r}_K$. The difference is that the likelihood function in this case is given by

$$\begin{aligned} f(\mathbf{r}_K|m) &= \int_0^{2\pi} f(\mathbf{r}_K|m,\theta) f(\theta) d\theta \\ &= \int_0^{2\pi} \frac{1}{2\pi} \left(\frac{1}{2\pi N_0}\right)^K \exp\left(-\frac{1}{2N_0}\sum_{k=1}^{K} \left|r_k - Ae^{\mathrm{j}\theta} s_{mk}\right|^2\right) d\theta \\ &= f(\mathbf{r}_N|m) \cdot \left(\frac{1}{2\pi N_0}\right)^{K-N} \exp\left(-\frac{1}{2N_0}\sum_{k=N+1}^{K} |r_k|^2\right). \end{aligned} \tag{2.225}$$

Obviously, $\mathbf{r}_N$ is suf£cient for the detection of the transmitted signal. Hence, we can just assume $K = N$ and maximize

$$\begin{aligned} f(\mathbf{r}_N|m) &= \left(\frac{1}{2\pi N_0}\right)^N \frac{1}{2\pi} \int_0^{2\pi} \exp\left(-\frac{1}{2N_0}\left\|\mathbf{r}_N - Ae^{\mathrm{j}\theta}\mathbf{s}_{mN}\right\|^2\right) d\theta \\ &= \left(\frac{1}{2\pi N_0}\right)^N \exp\left(-\frac{\|\mathbf{r}_N\|^2 + A^2\|\mathbf{s}_{mN}\|^2}{2N_0}\right) \cdot \\ &\quad \frac{1}{2\pi}\int_0^{2\pi} \exp\left(\frac{A}{N_0}\mathrm{Re}\left[e^{-\mathrm{j}\theta}\mathbf{s}_{mN}^H \mathbf{r}_N\right]\right) d\theta. \end{aligned} \tag{2.226}$$

This is the same as choosing m to maximize the noncoherent metric

$$\begin{aligned} \tilde{c}(\mathbf{r}_N, Ae^{\mathrm{j}\theta}\mathbf{s}_{mN}) &= \exp\left(-\frac{A^2\|\mathbf{s}_{mN}\|^2}{2N_0}\right) \frac{1}{2\pi}\int_0^{2\pi} \exp\left(\frac{A}{N_0}\mathrm{Re}\left[e^{-\mathrm{j}\theta}\mathbf{s}_{mN}^H\mathbf{r}_N\right]\right) d\theta \\ &= \exp\left(-\frac{A^2E_m}{2N_0}\right) \frac{1}{2\pi}\int_0^{2\pi} \exp\left(\frac{A}{N_0}\mathrm{Re}\left[e^{-\mathrm{j}\theta}\int_{-\infty}^{\infty} r(t)s_m^*(t)dt\right]\right) d\theta \\ &= \exp\left(-\frac{A^2E_m}{2N_0}\right) \frac{1}{2\pi}\int_0^{2\pi} \exp\left\{\frac{A}{N_0}\Big(\mathrm{Re}\left[\int_{-\infty}^{\infty} r(t)s_m^*(t)dt\right]\cos\theta + \right. \\ &\quad \left.\mathrm{Im}\left[\int_{-\infty}^{\infty} r(t)s_m^*(t)dt\right]\sin\theta\Big)\right\} d\theta \\ &= \exp\left(-\frac{A^2E_m}{2N_0}\right) \frac{1}{2\pi}\int_0^{2\pi} \exp\left\{\frac{A}{N_0}\left|\int_{-\infty}^{\infty} r(t)s_m^*(t)dt\right|\cos(\theta-\phi)\right\} d\theta \\ &= \exp\left(-\frac{A^2E_m}{2N_0}\right) I_0\left(\frac{A}{N_0}\left|\int_{-\infty}^{\infty} r(t)s_m^*(t)dt\right|\right), \end{aligned} \tag{2.227}$$

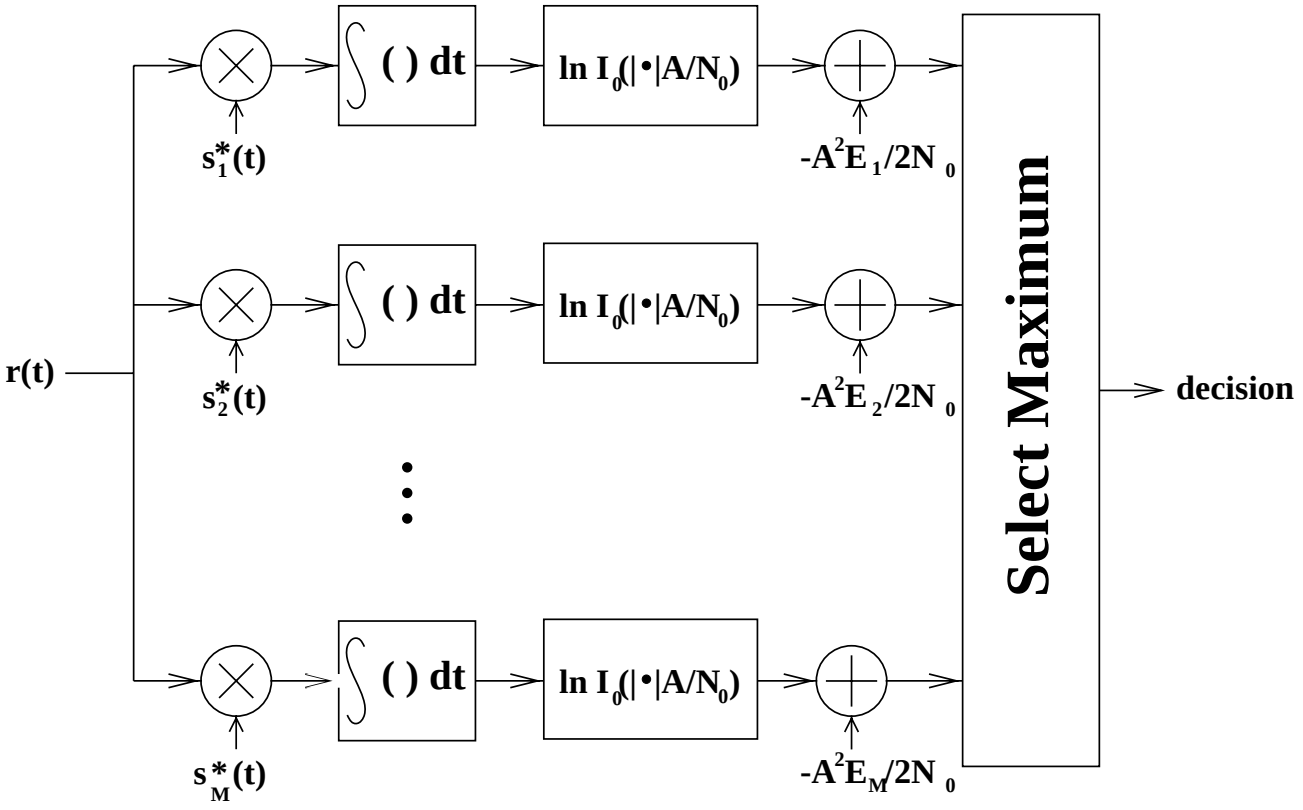

Figure 2.49: Maximum likelihood noncoherent receiver

where

$$\phi = \arctan\left\{\frac{\text{Im}\left[\int_{-\infty}^{\infty} r(t)s_m^*(t)dt\right]}{\text{Re}\left[\int_{-\infty}^{\infty} r(t)s_m^*(t)dt\right]}\right\} \tag{2.228}$$

and $I_0(\cdot)$ is the zeroth order modi£ed Bessel function of the £rst kind. Taking logarithm, the *maximum likelihood noncoherent receiver* can be implemented as shown in Figure 2.49 When all the M signals have the same energy, the ML noncoherent decision rule reduces to maximizing

$$\left|\int_{-\infty}^{\infty} r(t)s_m^*(t)dt\right| \tag{2.229}$$

or its square and hence the channel amplitude response A is not needed. The resulting simpli£ed receiver is shown in Figure 2.50. Finally, we point out that the noncoherent receiver we suggested for FSK in Figure 2.12 is in fact the ML noncoherent receiver for the non-dispersive channel.

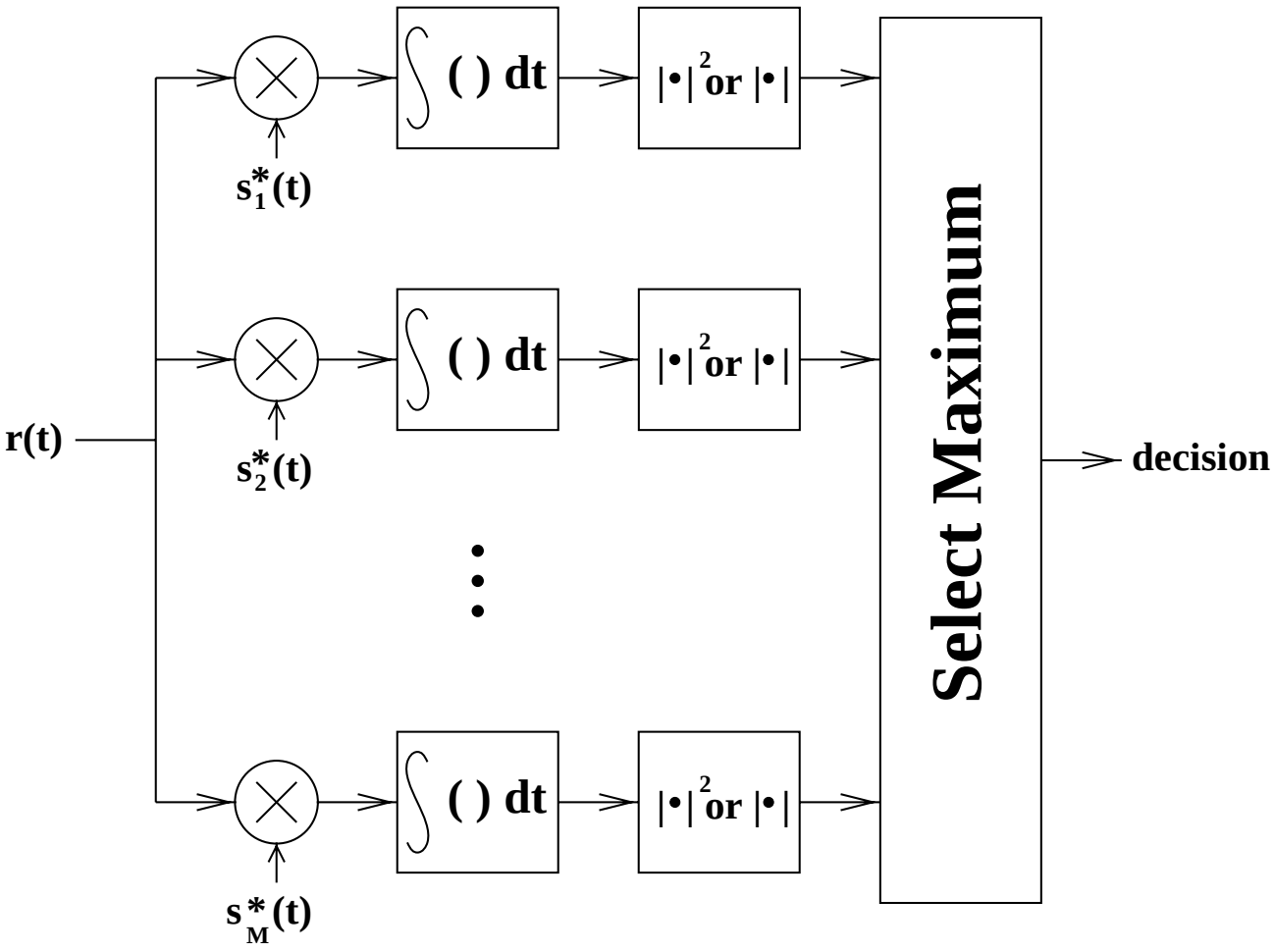

Figure 2.50: Simpli£ed ML noncoherent receiver for equal-energy signals

2.6 Comparison of Modulation Methods

We have introduced a variety of digital modulation methods and ways to demodulate them in this chapter. There are both pros and cons for each of the methods. A natural question one would ask is that which modulation method we should employ. Unfortunately, there is no easy answer to this question. The choice of modulation method (and the demodulation scheme) depends on many different considerations, such as constraints on the transmission power and the complexity of the receiver circuitry. However, there are several common comparison criteria based on which we can make a decision between different modulation methods. These design criteria are listed below:

Power ef£ciency

One of the many goals of a communication system is to use the least amount of energy per bit E_b to achieve reliable communication, i.e., to maintain the probability of bit error below a certain level. Of course, the amount energy we need to use depends also on the severity of the channel defects. For the simple case of the AWGN (or non-dispersive) channel model, we usually plot error probability versus the ratio E_b/N_0 to compare the error performance of different modulation methods. For example, let us consider binary communications with coherent demodulation. For BPSK, $P_b = Q(\sqrt{2E_b/N_0})$, while for FSK, $P_b = Q(\sqrt{E_b/N_0})$. To achieve a certain bit error probability, we need more energy if we employ FSK. Therefore, BPSK is more power ef£cient than FSK in this sense.

Bandwidth (spectral) ef£ciency

We also want to achieve the highest bit rate with a given frequency band. Given a certain frequency band (and a proper de£nition of bandwidth), we can compare different modulation methods by £nding the achievable bit rate with each method. For example, QPSK has the same PSD (up to a scale) as BPSK, but QPSK supports twice the bit rate of BPSK. Therefore, QPSK is better than BPSK in the sense that the bit rate per Hz is higher.

Complexity

Another design objective is to use the simplest transmitters and receivers. Different modulation methods could require different transmitters and receivers while the complexity of the transmitters and the receivers affects the cost of the system. Therefore, the complexity is certainly a factor of concern in determining which modulation method to use. For example, the receivers for binary communications are generally less complex than those for M-ary communications.

Robustness

Yet another consideration in choosing between modulation methods is the tolerance against variations from ideal situations, such as the AWGN model. Practical situations often contain non-ideal conditions and variations (foreseeable or not). A successful communication system must be able to tolerate (to a certain extent) unfavorable conditions. For example, FSK with noncoherent demodulation is more robust against changes in the channel phase response than BPSK which requires accurate estimation of the time-varying channel phase.

Spectral ef£ciency versus power ef£ciency plot

Very often, these criteria are in con¤ict, and it is not easy to make the choice. For example, the error performance of 16QAM is not as power ef£cient as QPSK, i.e., with the same E_b/N_0, the probability of bit error is larger for 16QAM. However, given the same bandwidth, the achievable bit rate for 16QAM is twice that of QPSK, i.e., 16QAM is more bandwidth ef£cient than QPSK.

For many of the common modulation methods described in this chapter, similar comparisons can be made. The comparison results can be summarized by a plot of the spectral ef£ciency versus the (relative) power ef£ciency of different modulation schemes. First, the spectral ef£ciency of a modulation method is obtained as the number of bits that can be transmitted by using the method per second per Hertz. For example, if we employ the null-to-null bandwidth as our working de£nition of bandwidth, then for BPSK, we can transmit 1 bit in T seconds using a bandwidth of $2/T$ Hz. Hence, the spectral ef£ciency of BPSK is 0.5 bits/s/Hz. Similarly for MPSK, the spectral ef£ciency is $\frac{1}{2}\log_2 M$ bits/s/Hz. For MFSK with $\Delta f = 1/2T$ (an M-ary orthogonal signaling method), the bandwidth is approximately $\frac{M+3}{2T}$ Hz, and hence the spectral ef£ciency is $\frac{2}{M+3}\log_2 M$ bits/s/Hz. To avoid the complexity involved

in calculating the exact error probability, we use the dominant terms in the union bound (the terms due to the nearest neighbors in the signal constellation) to compare the power ef£ciency of different modulation schemes. We note that this is equivalent to making the assumption that the ratio E_b/N_0 is very large. In this case, the symbol error probability (for coherent demodulation) is approximately given by[13]

$$Q\left(\frac{d_{min}}{2\sigma_n}\right) \approx \exp\left(-\frac{d_{min}^2}{2\sigma_n^2}\right), \tag{2.230}$$

where d_{min} is the distance between a pair of nearest neighbors in the signal constellation of the modulation method. Based on this, we can compare the power ef£ciency of modulation method by de£ning the relative power ef£ciency as the ratio of the exponent in (2.230) to that of BPSK which has the same energy per bit as the modulation method. Physically, the relative power ef£ciency of a modulation method represents the additional power needed to achieve the same asymptotic error probability as BPSK. A plot showing the spectral ef£ciency and the relative power ef£ciency of some of the modulation methods described before is given in Figure 2.51. From the £gure, we see that 16QAM and 8PSK are bandwidth ef£cient modulation methods while 8FSK is a power ef£cient modulation method. Neglecting other considerations, among the modulation methods shown in Figure 2.51, we would probably choose 16QAM or 8PSK if the channel is bandwidth-limited and 8FSK if the channel is power-limited.

[13]Strictly speaking, there should be a constant term, which accounts for the fact that there may be more than one nearest neighbors, in the approximate error expression in (2.230). However, as E_b/N_0 increases, only the exponent matters. Therefore we can neglect the constant term for simplicity.

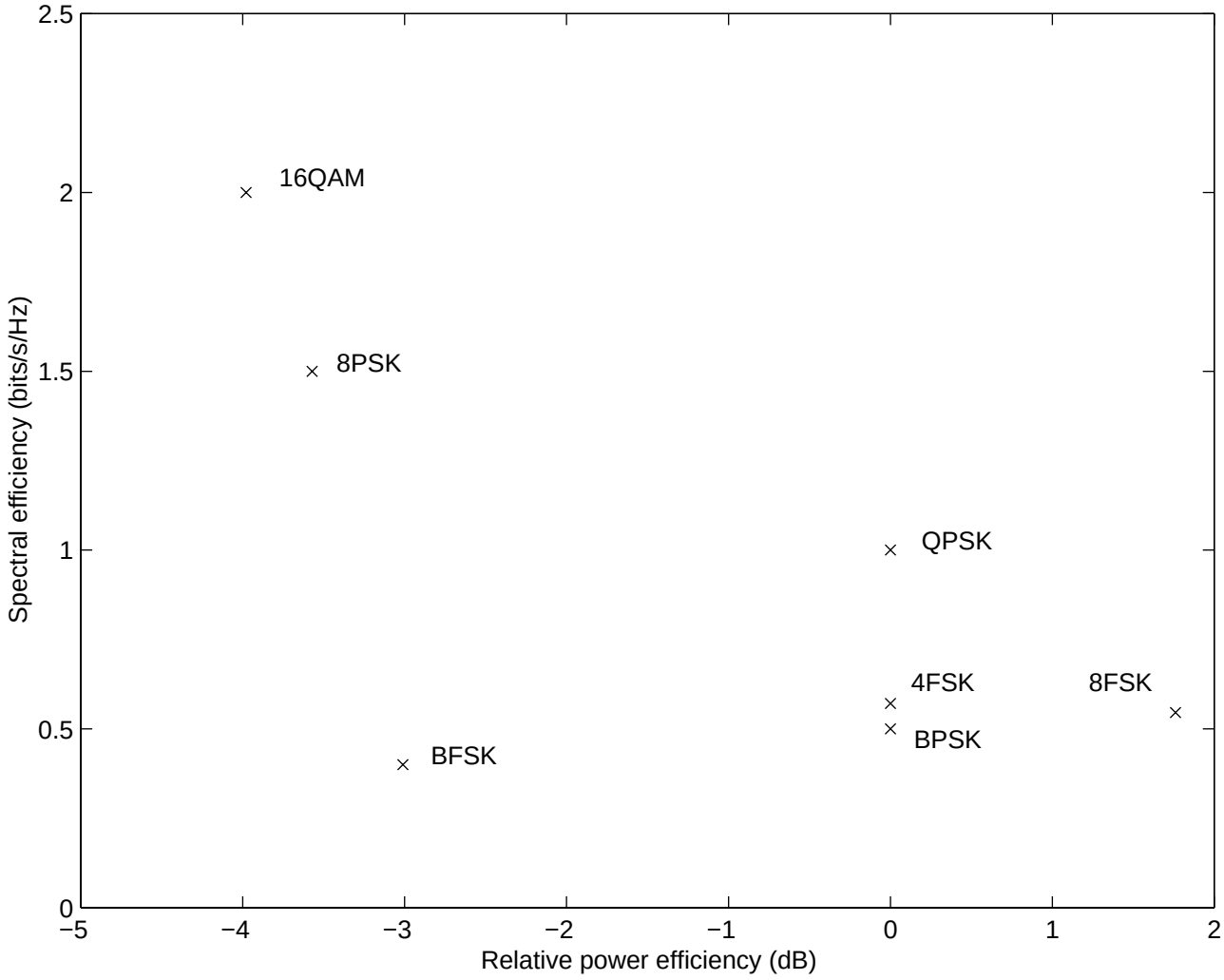

Figure 2.51: Spectral ef£ciency versus power ef£ciency plot